EUROPEAN Society for Hyperthermic Oncology

36th Annual Meeting | 6–8 NOVEMBER | 2024 | MALAGA SPAIN

ABSTRACTS

Content

Invited Talks

IT-03
Technology overview and recent advances in the delivery, monitoring and control of hyperthermia treatments

D. Rodrigues[1]

[1]University of Maryland School of Medicine, Baltimore, MD, United States

Hyperthermia therapy (HT) involves mild heating within 40-44 °C for one hour, which has been shown to be a potent enhancer of radiation and chemotherapy. Microwave (MW) and radiofrequency (RF) hyperthermia devices provide a variety of heating approaches that can treat most cancers regardless of tumor size and depth. This talk will introduce the physics of MW/RF HT, the current state-of-the-art systems for both local and regional heating, temperature monitoring approaches, and recent advancements in HT treatment planning and non-invasive treatment guidance using real-time magnetic resonance imaging.

Hyperthermia can be administered either invasively or noninvasively using externally applied power. Using RF/MW devices, HT treatments can be further divided into local or regional HT. Local HT can be applied to both superficial and deep-seated tumors by external, intraluminal or interstitial MW methods. Regional HT is delivered using RF phased array applicators to treat deep-seated pelvic or abdominal tumors. The key difference between these two HT modalities is the operating frequency, where localized heating is achieved with MW (434 or 915 MHz) and deep regional heating is achieved with RF (70-120 MHz) frequencies. Regardless of the heating mechanism, HT requires the use of RF/MW-insensitive temperature probes such as optical fibers or custom thermistors to monitor HT treatment.

Delivery of clinical HT is performed 1-3 times per week. As heat is applied, an increase in blood flow alters the heating dynamics, requiring precise control of the heat delivery. If temperatures reach levels above 44-45 °C, patients can experience pain or even thermal blistering, but continuous temperature monitoring, surface water cooling and patient feedback contribute to a high safety profile.

There are still several technical challenges to overcome toward optimal HT treatment delivery, including cumbersome applicators, limited thermometry, and simplistic treatment planning software. Despite these challenges, dozens of clinical trials strongly support the use of adjuvant HT since it significantly improves curative and palliative clinical outcomes. Recent technological advances will further improve treatment delivery and reduce its complexity, which are pivotal components for expanding the use of HT at medical and radiation oncology centers.

IT-09
Clinical magnetic hyperthermia – past and present

Quentin Pankhurst [1,2]*

[1]Healthcare Biomagnetics Laboratory, University College London, London; [2]Resonant Circuits Limited, London.

In its broadest sense, clinical magnetic hyperthermia – meaning thermal therapies based on the application of time-varying magnetic fields to the human body – has been practiced since the 1930s. For the first ca. 30 years, practitioners focused on the eddy-current heating of endogenous tissue, including the brain; but since the 1960s the field has focused on implant-mediated modalities, using exogenous materials such as particles or seeds. This is a more focused approach, with local hot spots being generated in and around the implanted materials when they are exposed to the time-varying magnetic field. The physical mechanisms for this heating depend on the material – they include eddy currents and hysteresis – but in all cases the key benefit of the approach is that the heat transfer is localized, so that potentially damaging peripheral or off-target tissue heating effects may be minimized or avoided.

In this contribution the speaker will provide a brief overview of the field of clinical magnetic hyperthermia, from its early days to the present. He will highlight some of the key challenges that practitioners in the field have faced

over the years, including the development of appropriate dose-response characteristics to enable reliable treatment planning and/or real-time thermal dose monitoring.

Oral presentations

OP-01

Fever-range hyperthermia restores sensitivity to anti-PDL1 therapy in pancreatic cancer by promoting mitotic catastrophe via deSUMOylation and cGAS-STING activation

G. Gong[1,2], N. Li[1,2,3], J. He[1], M. Chen[1,2,3], J. Yu[1,2,3], R. Wang[1,2]

[1]Affiliated Zhongshan Hospital of Dalian University, Department of Oncology, Dalian, China
[2]Affiliated Zhongshan Hospital of Dalian University, Laboratory for Brachtherapy and Hyperthermia Therapy, Dalian, China
[3]Affiliated Zhongshan Hospital of Dalian University, Hyperthermia Therapy Center, Dalian, China

Question: Immunological "cold" tumors such as pancreatic cancer remains a therapeutical challenge nowadays. They are notorious for the barren tumor microenvironment (TME) lacking dendritic cells (DCs) and cytotoxic T lymphocytes (CTLs) with little response to immunocheckpoint blockers. While early studies have suggested that hyperthermia therapy may regulate DCs infiltration and maturation, others observed increased mitotic errors in cells exposed to hyperthermia. This study questioned that whether and through which mechanism fever-range hyperthermia (FRH) may cause mitotic catastrophe, activate cGAS-STING-IFNβ signaling, attract DCs to TME, and synergize with immunotherapy.

Methods: Murine pancreatic cancer Pan02 were used to establish orthotopic tumors. Fever-range hyperthermia (FRH) was applied using a microwave physiotherapy device (41°C, 45mins, each other day, 5 times) +/- aPD-L1 therapy (10mg/kg, each 3 days, for 4 times) (BioXcell, clone.10F.9G2). In vitro hyperthermia experiments were carried out by heating various human and murine PDAC cells in a 41°C water-bath for one hour and cells were harvested 0-48 hour later. Tissues and cells were analyzed using routine histological and molecular techniques.

Results: FRH was shown to synergize with aPD-L1 therapy to reduce tumor burden in both heated side and abscopal side of Pan02 orthotopic tumors. Tissue analyses revealed that FRH significantly increased the infiltration (CD11c+) and maturation of DCs, as well as CCL5 and IFNβ expression. The combination therapy increased the infiltration (CD8α+) and activation (CD8α+GrzB+) of CTLs. No association was found with FoxP3+ T-reg cells, F4/80+ macrophages, Gr1+ neutrophils, CD11b+Ly6G+ MDSCs and HMGB1 expression. This synergistic effect was abolished by admistrating with STING antagonist Sn-011 (10mg/kg, i.p.). In vitro studies showed that cGAS-STING axis was activated by FRH. Mitotic catastrophe events, including micronucleated/macronucleated cells, chromosome lagging, multi-polar division, and cytoplasmic dsDNA was observed 0-48hrs after FRH. FRH was found to significantly decrease SUMO1 expression and nuclear protein sumoylation. SUMO1 overexpression was shown to counteract with mitotic catastrophe and cGAS-STING activation. The impact of FRH on human PDAC cells were also evaluated and the results revealed some (MIA-Paca2, HPAF-II) but not all (PANC-1, BxPC3) cells responded to FRH with STING activation. Additional factors such as genes involved in DDR and TP53/Wee1 checkpoints are under investigation.

Conclusion: Our results suggested that FRH may promote mitotic catastrophe, activate cGAS-STING-IFNβ axis and generate DC-mediated immunoactivating effect to synergize with aPD-L1 treatment. FRH could be a promising therapeutic companion with immunotherapy.

OP-02

Cell death kinetics after combined treatment of breast cancer cells with heat and radiation

S. Scheidegger[1], A. Sengedorj[2], S. Mingo Barba[1], U. S. Gaipl[2]

[1]Zurich University of Applied Sciences, ZHAW School of Engineering, Winterthur, Switzerland
[2]Universitätsklinikum Erlangen, Translational Radiobiology, Department of Radiation Oncology, Erlangen, Germany

Purpose: The presence of necrotic cells influences the anti-tumour and anti-host immune response. Slower cell death kinetics leading to more accumulation of primary and secondary necrotic cells potentially result in a stronger trigger for the immune system by the increased presence of necrosis-associated danger signals. The knowledge

about cell death kinetics can be used to evaluate the potential impact on the adaptive immune response after radiation therapy and hyperthermia.

Materials & Methods: Time-resolved cell necrosis - and apoptosis data (MDA-MB-231, as well as MCF-7 breast cancer cells) provided by Sengedorj et al. (Cancers 2022, 14, 2050) have been analysed regarding specifically the kinetic aspects for treatments with radiation only (2x5 Gy) or radiation and heat (HTRT). The time-resolved apoptotic and necrotic cell death data was generated by multi-color flow cytometry, using Annexin V/propidium-iodide staining. A kinetic cell necrosis model including the simulated application of 2x5 Gy was used to determine the kinetic model parameters. This model includes a pre-necrotic and a necrotic cell population. The resulting parameter values have been implemented in an artificial adaptive Immune-Tumour-Eco-System (aITES) model (Scheidegger et al., Alife 2023, The MIT Press Journals, in press) and the resulting dynamic scenarios have been evaluated.

Results: The analysis of the temporal cell death data exhibits comparable speeds for apoptosis - and necrosis development in the cell populations after the application of heat and radiation. For MDA-MB-231 cells and radiation only, the percentage of necrotic cells rises faster than for radiation and heat (independent of the order of application). The resulting fits of the radiation-only data by the mathematical necrosis model exhibit a faster kinetics compared to the fits using average HTRT data (Fig.1). Compared to Scheidegger et al. (2023), the slower kinetics derived by the cell necrosis data fit leads to an extended presence and subsequent higher accumulation of necrotic cells resulting in a higher danger signal level in the aITES model simulations. In consequence, an unrealistic strong anti-host immune response can be observed in silico. By adopting the danger signal activation level, the anti-host immune response can be reduced, but this is associated with faster tumour recurrence. As a preliminary result, the slower necrosis process and the higher accumulation of necrotic cells for HTRT lead to a stronger immune response in the model.

Discussion and Conclusions: The data analysis supports the hypothesis that hyperthermia protracts the necrotic cell death process. However, due to the lack of data for time points > 6 days, the evidence for this is still weak. In addition, this effect is not visible for the apoptotic cells. This analysis improved the estimation of the cell necrosis kinetics, but time-resolved data covering a longer period should be included in the future.

Fig. 1

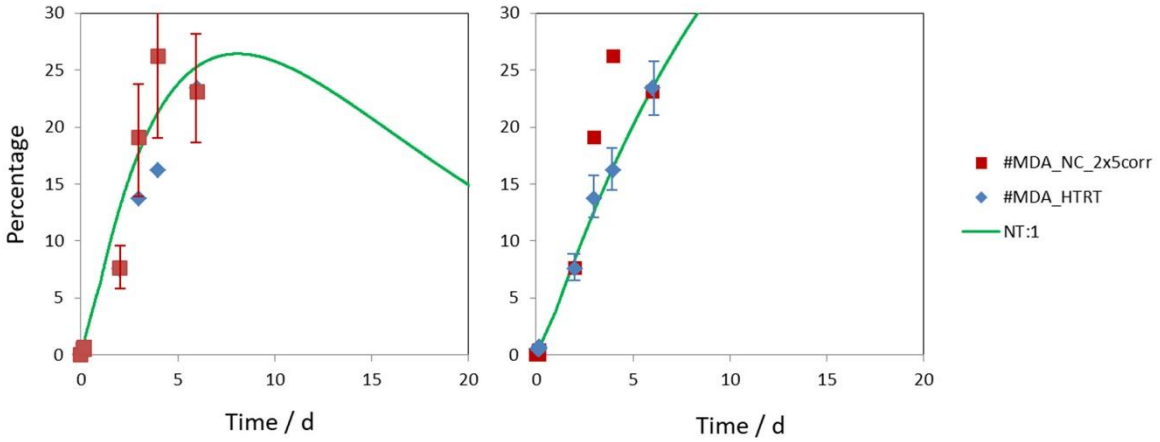

Fig.1. Resulting percentage of necrotic MDA-MB-231 cells *NT* (green line) by fitting the kinetic necrosis model data: (a) radiation-only (RT 2x5 Gy on day 0 and day 1, red squares) k_{pnecr} = 0.097 d^{-1}, k_{necr} = 0.163 d^{-1}, (b) model fit to average percentage after treatment with heat and radiation (blue diamonds;, hyperthermia prior or after radiation at different temperature rangig from 39-44°C) data, k_{pnecr} = 0.053 d^{-1}, k_{necr} = 0.026 d^{-1}.

OP-03

Hyperthermia-mediated immunogenic changes increase susceptibility of colorectal cancer metastases to immunotherapy

M. Tasker[1], R. Uzana[1], G. Lahat[1], E. Nizri[1]

[1]Tel-Aviv Sourasky Medical Center, Surgery B, Tel-Aviv, Israel

Question: Peritoneal metastases (PM) of colorectal cancer (CRC) are currently treated by cytoreductive surgery (CRS) and heated intra-peritoneal chemotherapy (HIPEC). However, tumor recurrence is common even after complete macroscopic resection, and the efficacy of current HIPEC regimens is debated. In previous experiments, we demonstrated that HIPEC induced immunogenic changes that increased tumor cells' susceptibility to immunotherapy. This study aims to investigate whether hyperthermia alone can achieve similar effects.

Methods: PM-CRC was induced in C57BL mice via intraperitoneal injection of 1x10^6 MC38 cells. After 7 days and establishment of PM, mice were treated according to the following groups: sham, HIPEC (with mitomycin C at a human equivalent dose of 0.01 mg/ml), HIPEC + anti-PD-1 (a-PD-1), Hyperthermia (Hyp), and Hyp + a-PD-1. Mice were monitored for overall survival (OS) and weight. Tumor tissue was collected at various time points post-treatment to analyze immune cell infiltration using FACS. In vitro studies on MC38 cells assessed the effects of Hyp and HIPEC on immunogenicity markers, specifically danger-associated molecular patterns (DAMPs) such as calreticulin, HSP70, HSP90, HMGB-1, and PDL-1.

Results: HIPEC treatment increased animal survival compared to sham (median OS: 25 vs. 18 days, 95% CI: 2.3-33.7 days). The combination of HIPEC and a-PD-1 further improved OS (29 days, 95% CI: 28.12-29.9), with Hyp + a-PD-1 showing the best outcomes (31 days, 95% CI: 27.1-34.9, p<0.001). HIPEC treatment resulted in increased CD8+ activity within metastases compared to sham (CD8+Ki-67+ positivity: 35% vs. 22%). Hyperthermia alone significantly increased the expression of calreticulin and HSP70 on MC38 cells (1.56 ± 0.02 vs. 1; 2.61 ± 0.65 vs. 1.2, respectively, $p < 0.05$), while HIPEC was more efficient in up-regulating HSP90 (2.37 ± 1.5 vs. 1.3 ± 0.2, $p < 0.05$). Ongoing experiments in our laboratory are evaluating protein expression of DAMPs and co-culture experiments of CD8+ T-cells and tumor cells to identify the specific signals mediating hyperthermia's anti-tumor effects.

Conclusions: Hyperthermia, without chemotherapy, induces immunogenic changes in tumor cells, enhancing the efficacy of immunotherapy for treating PM-CRC in experimental models. These in vivo and in vitro findings suggest that hyperthermia is more effective than HIPEC in augmenting tumor immunogenicity signals. This study could lead to novel applications of combined hyperthermia and immunotherapy for PM-CRC treatment.

Fig. 1. Overall survival of mice treated by sham, HIPEC (based on MMC), HIPEC+a-PD-1, Hyp, and Hyp+a-PD-1 (n=6 for each group, shown is one representative experiment out of 2).

Fig. 2. Expression of immunogenic cell death (ICD) signals by MC38 tumor cells upon exposure to hyperthermia and mitomycin C (MMC). mRNA expression of various ICD-related proteins was determined 24 hours after exposure to the conditions detailed above. The results are the summary of 3 different experiments performed on triplicates.*$p < 0.05$.

Fig. 1

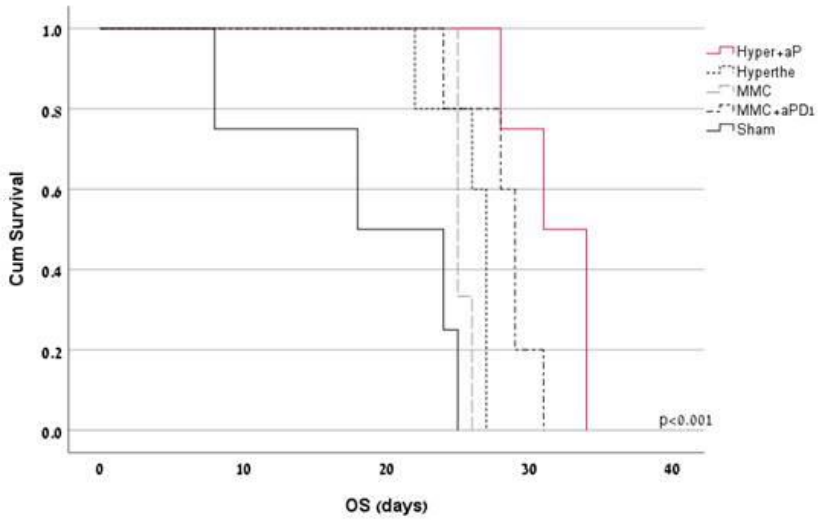

Fig. 2

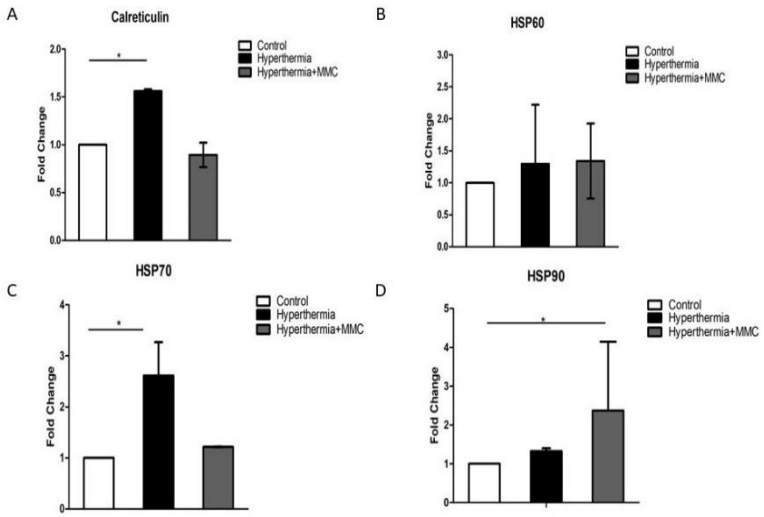

OP-04

Effect of photothermal therapy with gold nanoparticles conjugated with long chains of hyaluronic acid in an intracranial murine glioblastoma model

J. Domingo Díez[1], A. Foti[2], C. Satriano[2], L. Marrodán Bretón[1], Ó. Casanova Carvajal[1], R. Martínez Murillo[3], J. J. Serrano Olmedo[1], M. Ramos Gómez[1]

[1]Universidad Politecnica de Madrid, Centro de tecnología biomedica, Pozuelo de Alarcon, Spain
[2]University of Catania, Department of Chemical Sciences, Catania, Italy
[3]Instituto Cajal, CSIC, Department of Translational Neuroscience, Madrid, Spain

Purpose: This study aims to evaluate the efficacy of nanoparticle-mediated photothermal therapy (PTT) for treating Glioblastoma multiforme (GBM). We use gold nanorods (GNRs) conjugated with high molecular weight HA (HA-700kDa-GNRs) in a murine glioblastoma model due to its anticancer properties and affinity with CD44 marker presented in glioblastoma cancer cells.

Methods: C57/BL-6 adult male mice (N=15), 3-8 months old, were used for PTT experiments. The CT2A tumour model was established in mice as described previously. Briefly, CT2A cancer cells (8x104 cells/4 µL in PBS) were stereotactically injected into the mouse brain under isoflurane anaesthesia. Mice were randomly divided into three groups: control (tumour only, n=5), GNRs tumour + GNRs, n=5) and PTT treated (tumour + GNRs + laser, n=5). 4 µL of the high MW GNRs (HA-700kDa-GNRs) diluted 1:100 were injected gradually at a rate of 1 µL per minute into the GNRs and PTT-treated groups. After GNR injection, mice were laser irradiated at 0.98A (450mW) for 25 minutes for 3 consecutive days, with the laser placed over the hole in the skull where the cells and GNRs were injected.

Results: As observed in the analysis of tumour sizes obtained from all MR images, one week after PTT treatments (Figure 1), animals treated with laser following GNRs injection had a significantly smaller tumour size compared to control animals. PTT-treated animals also showed a smaller tumour size compared to animals treated with GNRs alone (Figure 1A).

Significant differences in tumour size between the PTT-treated and control groups were also observed in the second week after PTT treatment. Although tumours continued to grow in some PTT-treated mice due to the presence of residual cancer cells that were not removed by PTT therapy, the tumour size of PTT-treated mice was significantly smaller than that of control mice. In addition, PTT treatment significantly increased the life expectancy of treated mice compared to control mice (Figure 1C).

Conclusions: This study demonstrates the utility of PTT applied directly to the brain to target a glioma tumour mass into which the nanoparticles had previously been injected. This original work demonstrates the efficacy of PTT using long chains of HA attached to GNRs to target the CT2A tumour in mice, demonstrating non-cytotoxicity, partial reduction of tumour mass and prolongation of life in mice treated with PTT. HA-GNRs can target tumour cells by exploiting the anti-inflammatory and anti-cancer properties of the long chains of HA.

Figure 1: Volume of tumor mass analyzed in the three mice groups: control, 700kDa-HA-GNRs and PTT one week (A) and two weeks after treatment (B). Kaplan Meier survived curve shows the evolution of the survival mice population in every group along the time (C). Individualized images of RM one week after treatment of control (D) and treated mice one week after PTT was applied. Scale bar: 4mm. *p<0,05.

Fig. 1

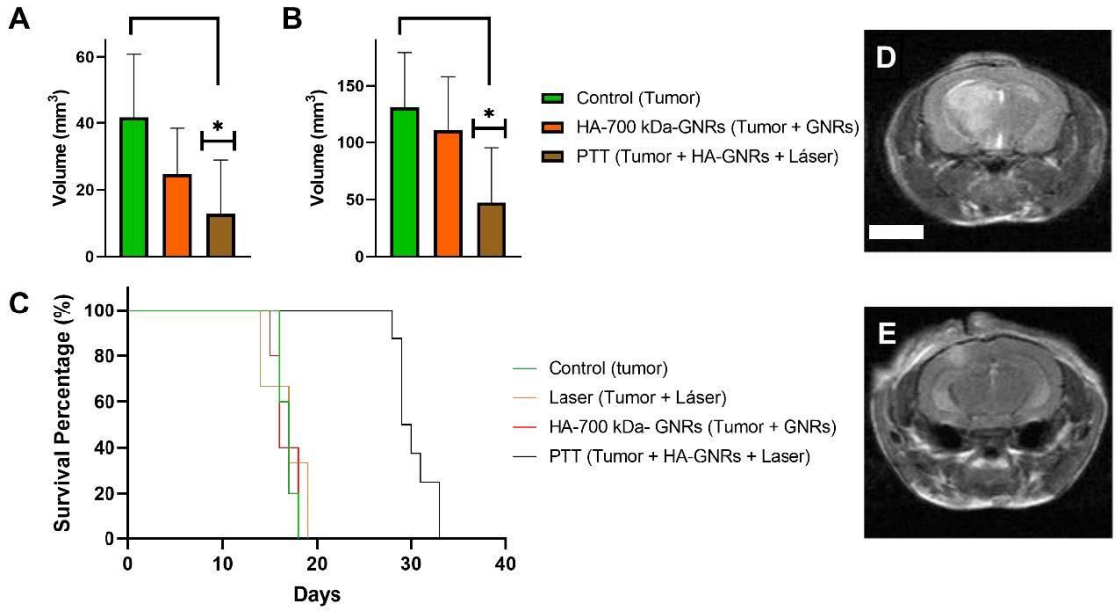

OP-05

Uncomplicated tumor control probability of hyperthermia plus radiotherapy treatments based on murine *in-vivo* data

S. Mingo Barba[1,2,3], P. M. Sinha[4], C. A. Folefac[4], M. R. Horsman[4], M. Lattuada[2], R. M. Füchslin[1,5], A. Petri-Fink[2,3], S. Scheidegger[1]

[1]Zurich University of Applied Sciences, School of Engineering, Winterthur, Switzerland
[2]University of Fribourg, Chemistry Deparment, Fribourg, Switzerland
[3]University of Fribourg, Adolphe Merkle Institute, Fribourg, Switzerland
[4]Aarhus University Hospital, Experimental Clinical Oncology-Department, Aarhus, Denmark
[5]European Centre for Living Technology, Venice, Italy

Purpose: Several authors have employed in-silico models to optimize the efficacy of radiotherapy (RT) combined with hyperthermia (HT). However, these optimizations often overlooked the increased normal tissue reactions induced by HT.

Methods: Tumor control (C3H mammary carcinoma) and acute skin reaction data from CDF1 mice under various HT+RT treatment regimens were analyzed. An extended Linear Quadratic (LQ) model was calibrated using these in-vivo data. These calibrations were used to perform Tumor Control Probability (TCP) and Normal Tissue Complication Probability (NTCP) calculations for different HT-related treatment conditions (number of HT sessions, temperatures, and time intervals between HT and RT). Conventional fractionation (31 x 2 Gy; 5 fractions/week) and hypofractionation (12 x 5.2 Gy; 2 fractions/week) RT schedules based on breast cancer treatment were assumed. Additionally, scenarios with three to six HT sessions with identical temperatures and time intervals, were considered. To mimic superficial HT+RT conditions, the same temperature and RT dose were considered both in the tumor and the skin. The optimal HT treatment conditions were determined by calculating the Uncomplicated Tumor Control Probability (UTCP=(1-NTCP)·TCP), for instance, the probability of controlling the tumor without inducing side effects.

Results: The extended LQ model accurately covered the in-vivo data. Under the studied conditions, the baseline TCP / NTCP (RT only) was 30% / 0% and 36% / 0% for the conventional and hypofractionated schedules, respectively. Additionally, TCP was not significantly affected by the time interval between HT and RT, whereas the NTCP was. Consequently, the time interval dependence of UTCP is primarily determined by the NTCP.

Figure 1A shows that, for conventional fractionation, the time interval between HT and RT was not critical since HT did not significantly increase NTCP. In contrast, Figure 1B indicates a strong time interval dependence for the hypofractionated schedule at high temperatures, where HT significantly increased NTCP. Moreover, increasing the number of HT sessions slightly increased the maximum UTCP achieved (77%, 85%, 91%, and 94% for three, four, five, and six HT sessions, respectively, in the conventional fractionation schedule).

Conclusion: For superficial HT, where normal tissue and tumor temperatures are comparable, high temperatures (approximately 43°C) and a short time interval between HT and RT (less than an hour) can significantly increase treatment side effects. However, the optimal HT treatment conditions strongly depend on the HT+RT schedule. But these results are based on the calibration of a model that does not fully incorporate repair dynamics, which could potentially alter the outcomes. In conclusion, in-silico models can help optimize HT+RT treatments to maximize tumor control while maintaining normal tissue reactions within acceptable limits, tailored to each patient.

Fig. 1

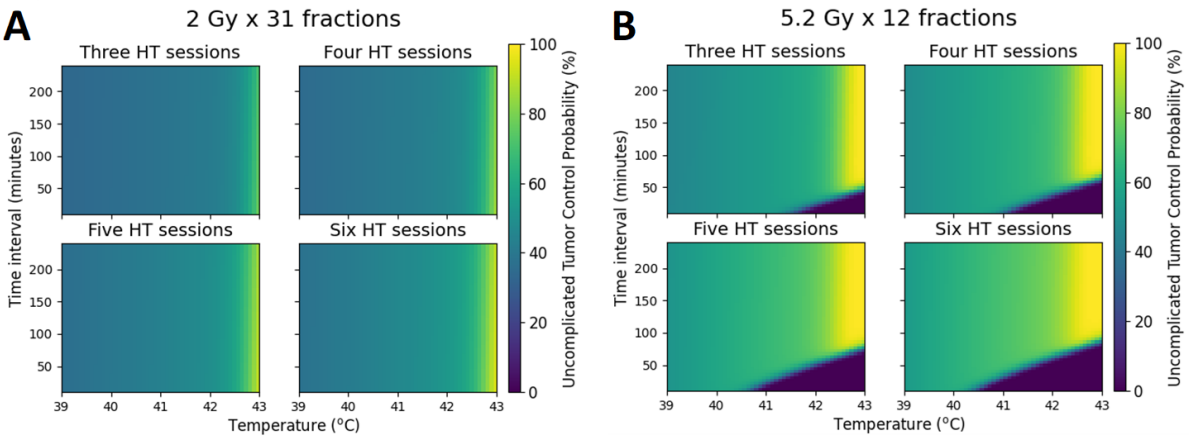

Figure 1: Uncomplicated Tumor Control Probability (UTCP) for various HT+RT treatment conditions. **(A)** An RT schedule of 31 fractions of 2 Gy (5 fractions per week) was assumed. Each subfigure considers different temperatures and time intervals between RT and HT for a specific number of HT sessions. **(B)** An RT schedule of 12 fractions of 5.2 Gy (2 fractions per week) was assumed. Each subfigure considers different temperatures and time intervals between RT and HT for a specific number of HT sessions.

OP-06

Benefit in local control for patients with oligoprogressive melanoma treated with radiotherapy combined with locoregional hyperthermia

A. Borkowska[1], M. Spalek[1,2], P. Chmiel[1], M. Telejko[1], P. Teterycz[1], P. Rutkowski[1]

[1]Maria Sklodowska-Curie National Research Institute, Department of Soft Tissue/Bone Sarcoma and Melanoma, Warszawa, Poland
[2]Maria Sklodowska-Curie National Research Institute, Department of Radiotherapy I, Warsszawa, Poland

Question: Is there a benefit in local control for patients with oligoprogressive melanoma treated with radiotherapy combined with locoregional hyperthermia?

Methods: The study included patients with oligoprogressive metastatic melanoma (MM) who were treated with radiotherapy (RTH) combined with hyperthermia (HT) at a melanoma center between 2019 and 2023. Oligoprogression was defined as up to 5 progressive metastases. Inclusion criteria was the availability of dimensions of the lesion subjected to RTH before and after treatment, patients without follow-up imaging after radiotherapy were excluded. The cut-off date was 01/10/2023. The benefit of RTH+HT was evaluated in terms of local control (LC) rates and, secondary, local benefit (LB) rates. Local control (LC) was defined as the percentage of patients who met the RECIST1.1 criteria for stable disease (SD), partial response (PR), and complete response (CR). Local benefit (LB) was defined as the proportion of patients who met the PR and CR criteria. Furthermore, overall survival (OS) rates were estimated. The association between BRAF status, age, concomitant systemic treatment, radiation dose, and LC was estimated. Additionally, data regarding adverse effects associated with RTH+HT were compiled. Survival analyses were performed using the Kaplan-Meier estimator and log-rank tests and were used to compare between groups. Hyperthermia was administered using Celsius and BSD200 equipment.

Results: 102 patients were included in the study, median follow-up was 15.3 months (14-18 months). There were 56.9% BRAF(-) and 43.1% BRAF(+) patients. Most patients (70.6%) were irradiated during immunotherapy, 10.8% received concomitant BRAF and MEK inhibitors and 3.9% had chemotherapy. LC and LB medians were not reached at the time of analysis. The 1- and 2-year LC rates were 93.5% (95% CI: 88.1-99.3%) and 88.3% (95% CI: 79.9-97.6%), respectively. The 1- and 2-year LB rates were 87.5% (95% CI: 80.5-95.2%) and 78.1% (95% CI: 67.9-89.9%), respectively. The mean reduction in tumor size across the entire cohort was 72%. The median total dose

administered to patients was 30 Gy, 11 patients received doses lower than the median, and no significant difference was observed in the impact on LC with doses below the median (p = 0.3). The mOS from radiotherapy was not achieved at the time of our analysis, accordingly 1- and 2-year OS rates were 100% and 95% (95% CI: 90.4-99.9%). Other evaluated factors did not influence LC among patients. There were no severe toxicities of radiotherapy or hyperthermia.

Conclusions: Hyperthermia with radiotherapy is an effective treatment for patients with oligoprogressive melanoma. This approach has resulted in excellent local control with minimal toxicity.

Figure 1 Spider plot on the change in tumor relative to the initial measurement among patients. Figure 2 The response to radiotherapy with hyperthermia in computed tomography.

Fig. 1

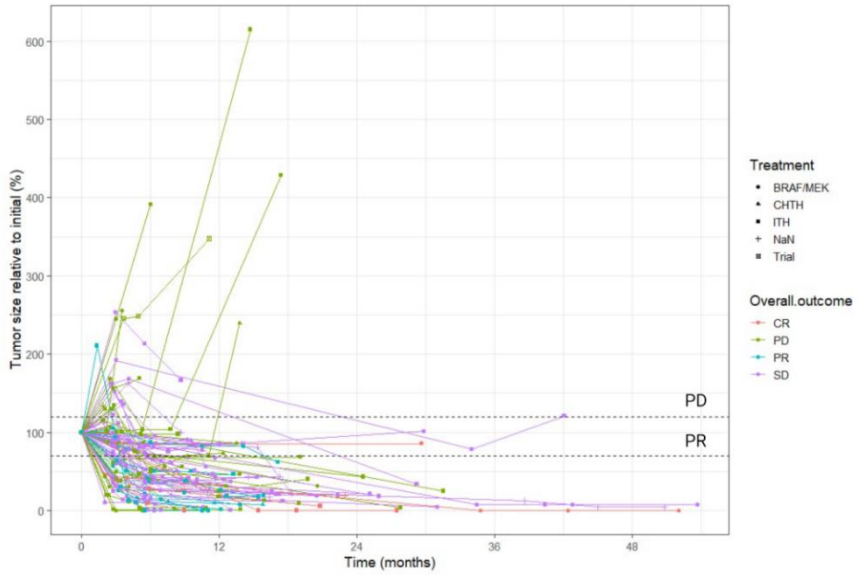

Fig. 2

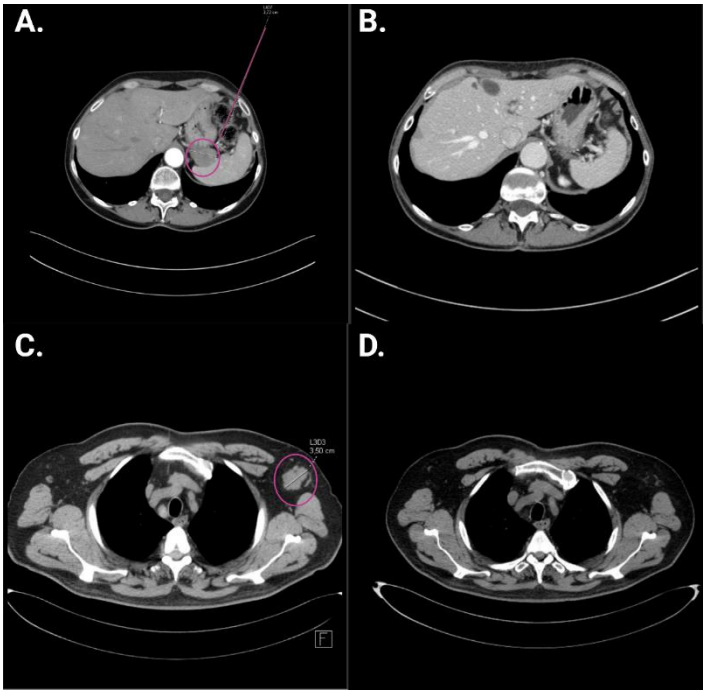

OP-07

Modulated Electrohyperthermia (MEHT, Oncothermia) as an effective and safe additional radiosensitizer for standard chemoradiation in Locally Advanced Cervical Cancer (LACC) IIb-IVa FIGO patients

Y. Kreynina[1,2], M. Kaskulova[2], V. Solodky[1], L. Shevchenko[1], Y. Mashkova[1], S. Isaeva[3]

[1]Federal State Budgetary Institution "Russian Scientific Center of Roentgenoradiology" of the Ministry of Healthcare of the Russian Federation (RSCRR), Moscow, Russian Federation
[2]Federal State Budgetary Institution "Volga Region Research Medical University", Ministry of Health of the Russian Federation, Nizhny Novgorod, Russian Federation
[3]I.M. Sechenov First Moscow State Medical University (Sechenov University), Moscow, Russian Federation

Question*:* To evaluate the medical feasibility, efficacy and safety of incorporating mEHT (oncothermia) into standard programs of chemoradiation in LACC IIb-IVa FIGO patients with massive parametrial invasion.

Methods*:* A retrospective-prospective study (2015-2019) included 133 LACC IIb-IVa FIGO patients with massive pelvic tissues involvement, eligible for standard platinum-based chemoradiation (CRT) – conformal external beam radiation therapy (EBRT) 45-50 Gy to the pelvis (1,8-2 Gy in 25-28 fractions), with weekly Cisplatin 40 mg/m2 or Carboplatin AUC2, followed by image-guided 192Ir HDR brachytherapy – who were randomly assigned to receive either CRT alone (Control Arm II, 65 pts.) or combined with mEHT sessions EHY-2000, 60-90 min, 110-130 W, 3 times a week, during EBRT, 9-14 sessions per course (Research Arm I, 68 pts). Clinical aspects, short- and long-term oncological outcomes, treatment toxicity data were compared in two groups. Molecular analysis of some key tumor apoptosis and cell proliferation markers was performed in 30 randomly selected LACC pts. from each arm to assess the influence of mEHT on immediate tumor response during CRT.

Results*:* 57 (83,8%) pts. in the research arm didn"t report any adverse events (AE), potentially associated with mEHT. Among the 35 AEs in 11 pts., no serious AEs were observed, and additional medications were mostly unnecessary. Objective response at the beginning of brachytherapy was significantly better in Research Arm I compared with control Arm II: complete tumor response in 5 (23,8%) vs 1 (3,8%) for IIb and 7 (15,9%) vs 1 (2,9%) for IIIa-c pts.: partial subtotal response ≥80% in 10 (47,6%) vs 3 (11,5%) for IIb and in 21 (47,7%) vs 4 (11,7%) for IIIa-c pts, p≤0,05. Optimal HR-CTV ≤ 30 cm3 at the beginning of brachytherapy was achieved in 38 (55,9%) vs 9 (13,8%) pts, p<0,001, complete resorption of parametrial infiltration – in 44 (64,7%) vs 9 (13,8%) (p<0,001) in arms I and II respectively. In 168 cervical cancer tissue samples, a significant decrease in apoptosis (BCL2, BAG1), proliferation (HER2, MYBL2, ESR1, P16INK4a) and tissue interaction (membrane protease MMP11) genes was noted. Differences in HER2neu, MYBL2, and P16INK4A expression between arms were significant already at TD 30Gy of effective EBRT, which may have predictive value.

Median follow up 46 mnth. Long-term results were significantly improved in Arm 1 vs Arm 2: DFS 80,7% ± 5,0% vs 64,8% ± 6.1% (p=0,041) for 36 mnths, 72,1% ± 6,7% vs. 58,3% ± 6,4% (p=0.047) for 60 mnths., LC 92.7% ± 8.7 versus 78.5% ± 9.4 (p = 0.048), no isolated local central relapses for 60 months in arms I vs II respectively. There were no significant differences in early or late toxicity rates and no differences in the type, frequency or severity of complications between arms during follow-up.

Conclusion: Incorporation of mEHT to standard CRT is an effective and safe way to improve treatment outcomes in LACC IIb-IVa FIGO patients with massive parametrial invasion.

OP-08

Optimising protocols for the use of modulated electro hyperthermia as a radiosensitiser

C. Minnaar[1,2], K. Dada[2]

[1]Wits Donald Gordon Medical Centre, Radiation Oncology, Johannesburg, South Africa
[2]University of the Witwatersrand, Radiobiology, Johannesburg, South Africa

Background: The optimal timing and temperature parameters for oncologic hyperthermia (HT) remain subjects of debate. In cervical cancer, HT is often administered post-radiotherapy (RT), with evidence suggesting that shorter intervals (2 hours or less) between treatments yield better outcomes. However, modulated electro-hyperthermia (mEHT), which uses modulated 13.56MHz radiofrequency waves to mildly increase tumour temperature, has also

been successfully applied pre-irradiation. This report aims to elucidate the radiodensitising effects of timing and temperature, focusing specifically on mEHT.

Methods: We present a comprehensive literature review and propose studies designed to test key hypotheses regarding the radiodensitising mechanisms of mEHT.

Results: Radiodensitising mechanisms at lower temperatures (39°C - 40°C), involve vasodilation, which increases tumour perfusion and oxygenation. When administered before RT, this boosts the Reactive Oxygen Species formed during irradiation, increasing tumour damage. Elevated oxygen levels can persist for up to two days, suggesting that flexible intervals between HT and radiation (RT) are feasible when HT is administered prior to RT. Additionally, an increase in the oxygen perfusion post-irradiation can slow DNA double-strand break (DSB) repair, which functions optimally in an anoxic environment and occurs up to 2 hours post irradiation. This latter effect may also be present when HT is applied within 2 hours post-irradiation. Mild hyperthermia independently affects enzyme activity, protein stability, cellular metabolism, membrane fluidity, and protein-protein interactions and this may account in part for the improved outcomes seen in patients treated with hyperthermia >2 hours post-irradiation. Higher temperatures (>43°C) induce vasoconstriction, counteracting radiodensitising effects by reducing tumour oxygenation. However, these temperatures cause protein denaturation and necrosis. Improved outcomes when HT is administered more than 2 hours post-irradiation may therefore be due to heat effects alone rather than HT-RT synergy, when HT achieves >43°C.

Conclusion: mEHT likely enhances radiosensitivity by increasing RT-induced damage, inhibiting DNA repair, and disrupting cellular metabolic and enzymatic processes. The developed protocols aim to test the effects of mild heat generated by mEHT alone versus mild heat combined with the electromagnetic field effect of mEHT. The studies include *in vitro* (spheroid cultures) and *in vivo* (murine) experiments. The models will be treated with mEHT and water bath heating combined with RT at various time intervals and temperature combinations. Key measurements will include DNA DSBs, repair of DSBs, and oxygen perfusion. The outcomes of these studies are anticipated to help standardise protocols that combine mEHT with radiation, thereby improving patient outcomes for cervical cancer and potentially other tumours.

OP-09
Radiosurgery reirradiation of high grade glioma in combination with modulated electro-hyperthermia: Preliminary results of a prospective study

E. Arrojo[1,2], M. Sallabanda[3], D. Arribas[1], Y. Hayde[1], M. C. Vaca[1], K. Sallabanda[3]

[1]Medical Institute of advanced oncology (INMOA), Madrid, Spain
[2]University Hospital Marques of Valdecilla, Santander, Spain
[3]IRCA, Madrid, Spain

Question: To analyze the potential benefits regarding tumor control and possible side effects of reirradiation with radiosurgery (RS) in combination with modulated electro-hyperthermia (mEHT) as radiosensitizer.

Methods: Data from 8 patients treated for 14 lesions with RS and mEHT between April and November 2023 were prospectively included in a database. Clinical, treatment and post-treatment data were analyzed with main focus on time from previous radiation, lesions volume, number of fractions and total radiotherapy dose, number and power of hyperthermia treatments, treatment delivery characteristics, local control and acute and subacute tolerance.

Results: Eight patients (5 females and 3 males) with a median age of 48 years (range 30-62 years) and a median of 2 lesions (range 1-3) underwent RS and mEHT during the study period. All patients had received standard Stupp protocol and 3 patients had a previous second course of radiation. The median time from previous radiotherapy was 11 months (range 21 – 6 months). A margin up to 1 mm was applied to the GTV. The median (2.8cm3), minimum (0.2cm3), and maximum PTV volume (51cm3) were registered. 57% (n = 8) of the lesions were treated in 1 fraction, 29% (n = 4) in 5 fractions and 14% (n = 2) in 3 fractions. Median dose in 1 fraction was 15 Gy (range 15 - 18 Gy). Lesions treated in 5 fractions received 25 Gy or 30 Gy and lesions treated in 3 fractions received 24 Gy. Median coverage of the prescribed dose was 95% (range 95%–98.4%). Median number of placed isocentres per lesion was 7 (range 1-16). Three to six mEHT sessions were administered during and after RS in alternating

days. Each mEHT had 60 minutes length. Power treatment from mEHT was between 45 and 100W wih most of the time at 80W. Time between RS and mEHT was ≤ 2 hours. Median clinical follow-up was 4 months (range 1-8 months). 1 patient died of multicentric spread 5 months after treatment, 2 patients received a second RS treatment for new lesions. One patient experienced a subependymal spread and started systemic therapy. Actuarial overall survival at 6 months was 67%. One patient, with a very aggressive tumor and a very low treatment-free survival experienced in field recurrence 3 months after RS with worsening of neurological symptoms. Acute and subacute treatment tolerance was acceptable, all patients needed ambulatory steroid medication adjustment. No specific toxicities from mEHT were found.

Conclusion: High grade glioma reirradiation with RS in combination with mEHT showed a favourable impact in local control and overall survival with low toxicity. Longer follow-up and larger series are needed to validate these results.

OP-10
Optimal operating frequencies for deep microwave hyperthermia: Are we missing the sweet spot?

I. Sykkö[1], A. Nguyen[1], R. Nilsson[1], M. Zanoli[1,2], K. Blomgren[1], H. Dobšíček Trefná[1]

[1]Chalmers University of Technology, Biomedical Electromagnetics, Gothenburg, Sweden
[2]Erasmus University Medical Center Rotterdam, Rotterdam, Netherlands

Historically, deep hyperthermia systems utilize frequencies between 70-110 MHz when targeting the pelvic region and frequencies above 400 MHz when aiming to heat delicate areas such as the head and neck [1]. This study investigated the optimal combination of frequencies in an ultra-wideband (UWB) system operating between 250-800 MHz, using intracranial targets of varying sizes, shapes, locations, and tissue properties, as well as different antenna arrangements.

Specific absorption rate (SAR) based treatment planning and thermal simulations were performed in COMSOL using pediatric models. The temperature exceeding 90% of the maximal temperature in the target volume, T90, was evaluated at frequencies between 250-800 MHz. First, a scenario with an 11-year-old female and a 12-channel array was considered for targeting craniopharyngioma (22 ml), diffuse midline glioma (DMG) (31 ml), ependymoma (49 ml), meningioma (55 ml), and a skull base tumor (12 ml). The heating was evaluated by using different tissue properties in the target: healthy, average, and tumor [2, 3]. Then, two different antenna arrangements within the applicator, a symmetric and an optimized 10-channel array, were investigated using a 13-year-old male with medulloblastoma (126 ml; tumor [2]). Finally, a simplified scenario was considered using healthy tissue (13-year-old male; 12-channel array), where target volume and location were incrementally changed; from small (7 ml) to large (45 ml), and from superficial to deep-seated. To alleviate target size dependency, the distance between the edge of the target and the skull was kept constant for each location.

The highest T90 was achieved for ependymoma and meningioma, ranging between 39-42 °C depending on target properties. Deep-seated targets around the skull base and brain stem reached lower T90 (37.5-39.5 °C). Surprisingly, the optimal operating frequencies were at the lower end of the tested range, regardless of target characteristics or antenna array. The optimal frequency was 250-275 MHz for medulloblastoma and the simplified scenario, 275 MHz for meningioma, 300 MHz for DMG and skull base tumor, and 250+350 MHz for craniopharyngioma and ependymoma.

This study affirms the feasibility of intracranial heating for a wide variety of cranial tumors. High variability in achieved T90 for different target tissue properties highlights the need for standardized parameters. Most importantly, it identifies that optimal frequencies lie at a lower band than expected from previous studies. Since the frequencies in the range of 350 MHz have seldom been investigated for regions of similar dimensions, such as the head and neck, these studies shall be revisited.

[1] Paulides, MM. et al., *Adv Drug Deliv Rev*, 163–164, 3 (2020)

[2] Paulides, MM. et al., *Int J Hyperthermia*, 38(1), 1425 (2021)

[3] Schooneveldt, G. et al., *Int J Hyperthermia*, 11(8), 1183; (2019)

OP-11

Integrating MR coils with heating antennas for hyperthermia of the intact breast: A simulation study

A. de Boer[1], I. Androulakis[1], M. Zanoli[1], K. Sumser[2], R. Forner[3], R. Nout[1], M. Paulides[1,2], S. Curto[1]

[1]Erasmus University Medical Center Rotterdam, Radiotherapy, Rotterdam, Netherlands
[2]Eindhoven University of Technology, Electrical Engineering, Eindhoven, Netherlands
[3]Hamburg University of Technology, Institute of Process Imaging, Hamburg, Germany

Introduction: The CARES consortium aims to revolutionize breast cancer treatment by developing a personalized magnetic resonance (MR)-guided local thermo-chemotherapy, striving for efficacy while minimizing toxicity. The overarching goal is to enhance the therapeutic window of neoadjuvant chemotherapy to ultimately enable breast conservative surgery.

This research focuses on the development of a novel thermotherapy device, with integrated coils for high SNR imaging and thermometry measurements of the intact breast at 1.5T. Hereto, an initial simulation study was set up investigating the imaging and heating performance of the thermotherapy heating antennas when integrated with MR coils.

Methods: Two different MR coil elements are investigated, a flat square coil and a square coil, both with sides of 9.5cm, the latter of which has been curved around the cylindrical waterbolus. Figure 1a and 1b show the simulation setups combining each coil type together with the heating antennas and a simplified cylindrical breast phantom. These elements are simulated using Sim4Life electromagnetic solver (ZMT, Zurich, Switzerland) and tuned to their respective resonance frequency using a co-simulation pipeline. Afterwards the B_1^- of the tuned coils (64 MHz), and the electric (E) field and specific absorption rate averaged over 1g (SAR_{1g}) distribution of the heating antennas (434 MHz), were investigated for the entire phantom as well as for a centrally located volume of interest (VOI) (2x2x2cm).

Results: Figure 1c and 1d show a near identical performance in average B_1^- field in the VOI with the flat and curved MR coils when simulated on their own. When simulating the heating antennas with the coils the difference in B_1^- is again minimal, however the average SAR_{1g} in the VOI decreases by over 95% for the setup with the curved coil in comparison with the other configuration, as seen in figure 2.

Discussion & Conclusion: The lower reduction in SAR_{1g} performance by the flat coils over the curved coils indicates that the former is the more suitable coil type for integrated use with the heating antennas for the breast applicator. However, these investigated setups are simplified models of reality, and more research will be done to optimize this design for effective clinical use, including simulations with realistic breast models [1] and an increased number of elements.

References:

[1] Androulakis, I (2022). Int J of Hyp, 39(1)

Fig. 1

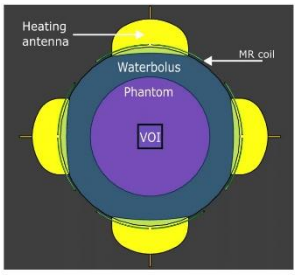

(a) Simulation setup combining 4 curved MR coils and 4 heating antennas around a 10 cm ⌀ cylindrical phantom surrounded by a 2.5 cm thick waterbolus.

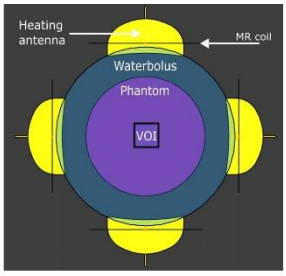

(b) Simulation setup combining 4 flat MR coils and 4 heating antennas around a 10 cm ⌀ cylindrical phantom surrounded by a 2.5 cm thick waterbolus.

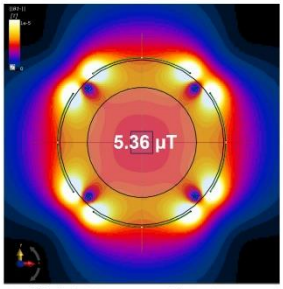

(c) $|B_1^-|$ field pattern of just the curved MR coils.

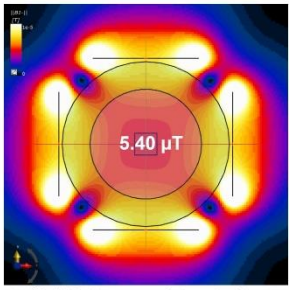

(d) $|B_1^-|$ field pattern of just the flat MR coils.

Fig. 1: Figures denoting the components of the simulation setups and the resulting $|B_1^-|$ field pattern of the two different coil array types in the xy-plane. Note that the individual components are pictured in each figure as well as the average value in the VOI.

Fig. 2

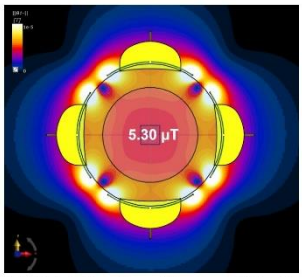

(a) $|B_1^-|$ field pattern of 4 curved MR coils combined with 4 heating antennas.

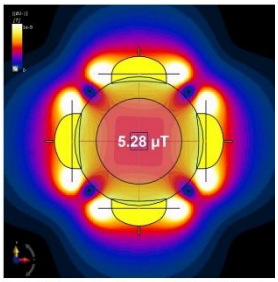

(b) $|B_1^-|$ field pattern of 4 flat MR coils combined with 4 heating antennas.

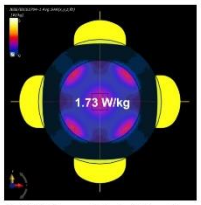

(c) SAR_{1g} of just 4 heating antennas.

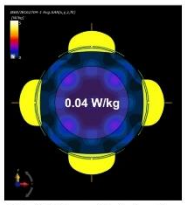

(d) SAR_{1g} of 4 heating antennas combined with 4 curved MR coils.

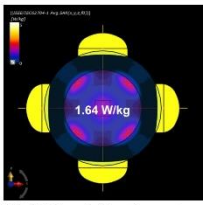

(e) SAR_{1g} of 4 heating antennas combined with 4 flat MR coils.

Fig. 2: Figures denoting the $|B_1^-|$ and SAR_{1g} distributions for the different setups in the xy-plane. Note that the individual components are pictured in each figure as well as the average value in the VOI.

OP-12
Effect of power delivery algorithms on microwave ablation zone extents: Results from computational modeling and experiments

P. Prakash[1]

[1]Kansas State University, Electrical and Computer Engineering, Manhattan, NY, United States

Question: With increasing interest in combination therapies involving thermal ablation that harness the hyperthermic temperatures at the ablation zone periphery, there is considerable interest in understanding how applied energy levels during microwave ablation influence the extents of the ablation and peri-ablational zones. The objective of the present study was to develop and experimentally evaluate the performance of a computational model of microwave ablation under varying power delivery schemes.

Methods: A coupled electromagnetic-bioheat transfer model was implemented to simulate 2.45 GHz microwave ablation. Models were implemented considering both ex vivo and in vivo conditions, and incorporated temperature-dependent thermal and dielectric properties. The model was employed to simulate the following conditions: (Phase 1) constant power ablation with 50, 75, or 100 W applied power for 5 – 10 mins; and (Phase 2) high power (65 W constant power for 10 min); ramped (step-wise increment from 25 – 65 W, followed by 65 W constant power for 8 min 46 s); low power (40 W constant power for 16 min, 15 s); pulsed (95 W intermittently applied for 6 min 51 s, with intermittent 31 s pauses); bookend (95 W, 1 min pulses on either end of a 65 W, 8 min segment); and high power, long duration (65 W constant power for 15 min). Model predicted extents of ablation zone were qualitatively assessed against experimental data from *in vivo* experimental studies reported in the literature (Hui et al, *Int J Hyperthermia,* 2020), and quantitatively assessed against data from *ex vivo* experimental studies presented herein.

Results: Phase 1 modeling results revealed ablation zone short axes of 29.8, 33.5, and 37.0 mm for 50, 75, and 100 W, 5 min ablations compared to 26.2 ± 1.0, 30.3 ± 2.1, and 34.1 ± 5.1 mm from experiments in *ex vivo* tissue. For 10 min ablations, models predicted ablation short axes of 38.6, 42.5, and 43.2 mm, compared to 35.0 ± 1.0, 38.2 ± 1.7, and 41.5 ± 2.8 mm from *ex vivo* experiments. These data indicate a 4-12 % discrepancy between model predicted and experimentally observed ablation zones. In the *ex vivo* setting, model-predicted ablation zone short axis diameters ranged between 38.0 – 39.2 mm for the high power, ramped, low power, and pulsed ablation configurations, with larger ablation zones observed for the bookend (39. 8 mm) and high power, long duration (44.0 mm) cases. Experiments revealed similar trends, with discrepancies relative to modeling ranging between 7-11%. Under the in vivo scenario, computational models predicted bookend and high power, long duration settings yielded larger short axis ablation zone diameters compared to the other phase 2 cases, in agreement with published experimental studies (Hui et al, *Int J Hyperthermia,* 2020).

Conclusions: This study demonstrates the usability of the presented computational model for predicting microwave ablation zone extents under a variety of energy delivery settings.

OP-13
A 12-channel phased array microwave source for targeted delivery of hyperthermia treatment

R. Choudhary[1]*, M. R. Subash Ramu*[1]*, K. Arunachalam*[1]

[1]Indian Institute of Technology Madras, Department of engeneering design, Chennai, India

A phased array microwave source with variable power and phase control has been developed for delivering targeted power deposition using site-specific microwave hyperthermia applicators developed in our research group. Twelve phase controlled 434 MHz microwave signals are generated digitally with a maximum of 50 W per channel. The phase of each channel can be varied independently to focus microwave power deposition in tissue. The twelve synchronous signals generated using direct digital synthesis (DDS) technique are fed to twelve solid state power amplifier modules equipped with high power digital attenuators for varying the output power. The forwarded and reflected power, delivered phase and temperature are continuously monitored to provide real time feedback and generate control signals to the master control unit. The output power can be varied from 1 to 50 W with an accuracy of less than ±5%. Phase control and monitoring is possible with an accuracy of less than ±5

degrees. The 12-channel phased array microwave source assembled in a compact 12U rack mount assembly has protection against over temperature, voltage standing wave ratio, faults and over current. The system characterization results indicate stable operation for hyperthermia treatment delivery.

OP-14
Electromagnetic wavefield inversion for (near) real-time monitoring of breast location and electric field distribution during breast hyperthermia treatment

A. Kanagaratnam[1,2], I. Androulakis[1], M. Zanoli[1], G. C. van Rhoon[1], S. Curto[1], K. van Dongen[2]

[1]Erasmus University Medical Center Rotterdam, Hyperthermia Unit, Radiotherapy department, Rotterdam, Netherlands
[2]TU Delft, ImPhys department, Applied Physics, Delft, Netherlands

Introduction: Hyperthermia (HT) is a promising approach for treating breast cancer as it can enhance the efficacy of chemotherapy and radiation therapy. To facilitate focused tumor heating in the breast region, our institutes have been developing a phased array electromagnetic (EM) applicator. Although magnetic resonance imaging (MRI) is currently the most accurate option for patient position and treatment monitoring, it is costly and can cause discomfort to the patient.

Objectives: The objective of this research is to investigate whether we can retrieve the location of the breast and the generated electric field distribution during HT by measuring the EM wavefield used for the HT treatment. If successful, this would offer a potential alternative to MRI for monitoring the patient position and the HT treatment.

Materials and Methods: We developed a hyperthermia treatment and monitoring prototype applicator consisting of 18 equally spaced Yagi-Uda antennas positioned in a single ring, where the antennas are operating at a center frequency of 434 MHz. Six equally spaced antennas were used as high-power transmitters for the focused treatment, and the remaining 12 antennas were used as receivers, for treatment monitoring (Figure 1). To reconstruct the location of the breast and the generated heating focus, a full-waveform inversion method similar to contrast-source inversion is used. First, the contrast-sources are reconstructed from the measured scattered EM wavefield. Next, the contours of the breast are computed. Finally, the electric field inside the breast is reconstructed.

Results: Our reconstruction method is tested first on four two-dimensional (2D) numerical breast models from real patients. For each breast model, we first solved the forward problem. Next, we used the resulting data to reconstruct the contours of the breast as well as the electric field inside the breast model (Figure 2). The reconstructed contours are accurate up to 13 mm whereas the location of the reconstructed heating focus is accurate up to 5 mm. Finally, we built a prototype applicator to test our approach on a homogeneous cylindrical phantom (Figure 3) and we succeeded in reconstructing the contour of the phantom as well as the location of the generated heating focus in the phantom.

Conclusion: A method has been developed to reconstruct the position of the breast within the applicator as well as the electric field distribution inside the breast during HT. For these reconstructions, the EM wavefield - as used for the HT treatment itself - is used. The method has been tested successfully using 2D simulations and a simple 2D hyperthermia device. In the future, this may mean that we have an alternative option to monitor the HT treatment.

Fig.1

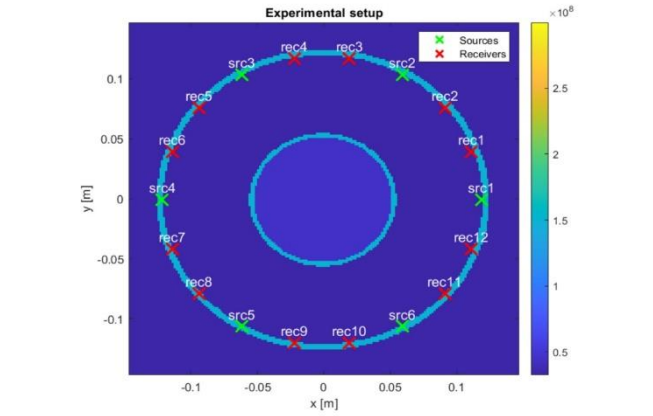

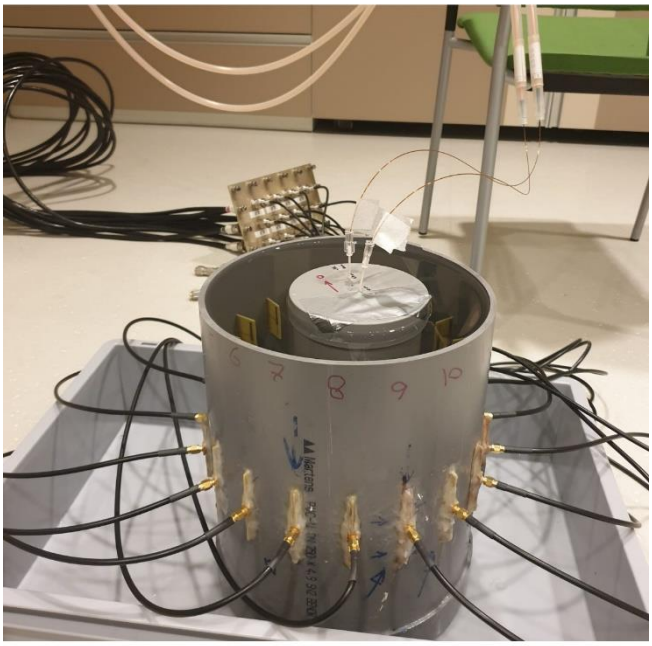

Figure 1 – Experimental setup with the prototype applicator. Top shows transversal view; bottom shows an image of the experimental setup.

Fig.2

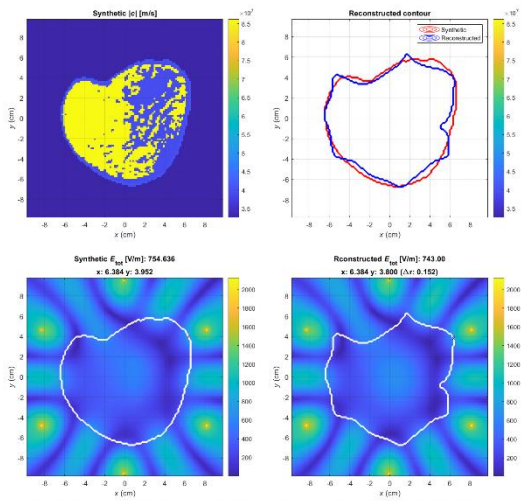

Figure 2 – Synthetic scenario. Top-left shows the absolute speed of light of the contrast (breast); Bottom-left shows the synthetic electric field using forward modelling; top-right shows the reconstructed contours using synthetic measurements; bottom-right shows the reconstructed electric field using synthetic measurements.

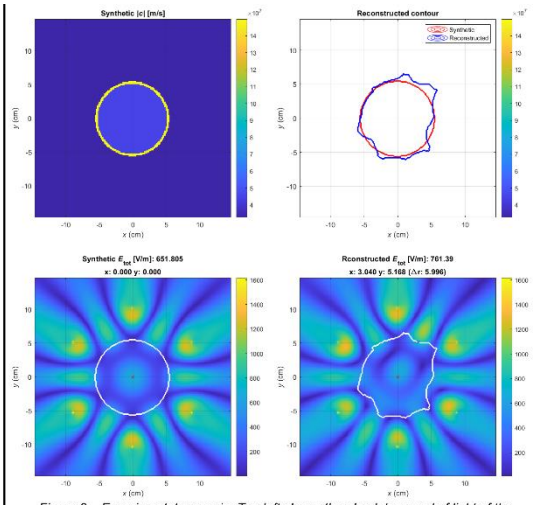

Figure 3 – Experimental scenario. Top-left shows the absolute speed of light of the contrast (phantom); Bottom-left shows the synthetic electric field using forward modelling; top-right shows the reconstructed contours using experimental measurements; bottom-right shows the reconstructed electric field using experimental measurements.

OP-15

Background, study design and treatment protocol of the upcoming TANCA-I trial: Thermoradiotherapy for locally advanced head and neck cancer patients-a phase I trial

Z. Kroesen[1,2], J. Elbers[1], M. Franckena[1], L. Tans[1], G. Verduijn[1], E. Van Meerten[3], H. Polinder-Bos[4], J. Hardillo[5], A. Rink[1], A. Sewnaik[5], B. Jonker[6], E. Van Werkhoven[7], M. Paulides[1,8], M. Zanoli[1], P. Granton[1], S. Curto[1], R. Nout[1]

[1]Erasmus University Medical Center Rotterdam, Radiotherapy, Rotterdam, Netherlands
[2]HollandPTC, Delft, Netherlands
[3]Erasmus University Medical Center Rotterdam, Medical Oncology, Rotterdam, Netherlands
[4]Erasmus University Medical Center Rotterdam, Internal Medicine/Geriatrics, Rotterdam, Netherlands
[5]Erasmus University Medical Center Rotterdam, Otorhinolaryngology head and neck surgery, Rotterdam, Netherlands
[6]Erasmus University Medical Center Rotterdam, Oral and Maxillofacial surgery, Rotterdam, Netherlands
[7]Erasmus University Medical Center Rotterdam, Hematology, Rotterdam, Netherlands
[8]Eindhoven University of Technology, Electrical Engineering, Eindhoven, Netherlands

Background and Rationale: Patients with a locally advanced head and neck squamous cell carcinoma (LA)-HNSCC are at high risk for locoregional recurrence following primary radiotherapy and have therefore an indication for radio-sensitisation, which is regularly achieved using either Cisplatin or Cetuximab. In some patients, however, these radiotherapy sensitizers are not effective and/or not possible to apply, due to age and co-morbidity. We select these sensitizer "unfit" patients for our study because of 1.) the clinical need for treatment intensification due to locally advanced disease, while 2.) no effective radio sensitizer is available and 3.) besides radiotherapy no other –systemic- therapy can interfere with the potential toxicity induced by the thermotherapy.

At the department of radiotherapy at Erasmus MC, the HyperCollar3D was developed. This is a medical device that allows for deep thermotherapy in the head and neck region, while avoiding sensitive structures. The device is equipped with advanced treatment planning software that enables the physician to mark the tumor area and predict the energy distribution.

We previously reported on two retrospective cohorts using the HYPERcollar (27 patients) and the next generation device, the HyperCollar3D (22 patients). We have used these devices in the past to apply thermotherapy in a compassionate use indication; patients having a recurrent or second primary HNSCC following previous RT in the head and neck area. We are now moving from the recurrent setting towards the first line treatment of HNSCC patients in order to find the maximal tolerable dose (MTD) in a phase I trial.

Objective: The main objective of this study is to determine the MTD of thermotherapy in HNSCC patients receiving radiotherapy as their first line treatment.

Study design: A phase I dose finding study using a Time-to-Event Bayesian Optimal Interval design. Five escalating dose levels will be tested in groups of 3-6 patients.

Study population: Patients with locally advanced oropharyngeal, hypopharyngeal and laryngeal cancer indicated for primary radiotherapy as monotherapy with curative intent

Intervention: Weekly thermotherapy treatments for one hour following the radiotherapy fraction, time interval as short as possible, maximal tow hours. The primary target of the thermotherapy treatment is the gross tumor volume including the primary tumor and pathological lymph nodes. Dose escalation will be performed using the maximal SAR to normal tissues. Skin and irta-oral thermometry will be standard and invasive neck thermometry will be performed in selected patients.

Study endpoints: Primary endpoint: MTD, defined as the incidence of dose limiting toxicity (DLT) over baseline radiotherapy toxicity and/or the probability of failure to apply the dose level more than 33%

Secondary endpoints: Local control, Disease Free Survival and Overall Survival, acute- and late toxicity, PROMs

OP-16

Multimodality therapy for high-risk soft tissue sarcomas of the trunk and limbs: evaluation of toxicity, efficacy and long-term outcomes of hyperthermia in combination with preoperative radiotherapy and chemotherapy

P. trecca[1], M. Fiore[1], G. D'Ercole[1], G. M. Petrianni[1], S. Minuti[1], C. Greco[1], E. Ippolito[1], S. Valeri[2], B. Vincenzi[3], S. Ramella[1]

[1]Fondazione Policlinico Campus Bio-Medico di Roma, Radiation oncology, Rome, Italy
[2]Fondazione Policlinico Campus Bio-Medico di Roma, General Surgery, Rome, Italy
[3]Fondazione Policlinico Campus Bio-Medico di Roma, Medical Oncology, Rome, Italy

Purpose: The aim of the study was to analyse the toxicity and efficacy of adding hyperthermia (HT) to radiotherapy (RT) and chemotherapy (CT) in patients with high-risk soft tissue sarcomas (STS) localised to the trunk and limbs.

Methods: We retrospectively reviewed patients with STS treated with HT combined with RT and/or CT. The treatment plan for all patients was decided by a multidisciplinary team. All patients underwent RT combined with HT according to quality and safety assurance guidelines. Radiotherapy was administered preoperatively using the VMAT technique with a total dose of 50 Gy in 2 Gy fractions. All patients eligible for surgery underwent wide resection. All patients underwent regular follow-up after treatment.

Results: Twenty-four patients (14 men and 10 women; mean age 62.5 years, range: 34-87) with STS were included in this study. The mean size of the treated tumours was 9.2 cm (range 2-20). The most common histology was undifferentiated pleomorphic sarcoma (8 patients, 33.3%). Eight patients (33.4%) received upfront concurrent chemoradiation and HT and 10 (41.6%) received RT and HT alone. Overall, the treatment was well tolerated and 22/24 (91.6%) patients completed the planned course of treatment. Only two cases of grade 3 toxicity (limb edema) were reported with RT. The objective response rate (partial response or stable disease) was 95.8% (23/24 patients). Twenty-three patients (95.8%) underwent surgery after completion of treatment and all achieved negative surgical margins except for two patients (8.2%) who had microscopic R1 margin involvement. Complete pathological response was achieved in 7 of 23 patients (30.4%). Two patients experienced local progression, four patients experienced distant progression and two patients experienced both local and distant progression. With a median follow-up of 18 months (range, 4.5-46.3), median disease-free survival (DFS) was 18.5 months and 3-year DFS was 44%. The 3-year overall survival (OS), local progression-free survival (LPFS) and metastasis-free survival (MFS) rates were 77%, 78% and 71%, respectively (median not reached).

Conclusions: In our experience, the integration of HT, RT and CT was feasible in patients with STS of the trunk and extremities, achieving good local control. However, a larger number of patients and a longer follow-up are needed to better evaluate the characteristics of this integration.

In our experience, the integration of HT, RT and CT was feasible in patients with STS of the trunk and extremities, achieving good local control. However, a larger number of patients and a longer follow-up are needed to understand the best way to synergize these therapies.

OP-17

The predictive value of hyperthermia temperature parameters for locoregional control in patients with locoregional recurrent breast cancer treated with postoperative re-irradiation and hyperthermia: An evaluation of invasive versus skin thermometry

C. P. Tello Valverde[1], H. P. Kok[1], W. Kolff[1], B. J. Slotman[1], J. Crezee[1]

[1]Amsterdam University Medical Center, Radiation Oncology, Amsterdam, Netherlands

Q: Hyperthermia (HT) at 40-43°C acts synergistically with ionizing radiation and chemotherapeutic agents and is used in combination with re-irradiation for treatment of locoregional recurrent (LRR) breast cancer. Extensive well-documented skin and invasive (i.e. interstitial) thermometry with multiple sensor thermocouple probes is crucial to maintain temperatures in the 40-43°C range during HT delivery. Skin cooling with a circulating water bolus is often applied to augment the heating depth during HT treatment. There is a debate whether both invasive and skin surface temperature measurements have a dose-effect relationship with locoregional tumor control (LRC).

We therefore investigated the association of invasive and skin HT parameters with LRC for patients with LRR breast cancer treated with postoperative re-irradiation and HT.

M: We analyzed a historical cohort of 112 women with LRR breast cancer treated between 2010-2017 with postoperative re-irradiation 8x4Gy (n=34) or 23x2Gy (n=78), combined with 4-5 weekly HT sessions. Superficial HT was given with 434 MHz microstrip applicators. Based on Weibull univariate and multivariate stepwise backward regression analysis, the highest invasively and skin surface measured thermal dose CEM43T50 (median cumulative equivalent minutes at 43°C) and average T50 (median cumulative temperature in °C) were selected to analyze relationships between thermal dose or temperature and LRC. Tumor location breast/chest wall, lymph node involvement and age were also included in the model. Additionally, Spearman's correlation coefficient analysis between invasive and skin surface HT parameters was performed.

R: Twenty-four patients (21.4%) developed an infield recurrence; with a median time to recurrence of 3.4 years (interquartile range (IQR) 2.7-4.6 years). Median highest HT session CEM43T50 for invasive and skin surface were 7.2 minutes (IQR 3.4-15.9) and 2.8 minutes (IQR 2.0-4.3), respectively. For average T50, the median invasive and skin temperatures were 40.7°C (IQR 40.0-41.3) and 40.6°C (IQR 40.3-40.8), respectively. Multivariate analysis showed no association between skin surface temperature parameters and LRC (*P*=0.131; *P*=0.215, respectively), where invasive temperature parameters CEM43T50 and T50 did show a significant association with LRC (*P*=0.013; *P*=0.021, respectively). Spearman's correlation analysis showed no significant association between the invasive and skin temperature parameters (Figure 1-2). The close proximity of the cool water bolus is likely to be a major reason for the absence of correlation between skin temperature measurements and LRC.

C: Only invasive thermometry was significantly associated with LRC in patients with LRR treated with postoperative re-irradiation combined with superficial HT when using a cooling water bolus to maximize heating depth. These results are clinically relevant for HT treatment delivery and stress once again the paramount value of invasive thermometry.

Fig. 1

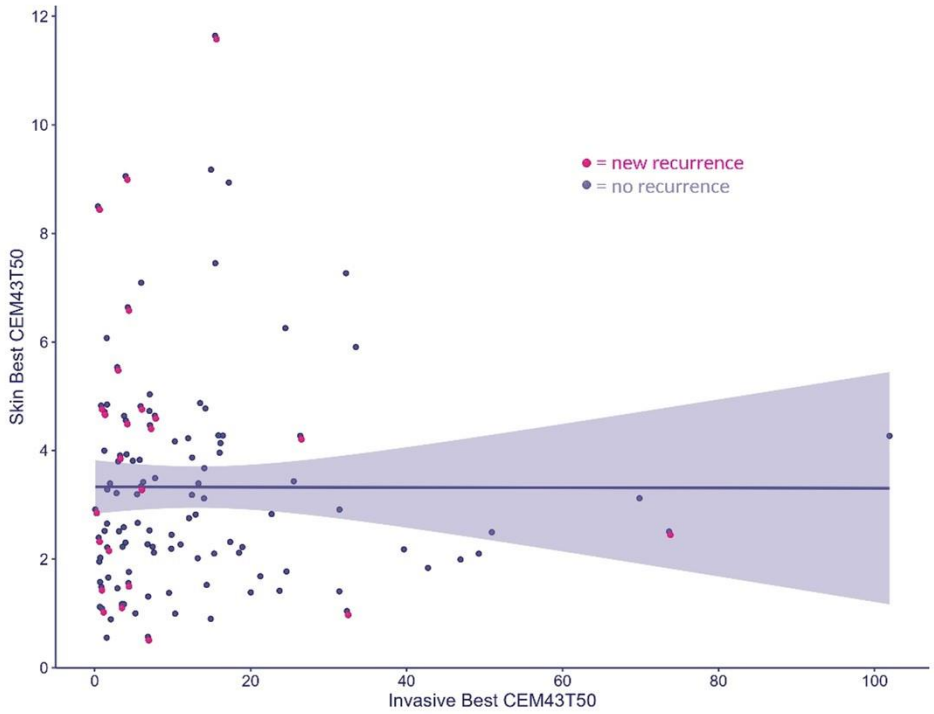

Figure 1. Scatterplot skin vs. invasive thermometry breast cancer

Fig. 2

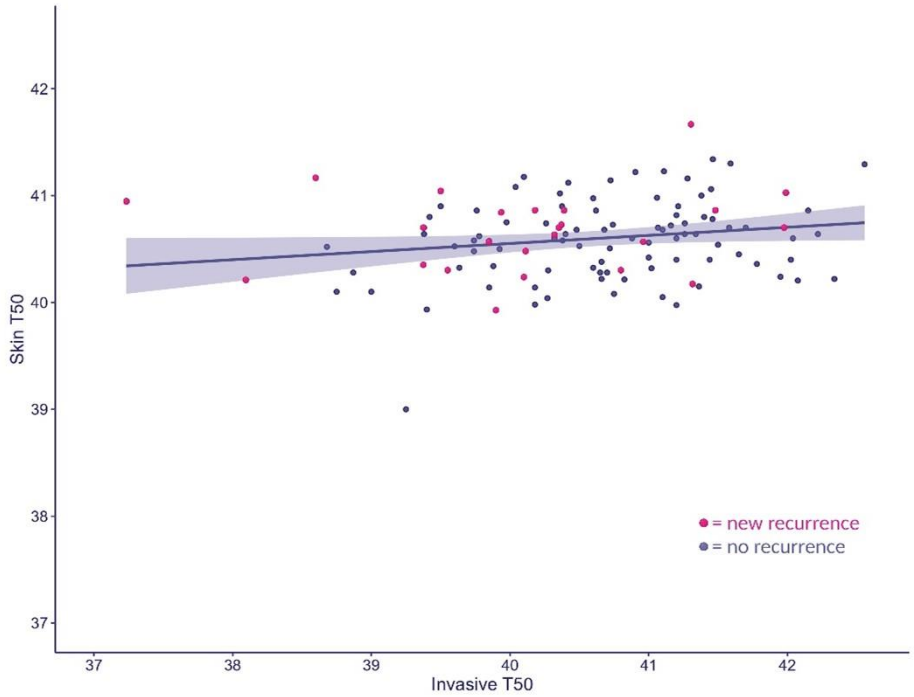

Figure 2. Scatterplot skin vs. invasive thermometry breast cancer

OP-18
Impact of uncertainties in the delivery of microwave hyperthermia treatments for head and neck cancer

R. Kwakernaak[1], M. Zanoli[1], Z. Perko[2], K. Sumser[3], M. Paulides[3], S. Curto[1]

[1]Erasmus University Medical Center Rotterdam, Radiotherapy, Rotterdam, Netherlands
[2]Delft University of Technology, Delft, Netherlands
[3]Eindhoven University of Technology, Eindhoven, Netherlands

Introduction: Between 2014 and 2018, 22 patients with head and neck (H&N) cancer were treated with the HyperCollar3D (HC3D), a clinical applicator for H&N hyperthermia developed at the Erasmus Medical Center. The results from this feasibility study and a subsequent retrospective evaluation were promising. Being the HC3D the only dedicated H&N hyperthermia applicator, literature regarding the robustness of treatment planning versus delivery in this anatomical area is scarce. To assess the impact of uncertainties, we studied the response of treatment quality metrics to variations in tissue properties, inaccuracies in patient positioning, and water bolus cooling efficacy, by means of uncertainty analysis using Polynomial Chaos Expansion (PCE).

Methods: A canonical treatment plan was prepared for a neck cancer patient using the segmented data from the available cohort. We constructed univariate PCE models to evaluate the impact of individual uncertainty parameters on the steady-state temperature distribution: permittivity, electric conductivity, thermal conductivity, and perfusion rate of each segmented tissue, patient positioning errors (x,y,z), and skin/bolus convection coefficient variations, for a total of 47 parameters. Subsequently, we constructed a multivariate PCE model to assess the combined effect of the uncertainty parameters that showed an impact on T90 in the univariate analysis. PCE models were validated on 100 independently generated random test scenarios. From the PCE models, we extracted statistical data about target temperatures and quality metrics (T90), and the probability of hot-spot formation (T > 44 °C in healthy tissue).

Results: In univariate analysis, the variations in patient positioning along the x-axis (left-right) had the largest impact with an induced standard deviation (STD) on T90 of 1.2 °C, followed by variations in muscle conductivity (0.9 °C), z-axis (rostro-caudal) positioning (0.9 °C), tumor conductivity (0.9 °C), and muscle perfusion (0.8 °C). Examples of mean and STD of the temperature distributions for patient positioning errors are reported in Fig. 1. Their impact on target temperatures and the corresponding probability of hot-spot formation are reported in Fig. 2. In multivariate analysis, the chosen polynomial order of the PCE model proved to be insufficient to accurately model the combined response to all the uncertainties. The combined impact of subsets of uncertainties grouped by type are reported in Fig. 2.

Conclusion: The construction and validation of large PCE models for H&N hyperthermia treatments, including all uncertainties impacting the delivery, is a challenging task. Our univariate analysis indicates that positioning alone has a large impact on achieved treatment temperatures. Work is in progress to develop an accurate PCE workflow including all clinically relevant uncertainties with limited computational complexity. Future work will extend the study to the entire patient cohort.

Fig. 1

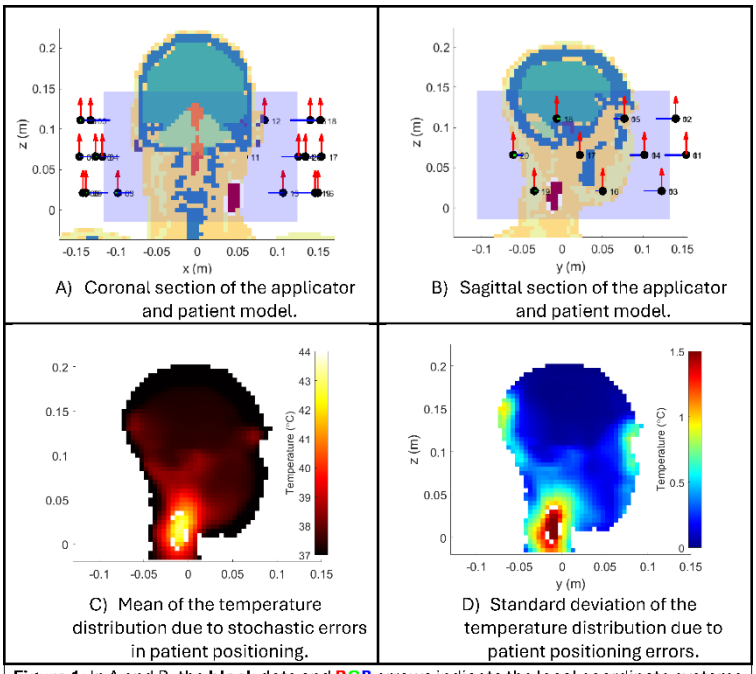

A) Coronal section of the applicator and patient model.

B) Sagittal section of the applicator and patient model.

C) Mean of the temperature distribution due to stochastic errors in patient positioning.

D) Standard deviation of the temperature distribution due to patient positioning errors.

Figure 1: In A and B, the **black** dots and **RGB** arrows indicate the local coordinate systems of the antennas in the applicator array, while the water bolus is represented in **light purple**. The target is delineated in a white contour and **dark purple** filling. An example of the impact of positioning errors (x,y,z) on the temperature distribution is reported in C and D. These are the expected value (mean) and standard deviation of 100000 PCE-generated random error scenarios.

Fig. 2

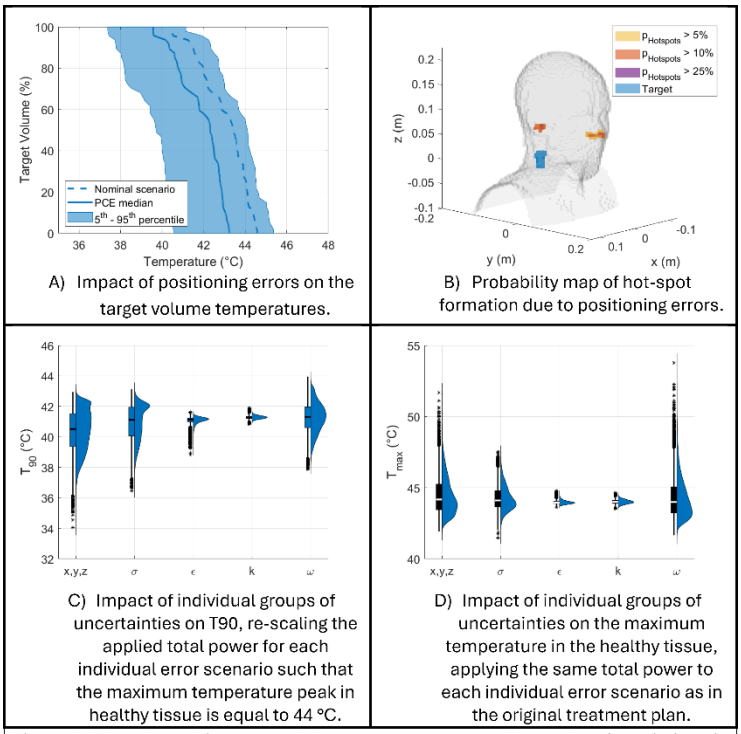

Figure 2: The volume histogram of the target temperatures for stochastic variations in patient positioning is reported in A. The probability map of hot-spot formation (T > 44 °C) outside the target is reported in B. The combined impact of subsets of uncertainties is reported in C and D. The uncertainties are grouped by positioning (x,y,z), electric conductivity (σ), permittivity (ε), thermal conductivity (k), and perfusion (ω).

OP-19

The HISTOTHERM study: wIRA-hyperthermia and hypofractionated radiation therapy for locally recurrent breast cancer – preliminary results

A. R. Thomsen[1,2], J. Sahlmann[3], P. Bronsert[4,5], P. Vaupel[1,2], A. L. Grosu[1,2], J. O. Gebbers[6], A. M. Lüchtenborg[1,2]

[1]Medical Center - University of Freiburg, Department of Radiation Oncology, Freiburg, Germany
[2]German Cancer Consortium (DKTK), Partner Site DKTK-Freiburg, Freiburg, Germany
[3]Medical Center - University of Freiburg, Institute for Medical Biometry and Statistics, Freiburg, Germany
[4]Medical Center - University of Freiburg, Institute for Surgical Pathology, Freiburg, Germany
[5]Medical Center - University of Freiburg, Tumorbank Comprehensive Cancer Center Freiburg, Freiburg, Germany
[6]University of Berne, Department of Pathology, Working Group Digital Pathology, Bern, Switzerland

Question: Hyperthermia (HT) combined with radiation therapy (RT) is a potent treatment modality for pre-treated breast cancer patients with locally recurrent disease[1]. While the radio-sensitizing effect of HT allows for re-RT with a reduced total radiation dose, treatment response is currently unpredictable. In addition, little is known about the patients" tissue reactions during the treatment. The HISTOTHERM study aims at filling this gap and at analyzing histological and clinical parameters longitudinally to evaluate treatment outcome and identify relevant tissue processes.

Methods: Patients with locally recurrent, non-resectable breast cancer treated with superficial HT and hypofractionated RT are included in the HISTOTHERM study. Local HT is applied with water filtered infrared A (wIRA) irradiation for 60 min to a temperature of 39-43°C. Radiation follows HT within < 5 min with a single dose of 4 Gy, to a total dose of 20-24 Gy, once a week [2]. Punch biopsies from tumor lesions are taken before start of the treatment, during treatment at a dose of 12 Gy and at first follow-up and stained by immunohistochemistry. Histological and clinical response are evaluated and correlated with clinical data. The study is registered (DRKS 00029221) and currently recruiting.

Results: Here, we present a first analysis of the HISTOTHERM data. So far, 41 patients have been treated in 70 regions with a maximum of six regions in one patient. In 75% of patients the tumor lesions were large (rClass III/IV according to Notter et al. [3]), extending across the midline and/or to the abdomen and/or back. Overall, the treatment was well accepted and caused only mild side effects. HT+RT yielded favorable clinical outcomes, with over 80% of patients achieving either complete or partial local response. Notably, local clinical outcome was found to correlate with histological regression. Additionally, the fraction of proliferating (Ki-67 positive) cancer cells decreased significantly ($p< 0.01$, $n=15$) at a radiation dose of 12 Gy, compared to initial histologies.

Conclusion: The combination of superficial HT+RT presents a viable treatment option for patients with recurrent, pre-irradiated breast cancer. Early histological regression is often followed by very good clinical results. Interestingly, histological regression often precedes the clinical response. Our longitudinal analysis of tissue markers allows, for the first time, evaluating tissue alterations throughout the course of the HT+RT treatment.

References:
[1] Water-filtered Infrared A (wIRA) Irradiation. From Research to Clinical Settings. Springer Nature, Cham, Switzerland. 2022.
[2] Notter, M et al. Int. J. Hyperth. 2017, 33; 227–236
[3] Notter, M et al. Cancers 2020, 12: 606.

OP-20
Harmonization of quality assurance and superficial hyperthermia-treatment delivery in The Netherlands: Nationwide multicenter monitoring and data-evaluation of thermometry procedures

A. Kanagaratnam[1], A. Ameziane[1], R. Zweije[2], M. van Wieren[3], M. Franckena[1], C. Carrapiço-Seabra[1], A. Rink[1], P. Granton[1], C. P. Tello Valverde[2], D. de Vries-Huizing[2], M. Essers[3], L. Wurfbain[2], D. van den Bongard[2], A. Bakker[4], J. Crezee[2], S. Curto[1]

[1]Erasmus University Medical Center Rotterdam, Hyperthermia Unit, Radiotherapy department, Rotterdam, Netherlands
[2]AMC, Hyperthermia, Radiotherapy department, Amsterdam, Netherlands
[3]Instituut Verbeeten, Hyperthermie, Tilburg, Netherlands
[4]Prinses Máxima Centrum, Kinderoncologie, Utrecht, Netherlands

Introduction: The European Society for Hyperthermic Oncology (ESHO) Quality Assurance (QA) guidelines for superficial hyperthermia specify necessary parameters but do not provide a uniform QA and data reporting protocol. Hyperthermia treatment procedures vary across institutes due to different heating and thermometry systems, complicating multicenter data comparison. This study systematically compared thermometry procedures at all Dutch institutes delivering hyperthermia: Amsterdam UMC (Amsterdam), Erasmus MC (Rotterdam), and Instituut Verbeeten (Tilburg). This study is part of the RT-HYPE project, which investigates postoperative re-irradiation alone versus re-irradiation with hyperthermia in patients with high-risk locoregional recurrent breast cancer, funded by the Dutch Cancer Society. The study focuses on harmonizing hyperthermia treatment delivery, essential for multi-institutional clinical studies.

Methods: Clinically used thermometry probes were benchmarked against a universal reference probe utilized across all institutes. Tests were conducted over a three-week period. During weekly assessments, temperature stability was assessed by continuously measuring temperature maintained at a constant 40 °C for 2 hours. Additionally, temperature accuracy and precision were monitored across the clinical range of 30 °C to 50 °C, with resolution steps of 1.0 °C. Within the hyperthermia-specific range of 37 °C to 43 °C, the resolution steps were reduced to 0.2 °C. Based on these assessments, we computed short- (2 hours) and long-term (3 weeks) stability, as well as temperature accuracy and precision.

Results: All institutes complied with existing guidelines for both short- and long-term temperature stability (Table 1). The average short- and long-term temperature stability across all institutes were -0.02 °C per hour and 0.04 °C per week, respectively. Initially, temperature accuracy and precision did not meet the QA guidelines at one institute. In response, the local calibration procedure and protocol were harmonized to match those of the other centers. The previously measured temperatures at this institute were corrected by applying new calibration values (see "before" and "after" in Table 1). After harmonization, the precision still did not meet the QA guidelines, likely due to the measurements being performed under prior sub-optimal conditions. However, the ESHO QA guidelines for temperature accuracy were met across all institutes.

Conclusions: The results presented here indicate that a joint evaluation of local QA guidelines for thermometry systems can identify and resolve discrepancies in QA procedures. These findings should be considered in the development of future QA guidelines, particularly concerning calibration protocols and thermometry systems, which are crucial for multi-center studies. The harmonized thermometry QA ensures optimal standardized treatment delivery during the prospective clinical study within the framework of RT-HYPE.

Fig. 1

Table 1. Thermometry results for different institutes in the Netherlands.
[1] Shrivastava et al.: Hyperthermia quality assurance guidelines (1989).
[2] Trefná et al.: Quality assurance guidelines for superficial hyperthermia clinical trials: I. Clinical requirements (2017).

Parameter	Unit	Definition	Description	Guidelines	Range	Institute 1 (before)	Institute 1 (after)	Institute 2	Institute 3
Probe	-	Universal reference thermometer: Fluke (United States) 1524 platinum resistance thermometer	Information about the clinically used probes and the total amount of sensors used for the assessments	-	-	16 ALBA (Italy) T-type copper-constantan thermocouple single-sensor probes: 16 sensors		4 Ella-CS (Czech Republic) copper-constantan multi-sensor probes: 35 sensors	2 FISO (Canada) fiber-optic multi-sensor probes: 10 sensors
Stability (short-term)	°C / hour	$S_S = \frac{\max((x_i - A_i) - \alpha(x_i) - (x_{t=0} - A_{t=0}))}{t}$	Maximum temperature drift per hour (including systematic error correction)	$\lvert S_S \rvert \leq 0.1$ [1]	30 ~ 50 °C	0.01	0.01	-0.02	-0.01
					37 ~ 43 °C	-0.03	-0.03	-0.02	-0.01
Stability (long-term)	°C / week	$S_L = \frac{\sum_{i=0}^{i=N-1}((x_{t=3,i} - A_{t=3}) - (x_{t=1,i} - A_{t=1}))}{N \cdot t}$	Average temperature drift per week (excluding systematic error correction)	$\lvert S_L \rvert \leq 0.1$ [1]	30 ~ 50 °C	-0.06	-0.06	0.02	-0.01
					37 ~ 43 °C	-0.09	-0.09	0.03	-0.04
Accuracy	°C	$\alpha(x_i) = \frac{\sum_{i=0}^{i=N-1}(x_i - A)}{N}$	Temperature offset relative to the actual/expected temperature	$\lvert \alpha \rvert \leq 0.2$ [2]	30 ~ 50 °C	0.33	0.12	0.03	-0.01
					37 ~ 43 °C	0.27	-0.01	-0.01	0.02
Precision	°C	$\mathrm{SD} = \sqrt{\frac{\sum_{i=0}^{i=N-1}(x_i - \bar{x})^2}{N-1}}$	Repeatability error in the temperature measurements	$\mathrm{SD} \leq 0.1$ [1]	30 ~ 50 °C	0.22	0.18	0.02	0.05
					37 ~ 43 °C	0.22	0.19	0.03	0.05

OP-21
Practical use of on-line adaptive treatment planning considering uncertainties in tissue parameters

P. Kok[1], J. Crezee[1]

[1]Amsterdam University Medical Center, Radiation Oncology, Amsterdam, Netherlands

Question: Treatment planning is a valuable tool to optimize phase-amplitude settings for locoregional hyperthermia treatments. However, the reliability of pre-treatment planning is affected by uncertainties in tissue parameters (i.e. dielectric properties and perfusion). On-line adaptive planning aims to support the operator to find optimal phase-amplitude steering strategies during treatment, and considers changes in SAR/temperature after phase-amplitude steering, rather than absolute levels. First applications so far indicated feasibility to ensure treatment quality. The question remains how uncertainties in tissue parameters influence the reliability of adaptive planning; this was evaluated in the present study.

Methods: Adaptive planning was evaluated for the 70 MHz ALBA-4D device, using the Plan2Heat treatment planning package. First, we considered steering in an inhomogeneous fat-muscle phantom, using SAR measurements for two different phase-amplitude settings from the literature. This was followed by evaluation of clinical steering strategies in a patient model. Uncertainties in electrical conductivity, permittivity and perfusion were mimicked by simulations using 100 random parameter samples from normal distributions, with a 20%, 10% and 30% standard deviation in electrical conductivity, permittivity and perfusion, respectively. Variations in absolute SAR/temperature values and in (relative) changes in SAR/temperature after phase-amplitude steering were evaluated. Next, correlations between measured and simulated SAR (changes) were determined for phase settings evaluated at the start of treatment for a treatment series.

Results: For the phantom, changing from setting 1 to setting 2 resulted in a measured SAR reduction of 28.5% SAR at the fat-muscle interface (from 60 to 43W/kg), which was predicted with minimal variation(~27-30%), despite large absolute SAR variations ranging between 47 and 74 W/kg for setting 1 and 34-52 W/kg for setting 2. In the patient model, predicted SAR/temperature changes after phase-amplitude adjustments varied typically within a few percent (Figure 1). For example at the tail bone, a common hot spot location, the predicted temperature was 44.9°C with standard tissue parameters. This local temperature could vary between 42.1°C and 50.5°C under parameter uncertainty; a spread of more than 8°C. After clinical steering, a 5.1% (0.4°C) reduction was predicted, varying between 2.6 and 7.2% (i.e. 0.2-0.9 °C) under parameter uncertainty. For the treatment series, correlations between measured and simulated (relative) SAR changes were much better(R^2=0.70-0.82) than for absolute SAR values(R^2=0.29).

Conclusion: The reliability of adaptive planning is minimally affected by tissue parameter uncertainties, with relatively small variations in predicted SAR/temperature changes after phase-amplitude steering. On-line adaptive planning proves thus robust and can effectively support clinical steering strategies.

Fig. 1

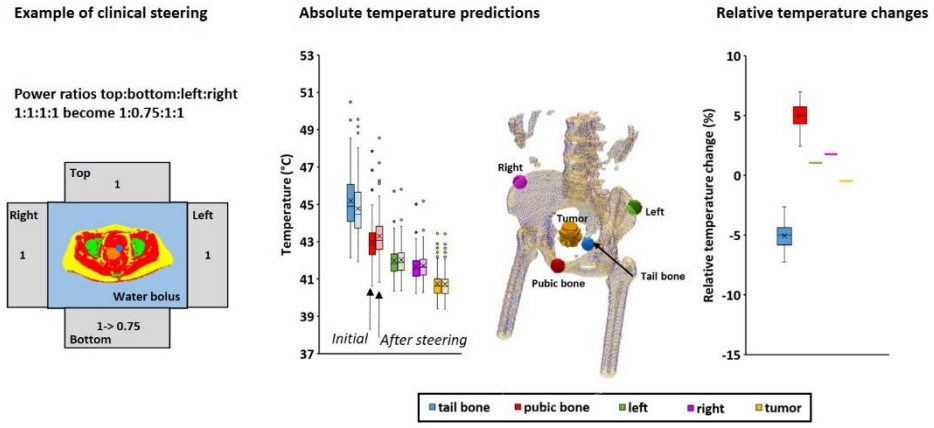

Figure 1: The influence of tissue parameter uncertainties (dielectric properties and perfusion) on predicted absolute temperatures and relative changes in temperature after clinical phase-amplitude steering.

OP-22

Imaging wide-band dielectric tissue properties through quantitative multinuclear MRI tissue composition assessment (tissue composition electrical properties tomography): A feasibility study

L. Barendsz[1], K. Sumser[1], D. Y. E. Tse[2], J. F. A. Jansen[1,3,4], R. M. C. Mestrom[1], M. Paulides[1,5]

[1]Eindhoven University of Technology, Electrical Engineering, Eindhoven, Netherlands
[2]Maastricht University, Neuropsychology and Psychopharmacology, Maastricht, Netherlands
[3]Maastricht University, Mental Health & Neuroscience Research Institute, Maastricht, Netherlands
[4]Maastricht University, Department of Radiology & Nuclear Medicine, Maastricht, Netherlands
[5]Erasmus University Medical Center Rotterdam, Radiotherapy, Rotterdam, Netherlands

Question: The accurate knowledge of the dielectric properties of human tissue is a crucial component of accurate hyperthermia treatment planning. In this study, we investigated the feasibility for determining dielectric tissue properties in the frequency range of 50 to 600 MHz using mixture models combined with quantitative multinuclear MRI-based tissue composition assessment (Tissue composition EPT (TiCEPT)).

Methods: Muscles can be approximated by protein, fat, sodium, and water. Four phantoms with different compositions were prepared (healthy, obese, obese+, and dehydrated) [1].

The Looyenga mixture model is used to relate the dielectric properties (DP) of the muscle to its constituents [2]. For muscle, the constituents are saline as background solution, protein and fat as additive, and the water fraction is used to find the volume fraction.

All MRI measurements were performed using a Siemens 7T whole-body MRI system at Scannexus (Ultra-High-Field MRI center, Maastricht). The water fraction was determined based on the measured T1 times. Calibration phantoms, consisting of water, sodium chloride and sugar, were used to correlate the T1 times with the water fraction [3].

The sodium concentration measurements of the phantoms were performed with a 23Na knee coil using an ultrashort TE sodium sequence. Four calibration samples with water, agar, and varying salt concentrations were used for a linear fit to find the sodium content in the muscle phantoms.

Results: The fit for the water fraction and sodium concentration is given in Fig. 1. The measured water fraction and sodium concentration were inserted into the Looyenga equation. Tab. 2 shows that the mean error is 8.2% for relative permittivity and 7.6% for conductivity.

Conclusion: This study demonstrates the feasibility of reconstructing the DP"s of human tissue by quantitative multinuclear MRI supplemented by the Looyenga mixture model.

[1] Barendsz, L.J.C., Sumser, K. , Beumer, S., Curto, S., Mestrom, R.M.C., & Paulides, M.M., "Phantom Material with Biological Composition for Muscle Equivalent Radiofrequency, Thermal and Magnetic Resonance Properties" In 2024 18th European Conference on Antennas and Propagation

[2] Looyenga H., "Dielectric constants of heterogeneous mixtures," Physica, vol. 31, no. 3, pp. 401–406, 1965.

[3] Hernandez D., Kim K.-N., "Correlation analysis between the complex electrical permittivity and relaxation time of tissue mimicking phantoms in 7T MRI," 04 2022

Fig 1. (a) Rational fit to the calibration phantoms, including the measurements for the muscle phantoms. (b) T1 relaxation time image, with ROI"s of muscle phantoms. (c) Linear fit to the calibration samples, including the measurements and the prepared value of the salinity of the muscle phantoms. (d) Magnitude image of the sodium scan with ROI"s, in yellow the muscle phantoms and in purple the calibration phantoms.

Tab 1. MAPE for the relative permittivity and conductivity found with the Looyenga equation.

Fig. 1

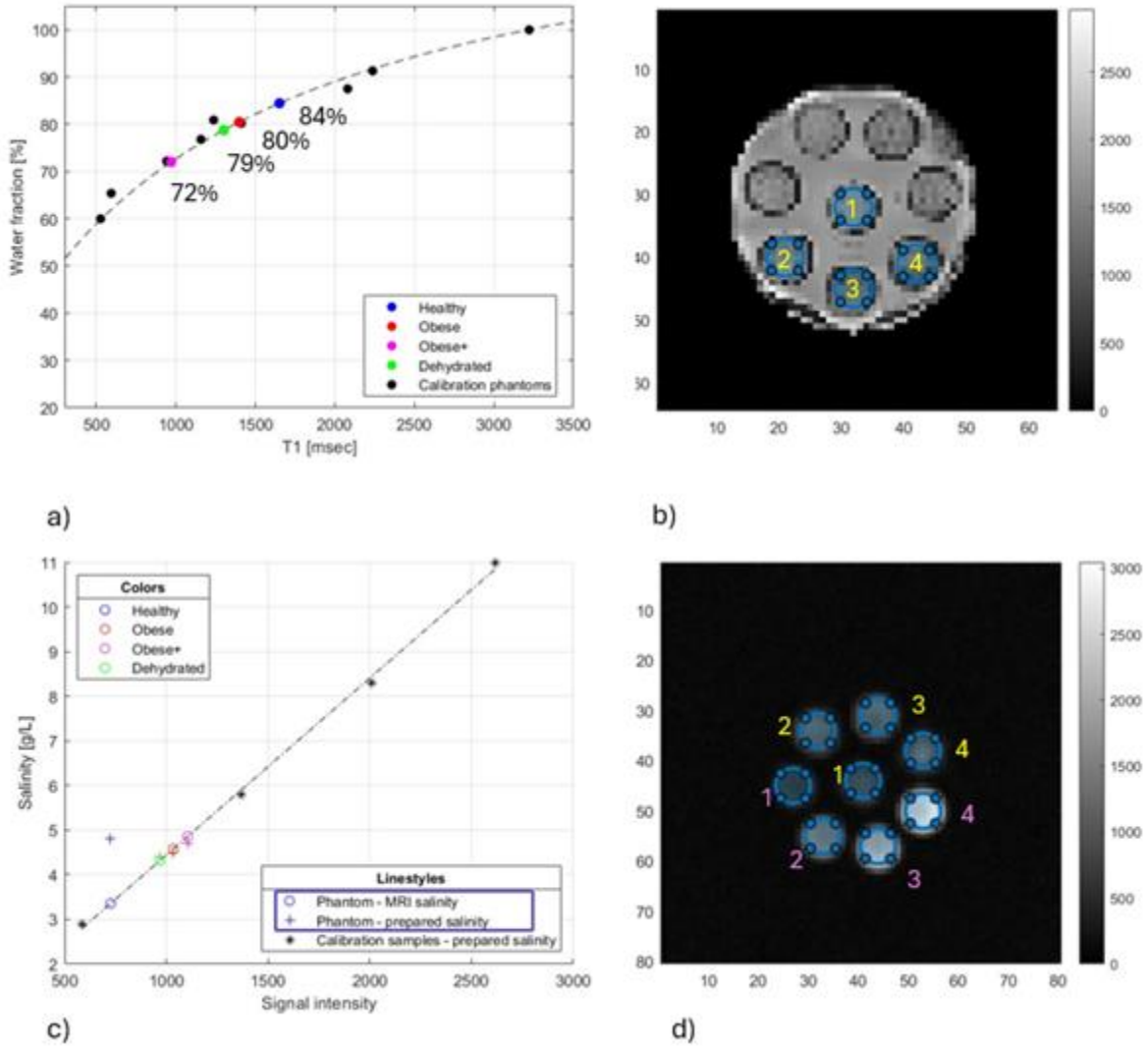

Fig. 2

Relative permittivity

Phantom	50 - 600 MHz	65 MHz	130MHz	300 MHz	400 MHz
Healthy	2.5%	6.0%	4.8%	2.1%	1.7%
Obese	8.0%	4.4%	5.1%	8.8%	8.9%
Obese+	18.0%	14.1%	14.2%	19.1%	18.9%
Dehydrated	4.4%	8.8%	7.2%	3.8%	3.3%

Conductivity

Phantom	50 - 600 MHz	65 MHz	130MHz	300 MHz	400 MHz
Healthy	14.5%	12.0%	12.4%	13.0%	14.8%
Obese	5.5%	7.5%	7.5%	7.3%	4.7%
Obese+	7.0%	8.0%	8.7%	10.0%	7.2%
Dehydrated	3.2%	1.5%	0.9%	0.1%	3.2%

OP-23

A framework for designing optimal multi-echo PRFS thermometry

M. Paulides[1], S. Nouwens[2], K. Sumser[1], M. Heemels[2]

[1]Eindhoven University of Oncology, Electrical Engineering, Eindhoven, Netherlands
[2]Eindhoven University of Technology, Mechanical Engineering, Eindhoven, Netherlands

Question: Magnetic resonance (MR) compatible hyperthermia devices enable real-time MR thermometry using the proton resonance frequency shift (PRFS). This PRFS with temperature is small, so there is a perpetual need to increase the temperature-to-noise ratio (TNR) to improve accuracy or reduce scan time to counteract motion. The thermo-dependent electrical conductivity is another PRFS confounder, which can be mitigated by the dual-echo (DE) technique. However, while the optimum single echo at the Ernst-angle (TE=T2*) maximizes the TNR, the additional DE echo enables the correction, but also adds noise. This might be overcome by adding the signal of additional echoes, for which we present a TNR-optimal echo-time placement framework.

Methods: We developed a weighted average approach to determine the PRFS from multi-echo MR scans, with the weights derived from the expected noise variance of a voxel. TNR-optimum echo placement was determined (T2* = 20ms, ΔTE = 2ms, and TEmax = 30ms) for the case that conductivity bias is & is not corrected for, and benchmarked the TNR results against those of an equidistant spacing (TEk = [5, 10, . . . , 30]ms). The benefit of the framework was experimentally demonstrated for a 6-echo gradient-echo sequence measurement of a cylindrical phantom inside the MRcollar in a 1.5T MRI scanner.

Results: Figure 1 (upper row) compares the optimal TNR for biased and bias-corrected reconstructions. Optimal placement outperforms the equidistant spacing for both regarding TNR. The TNR with conductivity bias correction was generally lower since some echoes are exploited to remove conductivity bias. For the biased reconstruction, the optimal echo placement is centered around T2* (lower row), whereas the echo placement is less straightforward for the non-biased reconstruction. Here, we observe an early echo (TE1 ≈ 0.1 T2*) followed by subsequent echoes located predominately after T2*. Note that these results are intuitive as echoes at the start are dominated by the conductivity bias, while later echoes have accumulated more temperature sensitivity. Figure 2 shows that the optimal echo placement reduced the noise standard deviation by 35% compared to that of non-optimal placement.

Conclusion: We presented an optimization-based framework to optimize echo placement for multi-echo PRFS-based thermometry. Our framework predicts that bias correction costs TNR. A 6-echo MRT experiment with optimal and non-optimal echo-time showed a 35% reduction in standard deviation.

Figure 1 upper row: TNR comparison for both optimal and equidistant echo placement with either biased (left) or bias-corrected (right) reconstructions (higher is better). Lower row: optimal echo placement for the biased (left) and bias-corrected (right) reconstruction of a multi-echo PRFS measurement.

Figure 2. Temperature increase distributions (°C) for DE gradient-echo sequence with optimal (4.9ms, 19.1ms) and non-optimal (9.2ms, 19.1ms) echo-times.

Fig. 1

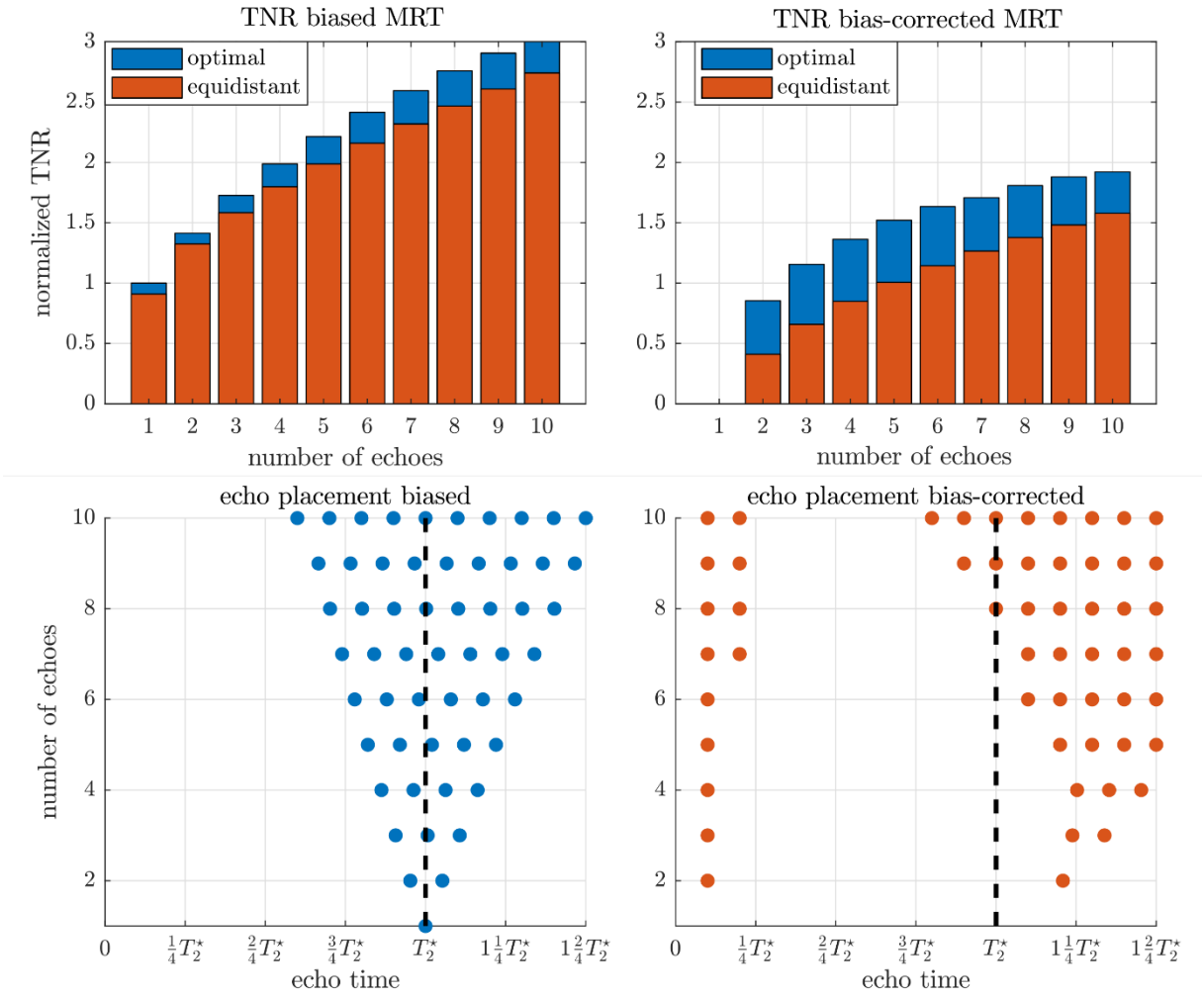
TNR biased MRT
optimal
equidistant
normalized TNR
number of echoes
TNR bias-corrected MRT
optimal
equidistant
number of echoes
echo placement biased
number of echoes
echo time
echo placement bias-corrected
echo time

Fig. 2

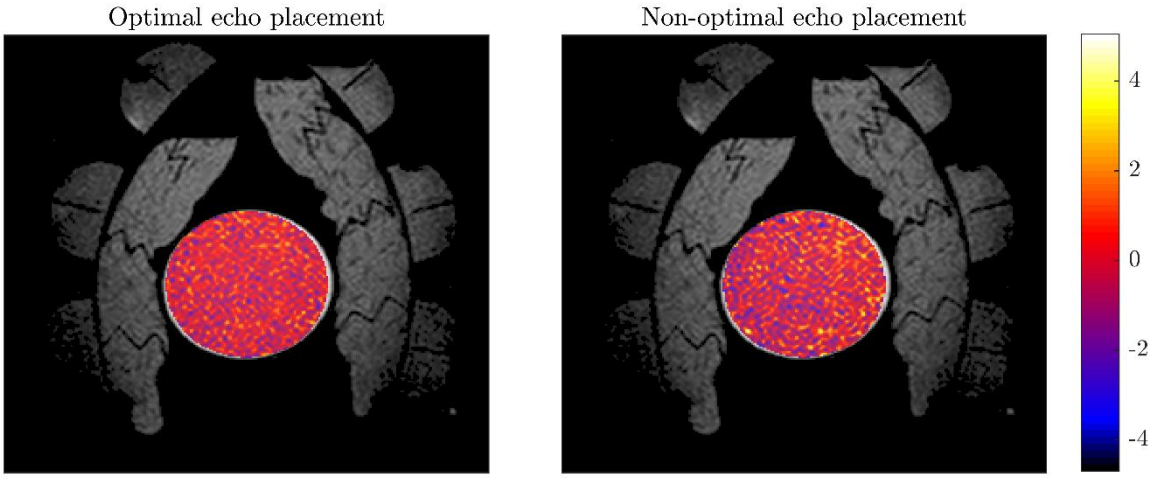
Optimal echo placement
Non-optimal echo placement
4
2
0
-2
-4

OP-24

Online hyperthermia treatment planning and delivery: Combining microwave imaging and heating

M. Zanoli[1,2], M. Jansen[1], H. Dobšíček Trefná[2], K. Sumser[3], M. Paulides[3], S. Curto[1]

[1]Erasmus University Medical Center Rotterdam, Radiotherapy, Rotterdam, Netherlands
[2]Chalmers University of Technology, Electrical Engineering, Gothenburg, Sweden
[3]Eindhoven University of Technology, Eindhoven, Netherlands

Introduction: Despite the long history and proven benefit of hyperthermia (HT) in the treatment of cancer, its clinical acceptance remains limited. Reasons for this can be attributed to one fundamental issue: the lack of control. Prescribed temperatures are difficult to achieve everywhere in the target, and dose-outcome relationships become challenging to determine. Measures to ensure treatment quality often result in stressful experiences for the personnel and the patient. The current trend towards MR-thermometry, while welcome and necessary, is only a partial solution, due to increased costs and cumbersomeness. In deep microwave HT, the use of the very same antenna array for the imaging, delivery, and monitoring of HT treatments could address several of these problems and make the clinical workflow more streamlined, as it is in radiotherapy. Here, we demonstrate the potential of an alternative HT workflow where the treatment plan is based solely upon the E-field and dielectric property distributions retrieved on-site via a novel microwave tomographic method compatible with HT applicators.

Methods: We present synthetic and experimental reconstructions at 434 MHz obtained from a numerical head and neck patient model and from a physical muscle phantom. We use a prototype applicator consisting of 16 antennas arranged inside an imaging/heating tank filled with deionized water. We prepare plans and perform heating at 434 MHz based on such reconstructions. In the synthetic case, the target and healthy tissue volumes are delineated in the original CT scan and registered to the contours of the reconstructed object. The plan is obtained by optimizing the power loss density (PLD) distribution derived from the reconstructed E-field and conductivity distributions. We validate the plan by feeding the antenna settings to commercial simulation software and obtaining the steady-state temperature distribution. In the experimental case, we focus on the center of the phantom and collect an infrared image after heating at 500 W for 10 minutes.

Results: Synthetic results for the patient model are reported in Fig. 1. Despite the resolution limits imposed by the large wavelength (7.8 cm in water), the accuracy is enough to optimize a plan to adequately heat a target volume located deep in the head. The target temperature (T90) is 41 °C, for a maximum healthy tissue temperature of 44 °C. Experimental results for the muscle phantom are reported in Fig. 2. The position of the phantom and its properties are retrieved at the imaging step. The infrared image confirms the presence of the central focus.

Conclusion: A novel approach to the planning and delivery of microwave HT treatments combining imaging and heating is reported and demonstrated. Microwave tomography seems sufficient for the planning, control, and monitoring of HT treatments. In ongoing work, we compare the novel approach to established offline treatment planning workflows in terms of robustness and accuracy.

Fig. 1

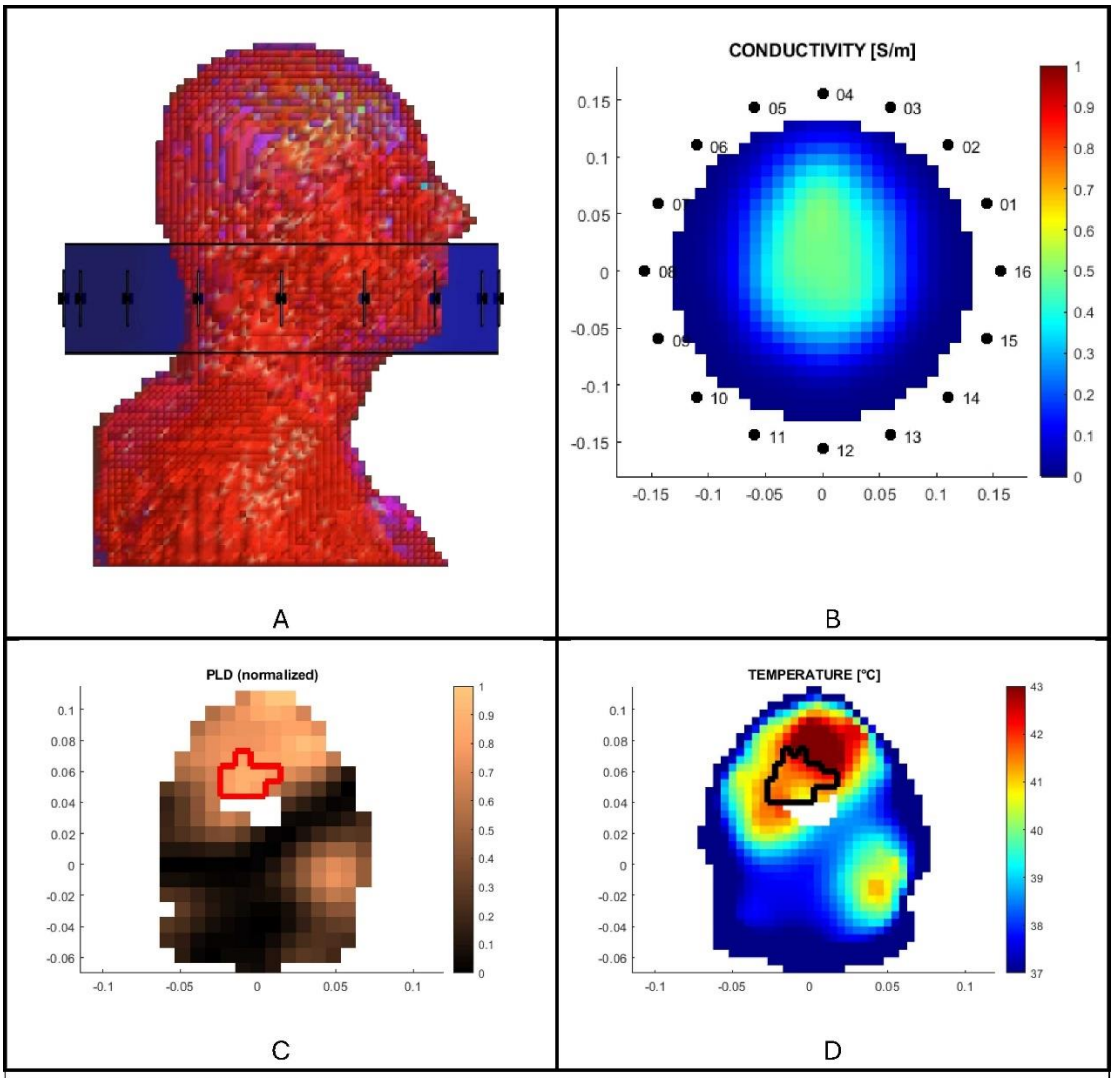

Figure 1: The synthetic patient and applicator models (water bolus + 16 antennas) are shown in Fig. 1A, side view. The reconstructed conductivity distribution is shown in Fig. 1B, transverse section at the array plane. The planned PLD distribution, based on tomographic data and clipped to the registered CT masks, is reported in Fig. 1C, with target contour in **red**. The resulting steady-state temperature distribution, based on an external simulation, is reported in Fig. 1D, with target contour in **black**.

Fig. 2

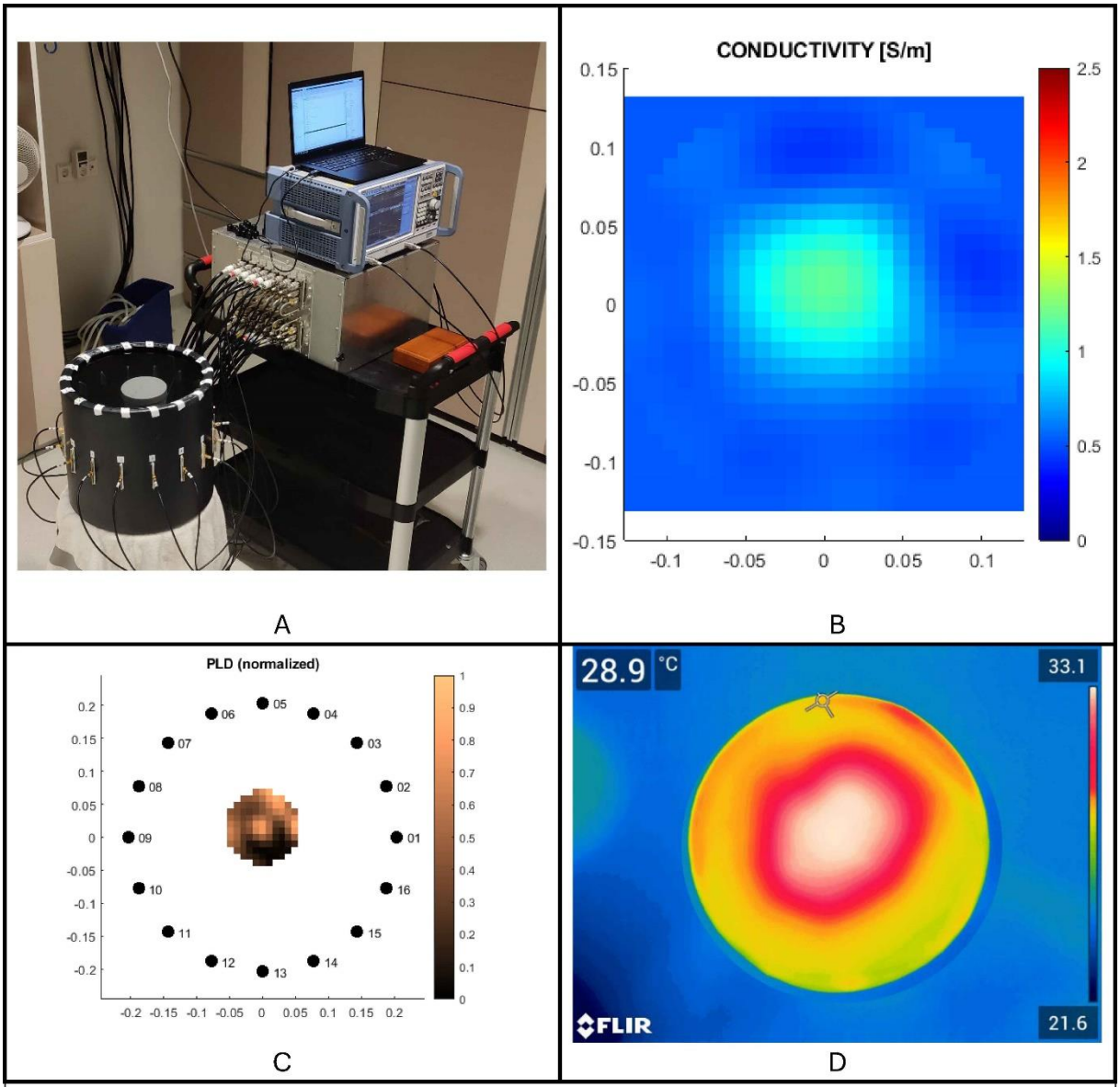

Figure 2: The experimental setup consisting of an applicator with 16 antennas, a cylindrical muscle phantom, and a switching system to alternate between imaging and heating, is shown in Fig. 2A. The reconstructed conductivity distribution is shown in Fig. 2B. Compare this with the actual phantom conductivity measured via dielectric probe: 0.95 [S/m]. The planned PLD distribution is reported in Fig. 2C. The resulting temperature distribution inside the split phantom at the array plane is reported in Fig. 2D.

OP-26

Feasibility and tolerance of deep hyperthermia combined with radiochemotherapy in locally advanced rectal cancer: First spanish experience

B. Salas-Salas[1], L. Ferrera-Alayón[1], A. A. Alayón Afonso[1], M. Sanchez-Carrascal[1], L. Lopez Molina[1], M. R. Elzo Vega[1], R. A. Hernandez-Santana[1], M. Lloret Saez-Bravo[1]

[1]Hospital Universitario de Gran Canaria DR. Negrín, Radiation Oncology, Las Palmas de Gran Canaria, Spain

Introduction: Hyperthermia has the potential to increase tumor cell sensitivity to both radiation and chemotherapy. This study focused on evaluating the feasibility, tolerability, and safety of integrating hyperthermia with conventional neoadjuvant treatment in patients with locally advanced rectal cancer (LARC).

Material and methods: From January 2020 to August 2023, patients with locally advanced rectal cancer (LARC) were considered for hyperthermia treatment in combination with standard neoadjuvant therapy and were enrolled in this prospective study (EudraCT 2020-335-1). Exclusion criteria included metal prosthesis in the treatment area, pacemaker, massive effusions (pleural or ascites), open wounds, abscesses, burns, hemorrhages, sensory disturbances, pregnancy, and patient refusal. Patients were treated with either short course radiotherapy (SCRT) of 5 Gy in 5 fractions or long course radiotherapy (LCRT) of 2 Gy in 25 fractions, following different chemotherapy regimens as per the tumor board's protocol. Hyperthermia was administered twice weekly for 60 minutes during radiotherapy (RT) using the ALBA 4D deep hyperthermia device. Tolerance and toxicity were evaluated using the integrated CTCAE 4.03/QMHT criteria, with an additional assessment of tolerance reported via the UMC scale.

Results: Of the 123 patients considered, 67 met the inclusion criteria and were enrolled in the study: 34 (50.7%) in the short-course radiotherapy (SCRT) group and 33 (49.3%) in the long-course radiotherapy (LCRT) group. A total of 243 hyperthermia sessions were conducted during radiotherapy (RT): 65 sessions for SCRT and 178 sessions for LCRT. All 34 patients (100%) in the SCRT group completed more than 50% of the prescribed sessions, whereas 21 out of 33 patients (63.64%) in the LCRT group achieved this adherence. The median and mean temperatures achieved during SCRT were 40.33°C and 40.37°C, respectively (range 38.72-41.45°C). For LCRT, the median and mean temperatures were 40.44°C and 40.21°C, respectively (range 38.56-41.66°C). Details of the temperature data are shown in Table 1.

Tolerance to the treatment varied among patients, as detailed in Table 2. Hyperthermia treatment was interrupted in 23 patients (34%) due to several reasons: pain in the treatment area (47.8%), radiotherapy toxicity (21.7%), technical issues (17.4%), pressure in the treatment area (8.7%), and claustrophobia (4.3%). Only 14 patients (20.9%) experienced grade 3 gastrointestinal toxicity from radiochemotherapy. The main symptoms among these patients included hemorrhoids, rectal obstruction, and diarrhea. All patients completed the prescribed course of radiotherapy without interruptions and underwent surgery within the scheduled timeframe.

Conclusions: Integrating regional hyperthermia with standard neoadjuvant therapy is a feasible and safe approach that enhances the treatment for locally advanced rectal cancer.

Fig. 1

Table 1. Temperature details.

Short Course					
T10	**T50**	**T90**	**TMin**	**Tavg**	**TMax**
40,99	40,99	40,99	40,99	40,99	40,99
Long Course					
T10	**T50**	**T90**	**TMin**	**Tavg**	**TMax**
41,14	40,44	39,48	38,56	40,21	41,66

Fig. 2

Table2. Effects observed by patients during hyperthermia sessions. Some patients encountered multiple effects throughout the sessions.

Effects on patients	Number of Patients	Percentage (%)
Pain		
Gluteus	40	59,7
Abdomen	33	49,2
Pelvis	29	43,3
Thighs	27	40,3
Dorsolumbar region	10	14,9
Lower limbs	5	7,5
Sensations		
Warm skin	21	31,3
Discomfort	15	22,4
Pressure from the bolus	14	20,9
Tingling	8	11,9
Deep pressure	7	10,4
Arterial hypotension	4	6
Other Effects		
Claustrophobia	3	4,5
Urinary urgency	2	3
Bradycardia, Tachycardia, Arterial hypertension, Dizziness, Shortness of breath	1	1,5

OP-27

Hyperthermia enhances spatially-fractionated radiation and immunotherapy in pre-clinical tumor models

S. V. Jenkins[1], A. Jamshidi-Parsian[1], A. Brint[1], H. Campbell[1], R. P. M. Dings[1], R. Griffin[1]

[1]UAMS, Radiation Oncology, Little Rock, AR, United States

Hyperthermia has been well-established as a radiation sensitizer and well as an immune adjuvant in pre-clinical and clinical settings. Spatially fractionated radiation therapy (heterogeneous dosing) offers the potential to spare normal tissues as well as spare immune cells in residence within the tumor and may enable improved antigen production/education of immune cells and retention of immunological memory. Both hyperthermia and spatial fractionation can be augmented using immune checkpoint inhibitor (ICI) therapies. Thermal therapy is associated with stimulation of the immune system and increased radiation sensitivity via increased oxygenation and inhibition of DNA repair. Spatial fractionation has also been demonstrated to induce local and remote bystander effects in the form of cytotoxicity and immune/abscopal actions. We thus hypothesized that combined hyperthermia and radiation might significantly increase the degree and frequency of response to ICI. Murine head and neck tumors (SCCVII) were implanted in immunocompetent (C3H) mice and treated with combinations of spatially fractionated radiation, immune checkpoint inhibitors, and mild hyperthermia. In vitro clonogenic assays revealed that hyperthermia causes a significant decrease in proliferative capacity when applied before or following radiation therapy. Our spatial fractionation system (GRID) is a honeycomb pattern with peak dose of 20 Gy and a valley dose of 3 Gy. Peak fields were 2 mm in diameter spaced 3 mm apart edge to edge. GRID alone did not significantly affect tumor growth relative to untreated controls. Addition of immune checkpoint inhibitors applied 3, 5 and 7 days after GRID, specifically anti-PD1 and anti-CTLA-4, led to tumor remission in more than 60% of tumors. Interestingly, application of 1 hour of hyperthermia at 42.5 °C immediately following GRID radiation and immunotherapy

resulted in less tumor growth delay and a lower percentage of remission. However, application of hyperthermia immediately prior to GRID radiation resulted in a similar growth delay as with GRID and ICI alone, but an overall increase in the percentage of tumor remission. Mice that demonstrated full remission were re-challenged by inoculation of the same tumor cell line, which resulted in delayed growth of the new tumor, but did not prevent tumor re-establishment. We are currently assessing the effect of hyperthermia and GRID combined on hypoxic cell bystander and direct effects on survival, immune recruitment and adhesion molecule expression.

OP-28

Phase I study of THE001 (DPPG2-TSL-DOX) combined with regional hyperthermia in patients with locally advanced or metastatic soft tissue sarcoma

D. Di Gioia[1], P. Reichardt[2], S. E. Güler[1], G. Schuebbe[1], S. Ghani[2], Z. Haramiova[3], F. Hermann[3], L. Lindner[1,3]

[1]LMU Munich, Department of Medicine III, University Hospital, Munich, Germany
[2]Helios Klinikum Berlin-Buch and Medical School Berlin, Berlin, Germany
[3]Thermosome GmbH, Martinsried, Germany

Objective: Doxorubicin (DOX) is the most relevant chemotherapy (CTx) for treatment of soft tissue sarcomas (STS). Regional hyperthermia (RHT) was shown to improve survival in locally advanced high-risk STS when combined with DOX-based CTx. THE001 ($DPPG_2$-TSL-DOX) is an innovative thermosensitive liposomal formulation of DOX, based on phosphatidyldiglycerol as key membrane component. After IV administration, THE001 releases DOX in the bloodstream once the temperature in the target area is above 40°C. The application of THE001 with RHT resulted in preclinical models in up to 15-fold higher DOX concentrations in the tumor and is expected to improve clinical treatment efficacy.

Methods: THE001 alone and in combination with RHT is investigated in an open-label, dose-escalation phase 1 study in participants with heavily pretreated locally advanced/metastatic STS and at least disease control on initial DOX-containing therapy (NCT05858710). The study explores different doses of THE001 as monotherapy and is applied in 21-day cycles to identify the maximum tolerated dose (MTD). From cycle 2, RHT is performed simultaneously. Tumor response is determined according to RECIST 1.1, and Choi criteria and safety findings reviewed by an independent Data Safety Monitoring Board. THE001 study began enrolling participants in April 2023 and is conducted in Germany at the LMU Klinikum Munich and the Helios Klinikum Berlin-Buch. Here, we report initial feasibility, safety, pharmacokinetic (PK), and anti-tumor activity results for THE001+RHT.

Results: At cut-off date 10 June 2024, no dose-limiting toxicity (DLT) or adverse event $\geq$ grade 4 occurred in dose level 1 (20 mg/m²) and dose level 2 (40 mg/m²). The safety profile characteristics are comparable to and known from non-liposomal DOX, and no dedicated formulation-related or RHT-related AEs were observed. The PK profiles from dose level 1 during cycle 1 (without RHT) and cycle 2 (with RHT) could confirm the proposed mechanism with RHT-mediated DOX release and high peak concentrations of free DOX during RHT. Encouraging signs of clinical activity were observed even in the initial dose levels, including durable disease control in two out of four participants for the period of the initial therapy of 6 cycles, and subsequently the option for continuation in case of disease control for another 6 cycles has been implemented.

Conclusions: THE001 is well-tolerated as monotherapy and in combination with RHT in the ongoing phase 1 study and confirms the feasibility of this innovative combined modality. Signs of clinical activity in heavily pretreated STS participants, together with the PK profile, indicate the potential of THE001+RHT as a promising tumor-targeted therapy with heat-triggered release of high peak concentrations of DOX in the tumor together with systemic exposure as a potential future treatment option for DOX-sensitive tumors such as STS. Recruitment is ongoing and further updates will be reported at upcoming conferences.

OP-29
Hyperthermia clinicals trials in Catalan Institute of Oncology: Initial results

M. Arangüena Peñacoba[1], J. Jové Teixido[2], S. Villà Freixa[2], M. A. Eraso Urién[3], C. Gutiérrez Miguélez[1], E. Martínez Pérez[1], H. Pérez Montero[1], J. González Viguera[1], L. Asiaín Azcárate[1], J. Valera Muñoz[1], M. C. Siria Lóez[1], J. Martínez González[1], P. Fernández López[1], M. Ventura Bujalance[1], F. Guedea Edo[1]

[1]Instituto Catalán de Oncología, Radiation Oncology, Barcelona, Spain
[2]Instituto Catalán de Oncología, Radiation Oncology, Badalona, Spain
[3]Instituto Catalán de Oncología, Radiation Oncology, Girona, Spain

Question: To evaluate whether Oncological Hyperthermia administered as adjuvant therapy to External Beam Radiotherapy is a safe technique that allows radical or palliative treatment of patients with locally advanced tumors without relevant acute or late toxicity in ICO Centers, as main objective, and local control at 6, 12 and 18 month and recurrence-free survival as secondary objective.

Methods: We have designed two open-label prospective Phase II Clinical Trials with 30 patients each: one for recurrences of breast cancer and another one for other locally advanced tumors, pelvic tumor relapses and palliative treatments for bone metastases. Patients are treated with External Beam Radiotherapy followed by twice-a-week hour-long Hyperthermia sessions, in non- consecutive days. Hyperthermia is given by a radiofrequency system with capacitive coupling with emission of non-ionizing waves.

Results: From September 2023 until June 2024, a total of 27 patients have been treated with Hyperthermia combined with Radiotherapy at ICO Hospitalet; 17 of whom were breast cancer recurrences, 2 pelvic recurrences, and 8 palliatives. The hyperthermia regimen comprised 4-6 sessions for palliative care and 10-12 sessions for breast cancer recurrence.

Regarding skin toxicity: Grade 0 in 12 patients (44.44%), Grade 1 in 7 patients (25.93% - 5 with radiodermatitis, 1 with hyperpigmentation, 1 with folliculitis), Grade 2 in 6 patients (22.22% - 5 with radiodermatitis, 1 with folliculitis), and focal Grade 3 in 4 patients (14.81%); taking into account that some patients have exhibited two different types of toxicities.

The Hyperthermia treatment tolerance was excellent in 23 patients (85.19%) and poor in 4 patients (14.81%) due to underlying disease pain/discomfort, extensive Grade 3 radiodermatitis, immune-mediated rectal bleeding not related to the treatment, and one patient requiring reduced power due to pain. Three of these 4 patients were withdrawn from the study.

Conclusion: Based on our experience, Hyperthermia is a safe treatment and to date the observed toxicity aligns with that typically associated with conventional Radiation Therapy alone.

Furthermore, a substantial body of scientific evidence strongly advocates for the use of hyperthermia to enhance local disease control. Consequently, our aim is to contribute with further evidence to solidify the integration of hyperthermia as a standard treatment modality in the future.

OP-30
Interim results of the european registry study for the treatment of recurrent glioblastoma (2019-2023) using the NanoTherm Therapy System (NTTS)

A. Jordan[1,2,3,4]

[1]Centrum Medyczne HCP Sp. z o.o., Dr. Jacub Moskal, Poznan, Poland
[2]Paracelsus Klinik Zwickau, Prof. Jan Peter Warnke, Zwickau, Germany
[3]Hufeland Klinik, Neurosurgery, PD Dr. Johannes Wölfer, Muehlhausen/Ruhr, Germany
[4]Medical University of Lublin, Department of Neurosurgery and Pediatric Neurosurgery, Prof. Radoslaw Rola, Lublin, Poland

Introduction: Since Penny Sneed et al published their resultsin 1998 about the survival benefit of Hyperthermia in a prospective randomized trial of brachytherapy boost ± hyperthermia for Glioblastoma multifirme [1], thermotherapy still has not become standard in this tumor entity although the median overall survival is still 14 months on average if molecular genetic prognostic are not taken into account. A newer method to apply heat to GBM is called NanoTherm Therapy System (NTTS).

Results: Here in this contribution, we report on recent interim results of a European Registry Study. The trial design is an open label, prospective multicentre trial, being a non-randomized observational study. The molecular genetic status was assessed from the primary tumour resection, particularly the MGMT promotor status. Between 2019 and 2023, 45 patients mostly with recurrent GBM were treated with thermotherapy using NanoTherm® AS1 nanoparticle dispersion in addition to surgery and (radio)-chemotherapy; chemotherapy is mostly TMZ temozolomide. The designation "NanoPaste" has been coined to a technique of covering the wall of a resection cavity with NanoTherm using a mesh of oxidized regenerated cellulose as matrix and fibrin glue as sealant. A closed-end catheter is inserted for intracranial temperature monitoring. Postoperatively, all patients underwent six one-hour hyperthermia sessions in an alternating magnetic field (mean maximum temperature 43.7°C ± 3.0°C) and – if still possible after primary therapy – were simultaneously treated with temozolomide and/or radiotherapy. Median time from first diagnosis to treatment for recurrence including NTT was 10.6 months (min = 3.3, max = 43.6), OS1 was 24.1 months (95% CI 19 – 35.6), and OS2 was 8.9 months (95% CI 7.5 – 13.8).

MGMT promoter was methylated in 8 (22%), unmethylated in 13 (35%), and unknown in 16 (43%) rGBM patients. The resulting OS1 for methylated, unknown and non-methylated MGMT promoter were 32.1, 24.4, and 23.3 months, respectively. For OS2 the resulting values are 11.8, 8.3 and 8 months.

Conclusions: The registry data for intracavitary thermotherapy of rGBM with superparamagnetic iron oxide nanoparticles show relevant results. Median OS for the total rGBM sample was 24.1 months, and even the non-methylated subgroup reached a median OS of 23.3 months. In our current series, only 5% of patients required surgical removal of nanoparticles due to refractory edema, thus indicating that the most serious specific adverse event can be effectively controlled.

The application of hyperthermia in the treatment of malignant tumors is well established in many areas apart from neurosurgery. With NTTS, this method is now also available for the treatment of glioblastoma. The reported results demonstrate efficiency, (improved) safety, and manageability of this treatment method.

Fig. 1

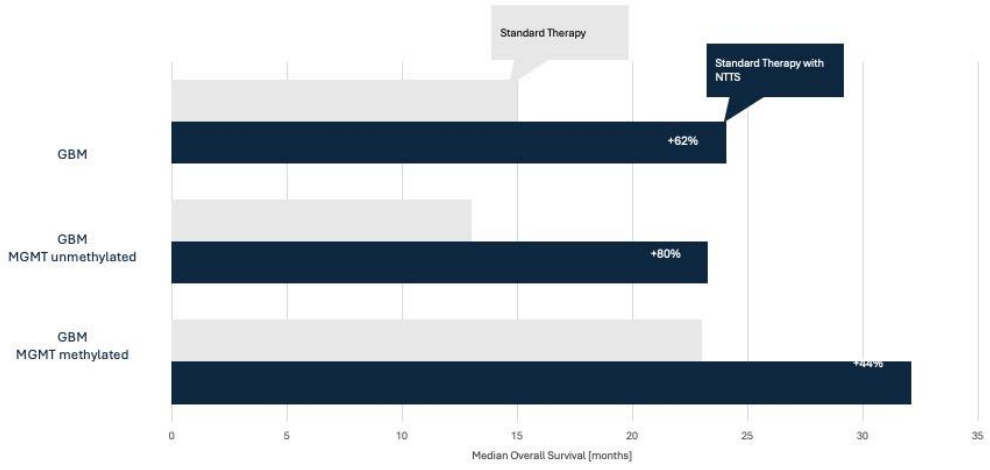

Multicenter Post-Market-Clinical Follow-up (PMCF) Data NTTS 2021-2023

OP-31

A pilot study of chemoimmunotherapy combined with deep hyperthermia and spatially-fractionated radiotherapy in advanced biliary tract cancer

J. Molitoris[1,2], D. Rodrigues[1,2], K. Baker[3,2], C. Eggleston[3,2], S. Mossahebi[1,2], M. Zakhary[1,2], A. Ciner[1]

[1]University of Maryland School of Medicine, Baltimore, MD, United States
[2]Maryland Proton Treatment Center, Baltimore, MD, United States
[3]University of Maryland Medical Center, Baltimore, MD, United States

Advanced Biliary Tract Cancers (BTCs) have a poor prognosis despite recent advances including the addition of checkpoint blockade to platinum-based chemotherapy. Novel techniques, including hyperthermia therapy (HT) and spatially fractionated radiotherapy (SFRT), can positively modulate the tumor microenvironment and potentially broaden the patient population who respond to frontline systemic therapy. In this single-arm pilot study, we plan to enroll up to 15 patients and assess the safety and feasibility of combining chemoimmunotherapy with deep HT and SFRT in patients with locally advanced unresectable or metastatic BTC. Per standard practice, participants in this study will receive up to 8 cycles of gemcitabine and cisplatin on days 1 and 8 and durvalumab on day 1 of each cycle (21 days/cycle). In addition to this chemoimmunotherapy regimen, HT and SFRT will be administered to 1 measurable lesion on cycle 2-day 1 and HT alone will be delivered to the same lesion on day 1 for cycles 3 and 4. Feasibility is defined as the ability of participants to receive a minimum of 30 minutes of heating at the target temperature (39-43°C) for at least 2 of the planned 3 deep HT treatments. We will monitor the temperature continuously using an intraluminal probe in the stomach/duodenum, placed via a nasopharyngeal tube, and verify its position relative to the tumor volume with CT immediately prior to HT treatment. Additional intraluminal temperature probes will be placed in the rectum, vagina, or bladder as recommended by the physician. Safety is defined by < 30% rate of grade 3 or higher non-hematologic adverse events. Radiographic response rates, oncological outcomes and immunological correlates will also be evaluated. Our protocol is FDA approved and undergoing IRB review, with expected enrollments to begin in September 2024.

OP-32

A randomized phase III trial comparing trabectedin to trabectedin combined with regional hyperthermia in patients with pre-treated soft tissue sarcoma: HyperTET a German Interdisciplinary Sarcoma Group (GISG) trial

G. Schuebbe[1], L. Lindner[1], D. Di Gioia[1], Y. Xu[2], E. Kampmann[1], S. Abdel-Rahman[1], W. Kunz[3], T. Roshchyna[1], R. Fenderle[1], V. Bücklein[1], P. Reichardt[4], D. Pink[5], A. Flörcken[6], R. Fietkau[7], U. Mansmann[2], R. D. Issels[1]

[1]LMU Munich, Department of Medicine III, Munich, Germany
[2]LMU Munich, Institute of Medical Informatics, Biometry, and Epidemiology, Munich, Germany
[3]LMU Munich, Department of Radiology, Munich, Germany
[4]Helios Klinikum Berlin-Buch, Berlin, Germany
[5]Helios Klinikum Bad Saarow, Bad Saarow, Germany
[6]Charité Universitätsmedizin Berlin, Department of Hematology, Oncology and Tumorimmunology, Berlin, Germany
[7]University Hospital Erlangen, Department of Radiation Therapy, Erlangen, Germany

Question: The German Sarcoma Group assessed the efficacy and safety of trabectedin (Tr) versus trabectedin plus regional hyperthermia (Tr + RHT) in patients with soft tissue sarcoma (STS) as treatment after progression following previous chemotherapy. In this trial, all patients received Tr in accordance with European Commission approval, while half of the patients additionally received RHT, adhering to the ESHO Quality Guidelines (Bruggmoser 2011).

Methods: The HyperTET trial was a multicenter, open-label, randomized phase III study in patients with histologically confirmed STS who progressed with local tumor or development of distant disease after ≥ one prior treatment lines. The study was carried out in 5 tertiary study centers in Germany. Pts were randomized (1:1) to receive either Tr 1.5 mg/m2 (24-hour infusion) every 3 weeks or Tr 1.5 mg/m2 (24-hour infusion) every three weeks combined with RHT (1-hour at the end of Tr infusion). Patients were stratified into histological type (L-STS (lipo-/leiomyosarcoma) vs non-L-STS), subsequent after incomplete surgery (yes/no), metastasis (yes/no), and ECOG (0 vs 1/2). The primary efficacy endpoint was progression-free survival (PFS) analyzed in the intention-to-treat population. Secondary objectives include assessing radiological response, overall survival (OS), and treatment-related toxicity through descriptive analysis for both treatment groups.

Results: From December 19, 2014, to December 7, 2021, 118 pre-treated patients from 5 German centers received either Tr (n=58) or Tr + RHT (n=60). Prior chemotherapy was given in the neoadjuvant/adjuvant setting to 55.3% in the Tr arm and 65.0% in the Tr + RHT arm. Enrolled patients received either Tr or Tr + RHT as second to fourth-line treatment. Additionally, 44.8% in the Tr arm and 55.0% in the Tr + RHT arm had previously received chemotherapy combined with RHT. Further baseline characteristics were well balanced between both treatment arms. In the Tr arm, 60.3% of patients had an ECOG 0, and 36.2% had an ECOG 1/2. In the Tr + RHT arm, 61.7% had an ECOG 0, and 35.0% had an ECOG 1/2. The proportion of L-STS was 69.0% in the Tr arm and 61.7% in the Tr + RHT arm. Overall, 80.5% of patients were metastatic, with 79.3% in the Tr arm and 81.7% in the Tr + RHT arm. Median cycles per patient were 4 (IQR 2-6) for Tr, with 36.2% receiving ≥ 5 cycles, and 3 (IQR 2-6.2) for Tr + RHT, with 30.0% receiving ≥ 5 cycles. In the Tr arm, 58.7% of cycles were given without delay or dose reduction, compared to 59.2% in the Tr + RHT arm. At least 80% of the dose was administered to 89.5% of patients in the Tr arm and 84.8% in the Tr + RHT arm. Dose modifications or delays, mostly due to hematological toxicity, were needed in 11.5% of Tr cycles and 15.2% of Tr + RHT cycles.

Conclusion: The study's initial results for the primary endpoint, secondary objectives and toxicity will be presented at the congress.

Clinical trial information: NCT02359474

Trial supported by PharmaMar.

OP-33
Feasibility and safety of MR guided high intensity focused ultrasound-induced hyperthermia in large volume near bone structure

M. Ayary[1], H. Grüll[1,2], J. Lindemeyer[1,2]

[1]Uniklinik Köln, Cologne, Germany
[2]Uniklinik Köln, Radiology, Cologne, Germany

Question: MR-guided High-Intensity Focused Ultrasound is a versatile, non-invasive therapeutic approach with a wide range of clinical applications. Mild hyperthermia which involves raising tissue temperature to a range of 40-43 °C for up to 60 minutes, has shown potential as an adjuvant therapy alongside radiotherapy and chemotherapy, as well as in combination with temperature-responsive drug delivery systems to enhance efficacy and minimize systemic toxicity[1]. However, treating tissue near bone structures presents a challenge due to acoustic energy attenuation caused by scattering and absorption, which can limit or alter the amount of heat delivered to the target area. This study investigates safety and spatial temperature distribution during MR-HIFU-mediated hyperthermia near bone structures.

Methods: To evaluate the feasibility of delivering hyperthermia near bone, we designed polyacrylamide-based tissue-mimicking phantoms with embedded Neoptix® TS1 Fiber Optic probes to provide reference temperature measurements. Using a clinical MR-HIFU system (3T Achieva®, Philips Healthcare; Sonalleve® V2 Transducer, Profound Medical), we investigated hyperthermia application in three scenarios, varying the focal distance from the bone: far field, near field, and lateral exposures. Employing a feedback loop temperature control system [2] we utilized three treatment cell sizes, measuring 18 mm, 32 mm, and 44 mm in diameter. Field drift was handled using a software-featured algorithm and a hand-drawn reference ROI around the treatment cell.

Results: The desired temperature range in the target area at focal depth was reached in all but one hyperthermia experiment, and was successfully maintained (Fig.1). MR thermometry demonstrated high accuracy, with measurements closely aligning with fiber optic sensor readings (average difference: -0.9 ± 0.5°C). Bone heating effects were observed, with heat reflection occurring after approximately 5 min when the focal target was at 25 mm from the bone surface, all sonications were successfully completed, with durations ranging from 30 to 60 min (Fig.2). Heat diffusion within the bone during the cooling period was observed, which helped to prolong hyperthermia duration in the target region before returning to baseline temperature.

Conclusion: The use of a feedback loop control system allowed for accurate and stable temperature maintenance within the target zone. While heating effects around the bone were observed, they could be mitigated by

incorporating a spatial safety margin. Notably, heat diffusion within the bone was observed to prolong hyperthermia duration in the target region. These findings suggest that MR-HIFU-mediated Hyperthermia has the potential to be a safe and effective treatment modality near bone structures.

Figure 1 Hyperthermia in 32 mm Treatment Cell temperature map in coronal (left) and sagittal (right) slices across HIFU Beam

Figure 2 MR Thermometry in 32 mm Treatment Cell (Above), MR temperature measurement versus fiber optic sensor in 32 mm Treatment Cell: 35 mm Target Depth to Bone (Below)

[1] *Partanen et al., International journal of hyperthermia, 2012*

[2] *Tillander et al., American Association of Physicists in Medicine,2016*

Fig. 1

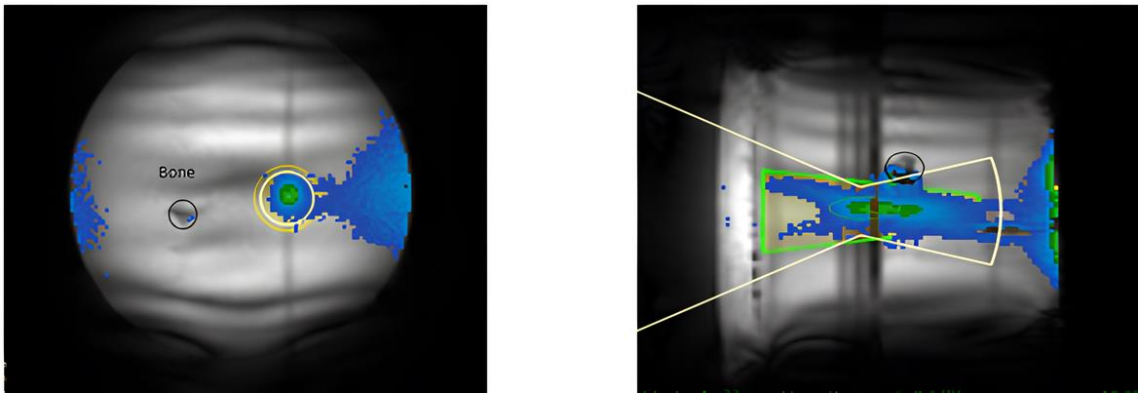

Fig. 2

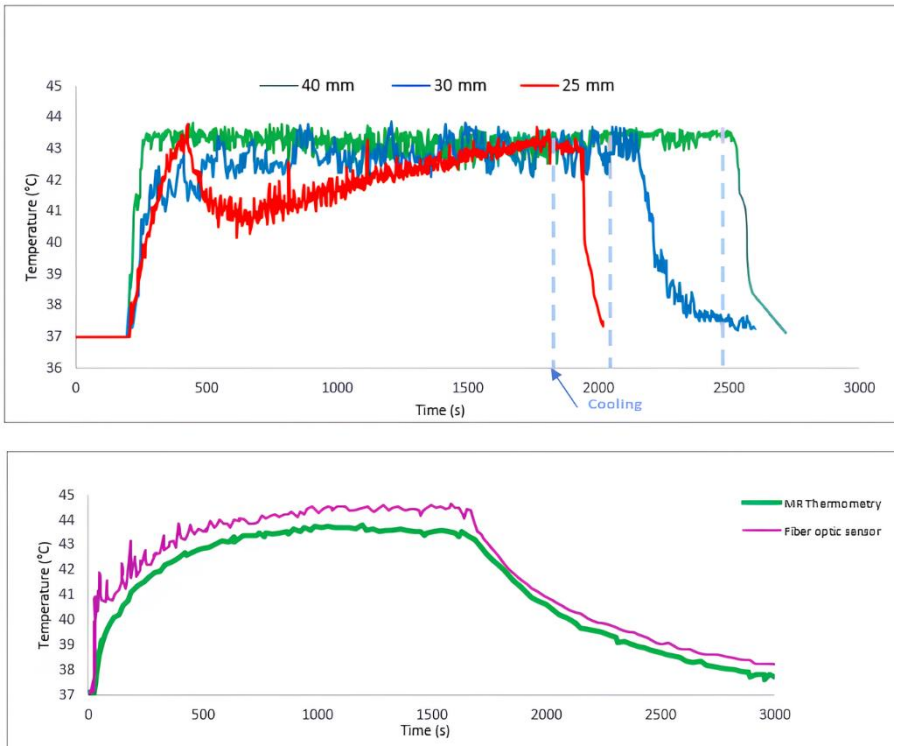

OP-34

The role of regional deep hyperthermia (RHT) and hyperthermic intraperitoneal chemotherapy (HIPEC) in children and adolescents with disseminated abdominal desmoplastic small round cell tumors (DSRCT)

R. Wessalowski[1], C. Staude[2], K. Harder[1], O. Mils[1], D. Klee[3], C. Matuschek[4], C. Vokuhl[5], W. T. Knoefel[2]

[1]Heinrich-Heine University, Medical Faculty, Duesseldorf, Germany
[2]Heinrich-Heine University, Medical Faculty, Department of General, Abdominal and Pediatric Surgery, Düsseldorf, Duesseldorf, Germany
[3]Heinrich-Heine University, Medical Faculty, Department of Pediatric Radiology, Duesseldorf, Germany
[4]Heinrich-Heine University, Medical Faculty, Department of Radiation Oncology, Duesseldorf, Germany
[5]University Hospital Bonn, Section of Pediatric Pathology, Department of Pathology, Bonn, Germany

Question: Desmoplastic small round cell tumors (DSRCTs) are rare but aggressive soft tissue tumors that occur mainly in adolescents and young adults. They usually appear as an extensive serosa infiltration of the abdominal cavity and have a fatal outcome in almost all cases. We wanted to determine whether objective response and complete remission can be achieved in patients with disseminated abdominal DSRCTs by salvage chemotherapy with additional regional deep hyperthermia and cytoreductive surgery ± hyperthermic intraperitoneal chemotherapy (HIPEC).

Methods: This single-arm prospective trial enrolled patients aged ≤25 years with histologically confirmed disseminated abdominal DSRCTs. PEI-chemotherapy consisted of cisplatin 40 mg/m2 or carboplatin 200 mg/m2 administered intravenously on days 1+4; etoposide 100 mg/m2 intravenously on days 1-4; and ifosfamide 1800 mg/m2 intravenously on days 1-4 plus concomitant 1-hour regional deep hyperthermia (41-43°C) on days 1+4. Patients received two to four treatment courses at 21-day intervals until residual tumor resection ± HIPEC was possib le; in case of a response they subsequently received two to four additional courses of PEI-regional deep hyperthermia. During HIPEC procedure chemotherapy was administered through 4 to 5 capillary drains in the peritoneal cavity for 60-90 minutes with an inflow-temperature varying between 41-42°C. Drugs for HIPEC consisted of cisplatin 60-100mg/m2 ± doxorubicin 15 mg/m2. The primary endpoint was the proportion of patients who had an objective response as assessed with Response Evaluation Criteria in Solid Tumors version 1.0 guidelines.

Results: Eleven patients aged 4;6-23;9 years (median17;5 years) with disseminated abdominal DSRCTs were enrolled in this study. At diagnosis, all patients were treated according to the guidelines of the Cooperative Soft Tissue Sarcoma Study Group (CWS guidance). Salvage therapy with PEI chemotherapy was combined with a total of 127 abdominal RHT treatments. In addition, 7 patients underwent HIPEC with cisplatin ± doxorubicin after cytoreductive surgery. Of the 11 patients, 8 had an objective response to treatment, 2 no change, 2 progressive disease. Nine of 11 patients received cytoreductive surgery (R1 resections in six patients, R2 resections in two patients). The follow-up period of our patients n was 5-53 months.

Conclusions: A multimodal strategy integrating PEI-regional deep hyperthermia and tumor resection ± HIPEC can achieve a complete remission in children and adolescents with disseminated abdominal DSRCTs. Accurate patient selection plays a key role in treatment related outcome and requires intensive cooperation between pediatric oncologists and surgeons. To improve long-term survival, further immunological or targeted therapy strategies are required to control residual tumor cells in the future.

Funding: Deutsche Krebshilfe e. V., Bonn, Elterninitiative Kinderkrebsklinik Düsseldorf e. V.

OP-35

Temperature optimization for locoregional hyperthermia accounting for tissue-property uncertainties using polynomial chaos expansion

T. D. Herrera[1], J. Groen[1], J. Crezee[1], H. P. Kok[1]

[1]Amsterdam University Medical Center, Radiation Oncology, Amsterdam, Netherlands

Question: Conventional temperature optimization in Hyperthermia Treatment Planning, aiming at maximising the tumor temperature (typically T90; the temperature reached in at least 90% of the tumor), with hard normal tissue temperature constraints (≤45°C), is accurate, but only assuming correct tissue/perfusion properties. In this work

we analyzed options to increase the reliability of temperature optimization for clinical application by developing novel robust optimization strategies that reduce the impact of tissue/perfusion property uncertainties.

Methods: Within Plan2Heat, temperature calculations during optimization apply efficient superposition of precomputed distributions using a temperature matrix (T-matrix), calculated with average tissue properties (dielectric properties, thermal properties and perfusion values). We extended the superposition method and combined it with stochastic Polynomial Chaos Expansion (PCE) models. We computed an average T-matrix (Tavg), representing the average temperature of 10.000 PCE samples with different tissue properties, and a covariance matrix C. This allows to estimate the average temperature and standard deviation by superposition. This was used in optimization and three new strategies were implemented:

(1) Tavg90 maximization, with a hard constraint on normal tissue temperature (max(Ttissue)),

(2) Tavg90 maximization, with a hard constraint on normal tissue temperature variation, and

(3) combined Tavg90 maximization and variation minimization, with a hard constraint on max(Ttissue).

Conventional and new optimization strategies were tested in a cervical cancer patient treated using the 70 MHz 4-waveguide ALBA4D system. One-hundred test cases were generated randomly sampling tissue-property probability distributions. Temperature distributions for conventional and new optimizations were calculated for each sample, comparing tumor T90 and the number of constraint violations (max(Ttissue)>45°C).

Results: Conventional optimization had 28 test cases without constraint violation, with a median T90 of 39.7°C. For strategies (1), (2) and (3), the number of samples without constraint violation increased to 33, 41 and 36, respectively. Median T90 was reduced only slightly, by ~0.1-0.3°C, for strategies (1-3). Also tissue volumes exceeding 45°C and variation in max(Ttissue) were less for the novel strategies, implying that fewer complaints would occur, requiring fewer and less extreme phase-amplitude adjustments, while maintaining the same T90 levels.

Conclusion: Optimization strategies considering tissue-property uncertainties demonstrated lower probability of normal tissue constraint violations, with marginal reduction in tumor T90. This suggests a potential clinical utility in reducing the need for device setting adjustments during hyperthermia treatment. The reduction in variation and volume of constraint violation also indicates that, when adjustments are needed, these could be less aggressive.

Fig. 1

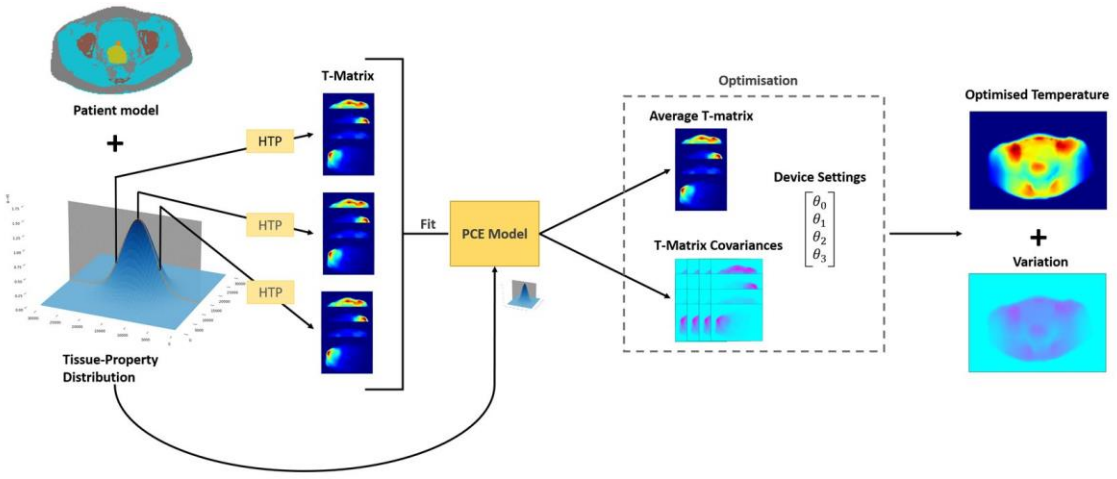

Figure 1. Workflow for robust temperature calculation and optimization using PCE models for the T-matrix elements. Using Polynomial Chaos Expansion (PCE), surrogate models are created for each element of the decomposed temperature matrix (T-matrix). The models are then used to estimate the average T-matrix and T-matrix variation (covariance matrix). Fast evaluation of device settings is performed using multiplication of device settings and the average T-matrix or the covariance matrix, resulting in the average temperature distribution or the standard deviation respectively.

Fig. 2

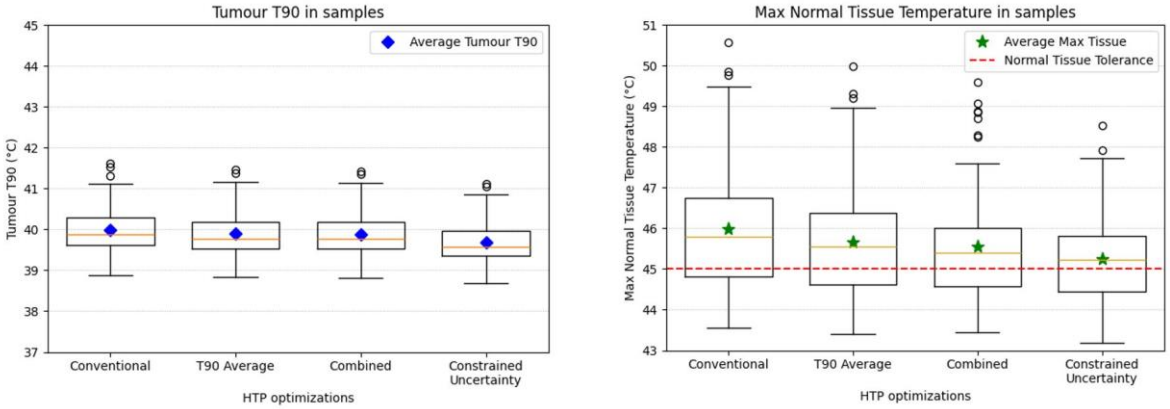

Figure 2. Box plots for the temperature reached in at least 90% of the tumour (T90) and maximum tissue temperature (max(T_{tissue})). The data are from 100 samples generated randomly from tissue-property distributions. Conventional temperature optimization was compared with PCE-model-based strategies that include the average T-matrix and covariance matrix: T90 Average (T_{avg}90 maximization, with a hard constraint on max(T_{tissue})), Constrained Uncertainty (T_{avg}90 maximization, with a hard constraint on normal tissue temperature variation), and Combined (T_{avg}90 maximization and variation minimization, with a hard constraint on max(T_{tissue})). Normal tissue tolerance of 45°C is shown as a dashed line. The novel optimization strategies achieve an important reduction in the variation of maximum normal tissue temperature with only a marginal reduction of tumour T90.

OP-36
Local temperature gradients and induced cell death in intracellular magnetic hyperthermia

A. Millan[1], Y. Gu[1,2], R. Pinol[1], C. Brites[3], R. Moreno-Loshuertos[4,5], J. Zeler[3,6], A. Martínez[7], G. Maurin[1], P. Fernández-Silva[4,5], J. Marco-Brualla[4,5], P. Téllez[1], R. Cases[1], R. Navarro Belsué[1], D. Bonvin[8], L. D. Carlos[3]

[1]INMA-CSIC, BioNanoMedicine, Zaragoza, Spain
[2]University Jaume I, Castellón, Spain
[3]University of Aveiro, Aveiro, Portugal
[4]University of Zaragoza, Bioquímica, Biología Molecular y Celular, Zaragoza, Spain
[5]University of Zaragoza, Instituto de Biocomputación y Física de Sistemas Complejos, Zaragoza, Spain
[6]University of Wroclaw, Faculty of Chemistry, Wroclaw, Poland
[7]University of Zaragoza, Electrónica de potencia, Zaragoza, Spain
[8]Ecole Polytechnique Fédérale de Lausanne, Lausanne, Switzerland

Question: The local intracellular magnetic hyperthermia hypothesis proposes that local temperature increases can be generated on internalized magnetic nanoparticles (MNPs) high enough to produce cell apoptosis without affecting the global cell temperature (Figure 1). That means destroying cancer cells with a small heat supply, and no damage to the adjacent healthy tissue.

Theoretical calculations predict that temperature gradients in internalized MNPs are not physically possible. However, most of experimental results of magnetic hyperthermia in MNPs suspensions as well as a previous experiment in life cells indicate the contrary.

We have measured the local temperature on cell internalized MNPs in during magnetic hyperthermia, and evaluated the cell apoptosis performance of this treatment.

Methods: Temperature was determined from the luminescent emission of two lanthanide complexes. Two types of thermometric probes were used: 1) dual magnetic/thermometric nanoparticles with a magnetic core and polymer shell containing the lanthanide complexes;1 and 2) copolymer micelles containing the lanthanides in the hydrophobic part.2 Temperature imaging was realized in a fluorescence microscope incorporating a beam splitter, and a electromagnet immersed in the cell culture. Hyperthermia performance experiments on were realized under controlled temperature (37 oC) in a square ferrite electromagnet providing a uniform magnetic field to several culture wells.

Results: It was observed in the first set of experiments that the temperature on the MNP surface increased rapidly after the onset of the AMF (*Hf*=2.4´109 A·m−1·s−1, *H*=30 mT, *f*=100 kHz) and then reached a plateau at DT=10 oC. The increase of the temperature in the vicinity of the MNPs measured with the thermometric micelles was linear and the DT=7 oC. However, the temperature on the cell membrane, and therefore the global cell temperature,

measured with the micelles did not change during hyperthermia. Actually, the heat input estimated from the heating power of the MNPs was too small to increase the temperature of the whole cell.

Cell magnetic hyperthermia experiments indicated that a magnetic field similar to that used in thermometry experiments could produce noticeable cell apoptosis. Furthermore, when the *Hf* of the magnetic field was increased to a value closer to the healthy limit (4.8´109 A·m−1·s−1, *H*=60 mT, *f*=100 kHz), the apoptosis ratio exceeded 60%, which is already relevant for therapeutical purpose.

Conclusions: It can be concluded that the local magnetic hyperthermia hypothesis could be feasible as an improved therapeutical approach in comparison with the actual global tumor heating treatment.

References:

1 Gu, Y., *et al. ACS Nano* **17**, 6822–6832, 2023.

2 Pinol, R. *et al. Nano Letters* **20**, 6466-6472, 2020.

Figure 1 legend. Scheme of local hyperthermia hypothesis. Taken from reference 1.

Fig. 1

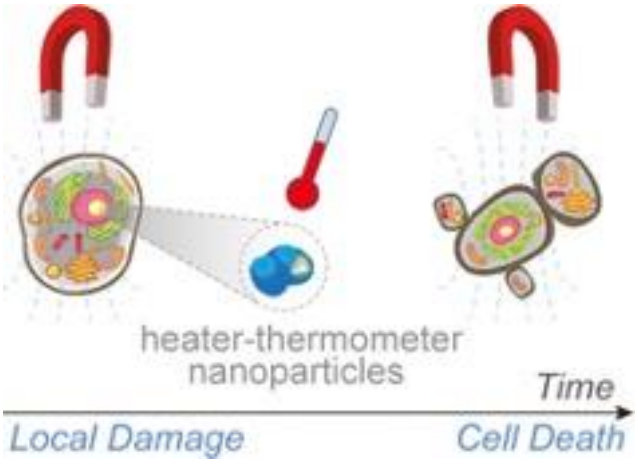

OP-37

Engineering NanoClusters of non-spherical magnetite particles with polydopamine for dual magnetothermal and photothermal therapy

G. García-García[1], G. Iglesias Salto[2]

[1]Universidad de Almería, Department of Nursing, Physiotherapy and Medicine, Almeria, Spain
[2]Universidad de Granada, NanoMag Laboratory Department of Applied Physics, GRANADA, Spain

Local hyperthermia has garnered significant interest due to its promising effects on the tumour microenvironment and tumour cells. In this context, photothermal and magnetothermal modalities are particularly notable. Developing novel antitumor hyperthermia agents has become an important objective. Consequently, the use of biodegradable nanomaterials such as polydopamine (PDA) and iron oxide (magnetite, Fe3O4) has been proposed. This research aims to develop an antitumor hyperthermia agent based on clusters of Fe3O4 particles using PDA and to assess their potential application in magnetothermal and/or photothermal modalities.

Non-spherical Fe_3O_4 colloids, obtained via a decanoic acid-modified thermal decomposition methodology, were utilized to form Fe_3O_4 particle clusters using PDA. Dopamine polymerization was induced in the presence of the Fe_3O_4 colloids at a PDA, ratio of 10:1 (Fig.1a). Physicochemical characterization of the resultant Fe_3O_4/PDA nanoparticles (NPs) was performed using transmission electron microscopy (TEM) and energy dispersive X-ray (EDX) spectroscopy. These have confirmed the nanostructure of the Fe_3O_4/PDA, demonstrating the formation of an Fe_3O_4 cluster embedded in a PDA polymeric nanomatrix.

The potential of the Fe_3O_4/PDA NPs as hyperthermia agents was investigated by measuring temperature increases upon applying an alternating magnetic field (18 kA/m and 165 kHz) and/or near-infrared (NIR) laser (850 nm, 0.75 W/cm²). Fe_3O_4/PDA NPs proved suitable for achieving antitumor effects by reaching temperatures of 42-45°C. (Fig.1b)

This study successfully developed a methodology to create a promising nanomaterial for antitumor hyperthermia, leveraging dual modalities of magnetotherapy and phototherapy.

Fig. 1. a) Transmission electron microscopy of Fe_3O_4 and Fe_3O_4/PDA particles and b) temperature rises for magnetotherapy, phototherapy and Fe_3O_4/PDA magnetotherapy/phototherapy double stimulus.

Acknowledgments:

Financial support of this investigation by the grant TED2021-131855BI00/AEI/10.13039/501100011033/Unión Europea Next Generation EU/PRTR and PID2023-151881OB-I00 (AEI, Spain) is gratefully acknowledged.

References:

[1] IJff, M., et al. (2022). *International Journal of Gynecologic Cancer*, *32*(3).

[2] Guardia, P., et al. (2010).*Chemical communications*, *46*(33), 6108-6110.

Fig. 1

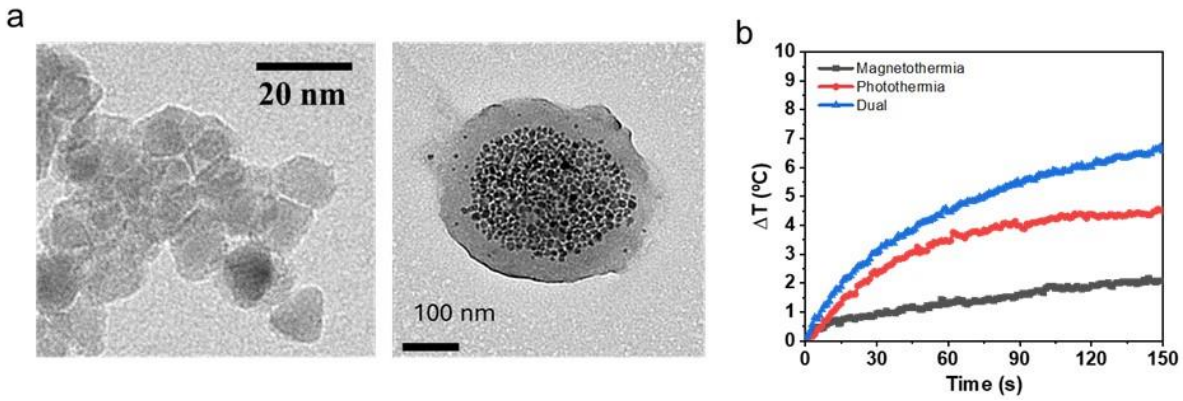

OP-38

Human-sized quantitative imaging of magnetic nanoparticles with magnetorelaxometry and optically pumped magnetometers

A. Jaufenthaler[1], F. Wiekhorst[2], D. Baumgarten[1]

[1]University of Innsbruck, Innsbruck, Austria
[2]Physikalisch-Technische Bundesanstalt, Berlin, Germany

Question: Magnetic nanoparticles (MNP) offer very promising biomedical applications, e.g. magnetic hyperthermia, where MNP are injected into a tumor and are heated by applying an RF magnetic field. Due to the treatment duration of several weeks, a quantitative MNP imaging procedure is required for a safe and efficient treatment. Currently there is no imaging technique available for large regions of interest and high iron amounts.

Methods: The quantitative spatial MNP distribution can be estimated by magnetorelaxometry imaging (MRXI), where the MNP within the region of interest are magnetized by pulsed DC magnetic fields. In-between the pulses, the relaxation of the MNP's magnetic moments is measured with highly sensitive magnetometers. The MNP distribution is then reconstructed by solving an inverse problem. We designed setups for imaging MNP inside the human head and inside the human torso. In the case of the human torso setup, we use a single optically pumped gradiometer and a single, large excitation coil for magnetizing the MNP (Fig. 1). The coil produces up to ~30 mT excitation fields. The MNP phantom consists of immobilized Perimag MNP (micromod, Germany) with 12 mgFe. Both, the gradiometer and the coil are moved mechanically during data acquisition. With the head setup (Fig. 2) we aimed at demonstrating a completely integrated setup with a 50 channel magnetometer array and 72 excitation coils. Both experiments were carried out within a magnetically shielded room.

Results: With our setups we were able to reconstruct point-like MNP phantoms with clinically relevant iron concentrations within our regions of interest.

Conclusions: With these measurements we demonstrated first human head and human torso sized MRX imaging measurements using optically pumped magnetometers. We are currently translating our setups to unshielded environments, which would drastically facilitate the use of our imaging technique in the clinics.

Fig. 1

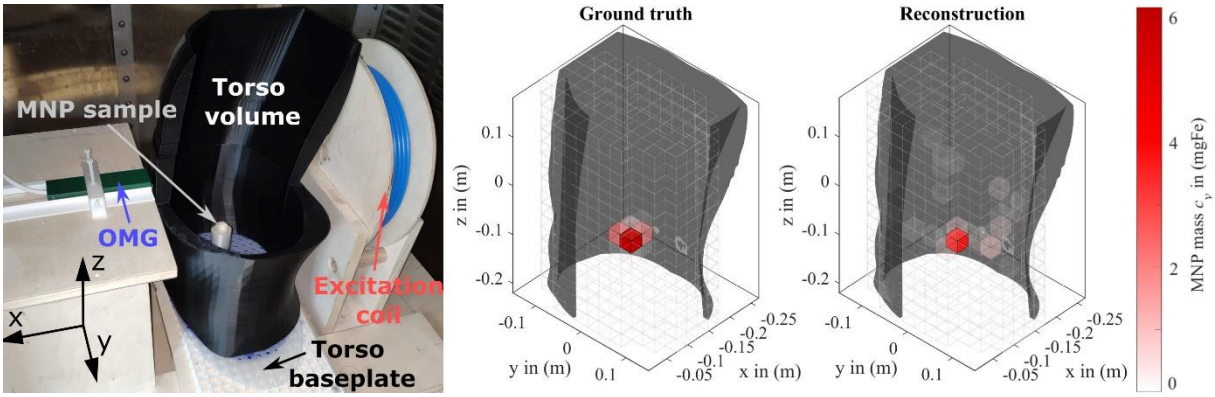

Fig. 2

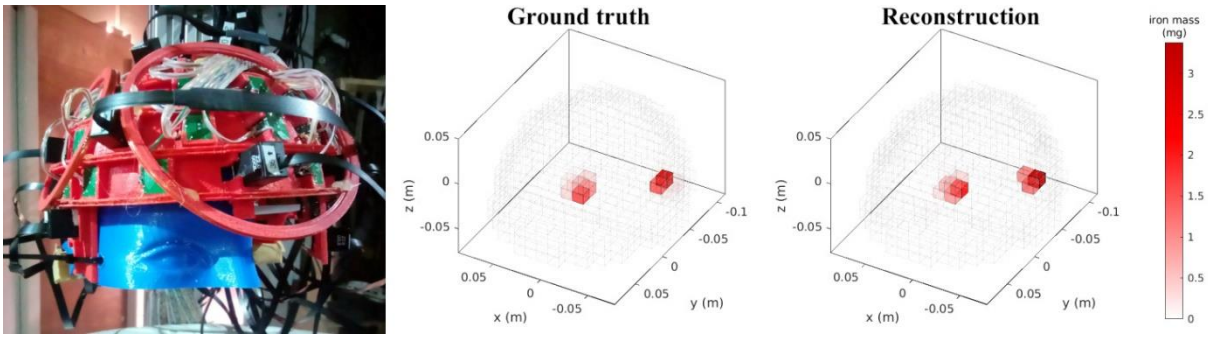

OP-39

Achieving temporal and spatial selectivity in chemotherapy: Remote activation of enzyme prodrug therapy

B. Torres-Herrero[1], I. Armenia[1,2], M. Alleva[1], L. Asín[1,3], L. Gutierrez[1], C. Ortiz[4], J. M. de la Fuente[1,5], L. Betancor[4], V. Grazu[1,5]

[1]INMA-CSIC, Zaragoza, Spain
[2]Università degli studi dell'Insubria, Dipartimento di Biotecnologie e Scienze della Vita, Varesse, Italy
[3]Universidad de Zaragoza, Zaragoza, Spain
[4]Universidad ORT-Uruguay, Montevideo, Uruguay
[5]Centro de Investigación Biomédica en Red de Bioingeniería, Biomateriales y Nanomedicina, MAdrid, Spain

Problem: Global projections estimate 29 million cancer cases by 2040, with over half leading to fatalities, highlighting an urgent need for new treatments. Although chemotherapy is the most effective treatment, it has a 90% failure rate in clinical trials for new drugs. This high failure rate is largely due to off-target toxicity (35% of failures) and difficulties in balancing efficacy with toxicity, resulting in low drug bioavailability and 45-50% of failures due to inefficiency, recurrence, or resistance**1**. Additionally, approved chemotherapeutics often cause both temporary and chronic adverse effects, such as chronic fatigue, neuropathy, cardiomyopathies, osteoporosis, and compromised immunity. These side effects can lead to functional and cognitive decline or be fatal, with additional costs estimated at $15,000 to $45,000 per patient annually**2**. Exogenous therapeutic enzymes that convert harmless prodrugs into potent chemotherapeutic agents offer a promising breakthrough. However, enzymes active at body temperature may lose selectivity if they accumulate outside the tumor. This work proposes strategies for spatial and temporal control of therapeutic enzymes by using those with optimal temperatures above 37 °C and applying alternating magnetic fields (AMF) externally.

Methodology:. Nanosized carriers for co-entrapment of Horseradish Peroxidase (HRP) and magnetic nanoparticles (MNPs) have been developed to enable remote control of prodrug conversion via magnetic heating**3**. These carriers were created by co-encapsulating HRP and MNPs in a biomimetic silica matrix through a rapid reaction under mild, enzyme-compatible conditions. Silica deposition was achieved by adding hydrolyzed tetramethyl orthosilicate (TMOS) and phosphate ions, which facilitated the assembly of polyethyleneimine (PEI) to entrap HRP and MNPs within the matrix.

Results: The effectiveness and remote activation of these nanocarriers (nHs) were demonstrated in pancreatic cancer models. Cytotoxicity from prodrug conversion into toxic oxidative species confirmed that enzyme activity, triggered remotely, was responsible for cell death in vitro using MIA PaCa-2 2D cell cultures. Exposure to nHs and prodrug without AMF or to nHs with AMF did not significantly affect cell viability. In vivo, treatment with nHs and the prodrug combined with AMF exposure resulted in greater reductions in tumor volume growth.

Conclusions: While this treatment could be applicable to various tumors, pancreatic cancer was prioritized due to its low survival rate, limited surgical options, and palliative current chemotherapy. This innovative approach promises to significantly reduce the side effects associated with traditional chemotherapy, improving patient quality of life and potentially enhancing survival rates by minimizing severe chronic issues in healthy organs.

1. Acta Pharm. Sin. B. 2022, 12(7): 3049;2. PLoS One 2018; 13(4): e0196007;3. *ACS Nano 2023, 17, 13, 12358–12373.*

Fig. 1

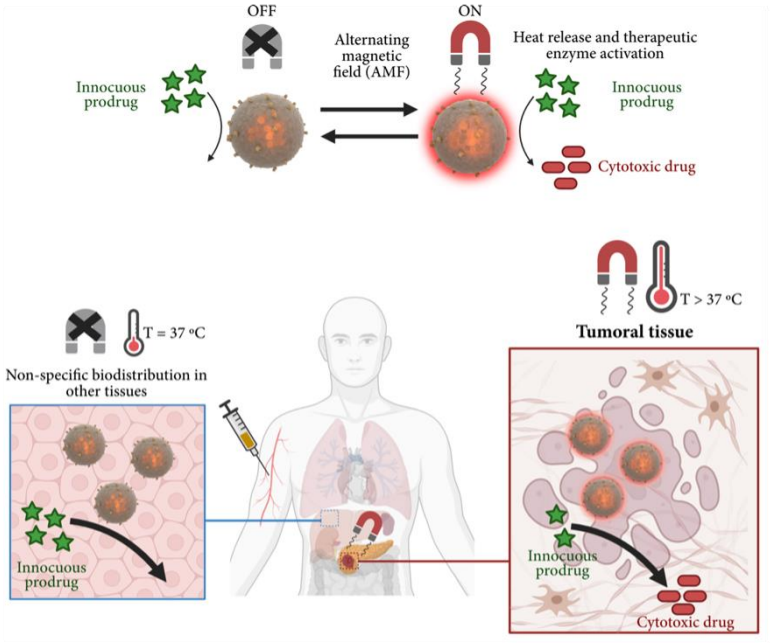

OP-40
In silico evaluation of metallic implants safety during magnetic hyperthermia

D. Ortega[1,2,3], I. Rubia-Rodríguez[4], A. Arduino[5], L. Zilberti[5], O. Bottauscio[5]

[1]University of Cadiz, Condensed Matter Physics, Puerto Real, Spain
[2]Institute of Research and Innovation in Biomedical Sciences of Cádiz (INiBICA), Cádiz, Spain
[3]IMDEA Nanoscience, Madrid, Spain
[4]Department of Applied Mathematics and Computer Science Cognitive Systems, DTU, Lyngby, Denmark
[5]Istituto Nazionale di Ricerca Metrologica (INRIM), Turin, Italy

Question: The aim of this study is to develop and validate an in silico methodology for assessing the thermal safety of metallic implants during magnetic hyperthermia (MH) treatments. The focus is on evaluating the heating effects induced by MH across different types of metallic implants, considering the variability in implant materials, geometries, and magnetic field orientations. The study also introduces a risk assessment equation that integrates these parameters into a framework for clinical treatment planning.

Methods: We have used an in silico testing approach, incorporating the numerical solution of Maxwell"s equations to simulate the electromagnetic response of metallic implants under magnetic hyperthermia conditions. The bioheat transfer was modeled using a modified Pennes" equation, which accounts for temperature-dependent blood perfusion and metabolic heat production. The study considered a range of implant materials, including Elgiloy, Nitinol (both austenitic and martensitic phases), and Ti-6Al-4V, with wire diameters varying from 0.1 mm to 0.4 mm. The applied magnetic field intensities ranged from 5 to 15 mT at 300 kHz, and different orientations relative to the implant geometry were explored. A risk assessment equation was developed to quantify the potential for adverse thermal effects, incorporating factors such as implant material properties, field intensity, and tissue-specific heat dissipation.

Results: The simulations revealed significant variations in heating behavior based on the material and geometric properties of the implants. In general, implants composed of lower electrical conductivity materials, such as Ti-6Al-4V, exhibited lower temperature increases. For instance, the maximum temperature increase observed for Nitinol (austenitic) implants was 57.3°C under a 10 mT magnetic field, with the martensitic phase showing even

higher temperatures. The orientation of the magnetic field relative to the implant geometry was identified as a critical factor, with specific orientations leading to localized temperature spikes exceeding 100°C, depending on the implant's final positioning within the body. The proposed risk assessment equation effectively identified scenarios where the induced heating posed significant risks, allowing for more informed decision-making in clinical treatment planning.

Conclusions: We present an in silico methodology for assessing the thermal risks associated with metallic implants during magnetic hyperthermia treatments. The proposed risk assessment framework intends to become a practical tool for clinicians to evaluate and mitigate potential hazards, ensuring patient safety across various clinical scenarios. The findings highlight the importance of careful consideration of implant materials and geometries, as well as magnetic field parameters, in MH treatment planning. This research underscores the need for further experimental validation and clinical trials to refine the proposed methodologies and integrate them into standard clinical practice.

OP-41

Moderate hyperthermia in Switzerland – A survey among Swiss radiotherapy centers on current practice, obstacles and opportunities of hyperthermia

N. Bachmann[1], E. Puric[2], M. Notter[3], B. Hübenthal[4], W. Arnold[5], S. Brodmann[6], T. Mader[7], F. Martucci[8], P. Tsoutsou[9], J. Crezee[10], O. Riesterer[2], E. Stutz[1]

[1]Inselspital Bern, Bern, Switzerland
[2]Centre for Radiation Oncology, Kantonsspital Aarau, Aarau, Switzerland
[3]Department of Radiation Oncology, Lindenhof Hospital, Bern, Switzerland
[4]Zentrum für Integrative Onkologie, Zürich, Switzerland
[5]Department of radiation oncology, Luzerner Kantonsspital, Lucerne, Switzerland
[6]Institute for Radiation Oncology, Cantonal Hospital Winterthur, Winterthur, Switzerland
[7]Department of Radiation Oncology, Kantonsspital Graubünden, Chur, Switzerland
[8]Department of Radiation Oncology, EOC Bellinzona, Bellinzona, Switzerland
[9]Department of Radiation Oncology, Hôpitaux Universitaires de Genève, Geneva, Switzerland
[10]Department of Radiation Oncology, Cancer Center Amsterdam, Amsterdam UMC, University of Amsterdam, Amsterdam, Netherlands

Aims: Growing interest in moderate hyperthermia (HT) is observed in Switzerland. The Swiss Hyperthermia Network (SHN) coordinates HT activities on a national level. On its behalf, an anonymous survey among Swiss radiotherapy (RT) centers was conducted to assess the current practice and opinion on HT, the interest of adopting HT and to identify obstacles to its implementation.

Methods: All head of departments of the 30 independent Swiss RT centers were invited to take the survey. A 25-item questionnaire was sent to the centers currently not offering HT (= non-HT-centers), while a more detailed 36-item questionnaire was sent to the centers having at least one HT device (= HT-centers). Thirteen matched questionnaire items were implemented to detect differences between HT-centers and non-HT-centers.

Results: The responses from 25/30 (83%) Swiss RT centers received by July 10, 2024 were taken into account. Ten (33%) centers have a HT unit. Of the 15 non-HT-centers, the majority is either interested in implementing HT (n=5, 33%) or is planning to consider it in the future (n=3, 20%), 5 (33%) centers do not intend to implement HT and 2 (13%) did not wish to comment on this topic. Lack of staff (46%) or patients (46%) and a too substantial initial investment (38%) were the most frequent reasons for not offering HT. However, the vast majority (n=24, 96%) of the 25 responding centers stated to believe in the benefit of HT. All (100%) non-HT-centers reported to refer 1-5 patients per year for HT, most commonly due to re-irradiation (92%), radioresistant histology (46%) or for increasing the likelihood of organ preservation (46%). After referral, 92% deliver RT fractions on days without HT in their own RT center. Correspondingly, HT-centers selected re-irradiation (100%), radioresistant histology (70%) and bulky/hypoxic tumors (60%) as most beneficial indications for HT. All (100%) centers with deep HT and 70% of centers with superficial HT stated that overall 1-3% of their RT patients is treated with additional HT. The sequence HT before RT is favored by 7/10 (70%) of superficial HT users and by 3/4 (75%) of deep HT users. 85% of non-HT-centers and 70% of HT-centers believe that there is enough data in the literature to support the wide use of HT, while 22 (88%) respondents believe more randomized phase III trials with HT should be conducted. Additionally, half (50%) of the non-HT-centers and 60% of HT-centers state that a national hyperthermia database would enhance HT legitimacy.

Conclusions: Ten RT centers in Switzerland offer HT and at least 8 more are interested to implement HT. Currently, about 1-3% of all RT patients receive additional HT in Swiss RT centers with a HT unit. Re-irradiation and radioresistant tumors seem to be well accepted indications for hyperthermia in the whole RT community. More randomized phase III trials and a national HT database would further promote legitimacy for HT.

Fig. 1

Table 1: Comparison of 13 matched questionnaire items designed to detect differences between HT-centers and non-HT-centers (green = match, 0-10% difference, yellow = 11-20% difference or partial match in multi-answer questions, red = no match, >20% difference)

	HT-centers	non-HT-centers	
(Deep) HT devices are not yet capable to guarantee a reproducible adequate heating.	Yes: 14%	Yes: 29%	
Are you referring patients for HT? vs. Do you refer patients to other HT if you do not offer the required HT modality?	Yes: 90%	Yes: 100%	
Why do you refer patients to HT? vs. In which situations is HT most beneficial?	- Re-irradiation: 100% - Radioresistant histology: 70% - Bulky/hypoxic tumors: 60% - increasing the chance of organ preservation: 50%	- Re-Irradiation: 92% - Radioresistant histology: 46% - Bulky/hypoxic tumors: 38% - increasing the chance of organ preservation: 46%	
Is there enough data in the literature to support and legitimate the wide use of HT?	Yes: 70%	Yes: 85%	
What would be the most effective way to enhance the legitimacy of hyperthermia?	- Randomized studies with modern control arm (100%) - National HT database (60%) - Modern prospective studies (50%)	- Randomized studies with modern control arm (100%) - National database (50%) - Modern prospective studies (50%)	
Should we aim for more randomized phase III HT studies?	Yes: 100%	Yes: 92%	
Is there a need for national technical HT quality guidelines?	Yes: 60%	Yes: 92%	
Could HT have a negative impact on the oncological outcome?	Yes, increased toxicity: 30%	Yes, increased toxicity: 15%	
Could HT have a negative impact on the patient's quality of life?	Yes: 0%	Yes: 38%	
Could HT have an immuno-modulatory effect and increase the effect of immunotherapy if applied concurrently?	Yes: 100%	Yes: 69%	
Is invasive intratumoral temperature measurement mandatory to generate reliable data to assess the benefit of HT?	Yes: 40%	Yes: 38%	
Is superficial HT sufficiently available in Switzerland?	Yes: 70%	Yes: 46%	
Is deep HT sufficiently available in Switzerland?	Yes: 40%	Yes: 38%	

OP-42

Heating through intact bone cortex with a radiative deep hyperthermia system: A proof-of-concept phantom study

M. Fürstner[1], A. Ethesam[1], A. Joosten[1], M. Künzler[2], D. M. Aebersold[3], P. Manser[1], M. Reist[3], D. Frauchiger[1], E. Stutz[3]

[1]Division of Medical Radiation Physics and Department of Radiation Oncology, Inselspital, Bern University Hospital, University of Bern, Bern, Switzerland
[2]Orthopaedic Surgery and Traumatology, Inselspital, Bern University Hospital, University of Bern,, Bern, Switzerland
[3]Inselspital Bern, Bern, Switzerland

Question: There is no experimental and clinical data available whether a space within an intact bone cortex can be heated with moderate radiative hyperthermia (HT). In clinical routine, this leads to the pragmatic assumption that tumors surrounded by an intact cortex might not be heated to required therapeutic temperatures. This early phantom study aims to provide initial insights into the achievable heating rates within an intact bone cortex.

Methods: A phantom was built that closely mimics an in vivo situation of an upper thigh, using a polypropylene cylinder (length 50cm, inner diameter 19.4cm, outer diameter 20cm) filled with minced meat (dielectric properties of a human muscle) and a pig femur placed in the center aligned the longitudinal axis of the cylinder. The intact bone cortex had a thickness of 5mm. Six catheters were embedded in the phantom to accommodate the temperature probes, one in the center of the bone marrow, two on the cortex surface outside the bone and three in the space between femur and cylinder wall. A planning CT was performed and treatment settings were calculated using the planning software EasyPlan (Med-Logix, Italy). The phantom was centered in the radiative deep hyperthermia system (ALBA 4D, Med-Logix, Italy) between the four antennas. A heating pattern with two phases was repeated three times in succession. During the first phase, each antenna was supplied with 150 W for 5 minutes, followed by a second phase where all antennas were off for 15 minutes.

Results: Average heating rates in the bone marrow, on the bone surface and in the minced meat are 0.6°C/min, 0.64°C/min and 0.8°C/min, respectively. In the second phase, the temperature of the bone marrow initially drops first but then starts to rise whereas all other thermocouples either exhibit an exponential temperature drop or stable temperature levels.

Conclusions: Based on our pilot experiment in a model without perfusion, a space completely covered by intact cortex bone seems to be heatable without a substantial time delay. We further observed that heat conduction from surrounding bone and meat might play an additional role. If this can be consistently demonstrated in further experimental setups, it could have implications for new hyperthermia indications. Further investigations, nevertheless, are mandatory to validate this early promising result.

OP-43

Evaluation of magnetic resonance thermometry performance during MR-guided hyperthermia treatment of soft-tissue sarcoma in the pelvis and lower extremities

M. Göger-Neff[1], S. Karkavitsas[1,2], B. Zilles[1], M. Kawula[3], K. Sumser[4], M. Wadepohl[2], G. Landry[3], C. Kurz[3], W. Kunz[5], O. Dietrich[5], L. Lindner[1], M. Paulides[4]

[1]LMU Munich, Medicine 3, Munich, Germany
[2]Sennewald SMT, Munich, Germany
[3]LMU Munich, Radiotherapy, Munich, Germany
[4]TU Eindhoven, EMC4C, Eindhoven, Netherlands
[5]LMU Munich, Radiology, Munich, Germany

Goal: To evaluate magnetic resonance thermometry (MRT) temporal precision and accuracy during deep-regional hyperthermia therapy (HT) of soft-tissue sarcoma (STS) in the pelvis and lower extremities and to investigate the influence of pre-treatment motion on MRT precision.

Materials and Methods: Patients with STS in the pelvis (17, 45 treatments) and lower extremities (16, 42 treatments) received HT combined with chemotherapy at the LMU Klinikum according to our clinical standard protocol. The temperature increase was monitored non-invasively using MRT: two consecutive Double-Echo Gradient-Echo (DEGRE) sequences every 10 minutes. 3D temperature maps were created from the MR phase data with an in-house developed algorithm, using only the 2nd echo of the DEGRE sequence. For the correction of the magnetic field drift, we applied a second-order drift correction, taking into account the signal from subcutaneous body fat in addition to the oil reference tubes built into the applicator. MonAI Label (https://github.com/Project-MONAI) was used to automatically segment patient and body fat volumes. Our results were benchmarked against the clinical standard software for MRT, SigmaVision (Sennewald SMT, Germany), utilizing both echoes but only the oil reference tubes for a linear drift correction. For each pair of consecutive DEGRE scans, temporal precision was quantified by the standard deviation of the voxel-wise temperature difference within the patient contour. Accuracy was assessed in three lower extremity patients (six treatments), using invasive tumor probes as reference, and quantified by the mean absolute difference between probes and MRT in a small ROI (1cm) around the probe. To investigate if pre-treatment motion could be used to select patients in which good MRT precision can be expected, we quantified pre-treatment gross motion and intestinal gas motion by the Jaccard Coefficient (JC). We then assessed the predictability of the JC for acceptable temporal precision (<1°C) using a ROC analysis.

Results: Compared to the clinical standard dual-echo MRT, our post-processing algorithm (single-echo /body-fat + oil tubes) improved the mean temporal precision from 1.3±0.4°C to 1.1±0.3°C for the pelvis and from 1.0±0.3°C to 0.8±0.2°C for the lower extremities. Accuracy improved from 1.1°C to 0.8°C in the lower extremities. Pre-treatment gross motion was a good predictor of precision with AUC=0.80-0.86 (pelvis) and 0.81-0.83 (lower extremities), and better than intestinal gas motion (0.52-0.58).

Conclusion: Single-echo MRT had significantly better precision than dual-echo MRT. Body-fat-based field drift correction significantly improved MRT accuracy. If these results can be confirmed in other clinical settings, they should be incorporated into clinical MRT software. Pre-treatment gross motion was a good predictor of acceptable MRT precision in contrast to intestinal gas motion, so strategies to avoid or mitigate the effect of such motion are needed.

OP-44

Feasibility study for optimizing the treatment of pathological lymph nodes in locally advanced cervical cancer patients treated with radiotherapy and hyperthermia

A. Rink[1], E. Meijer[1], H. Westerveld[1], Y. Seppenwoolde[1], M. Franckena[1], P. Granton[1], A. Cruz Perdomo[1], S. Curto[1]

[1]Erasmus University Medical Center Rotterdam, Hyperthermia, Rotterdam, Netherlands

Background: Approximately 10% of patients treated for locally advanced cervical cancer (LACC) develop nodal failure (NF). The standard treatment for LACC is chemoradiotherapy followed by a brachytherapy boost. In the Netherlands, patients with a contraindication for chemotherapy are treated with deep hyperthermia (DHT). Currently, hyperthermia is locally applied to the hyperthermia target volume (HTV) defined as the intermediate risk CTV. Therefore, there is minimal sensitization to the pathological Lymph Nodes (pLNs) when DHT is applied. The aim of this study was to investigated if it is feasible to include pLNs for DHT plan optimization.

Methods: 28 patients with a total of 107 pLN were included in the study. 13 patients were treated in the Sigma 60 (S60) and 15 in the Sigma Eye (Seye). The CT for EBRT planning was matched with the CT for HT planning and the pLN contours were rigidly transferred to the HT scan. In the HT planning system VEDO two different hyperthermia treatment plans (HTP) were conducted, one optimized on the HTV only, and one optimized on HTV and pLNs. To compare these plans the TC25 and THQ were extracted for the HTV and each pLN. The HTP for pLN was considered improved when it had a minimum target-to-hot-spot-quotient (THQ) of 0.33 and both the TC25 and THQ increased 5% compared to the HTP without pLN. In addition, pLN optimisation was not considered feasible when the TC25 and THQ of the HTV were more than 5% lower in the HTP with pLN compared to the HTP without pLN – defined as a clinically significant deterioration from the initial plan.
To determine the maximum distance between the HTV and pLN, the distance between the centre HTV and centre pLN was measured. To validate the optimisation results of a HTV + pLN HTP, a lamp phantom study was performed. For the S60 and Seye, 3 HTP for the lamp phantom were made per applicator: 1st with an HTV only, 2nd with LN

at 9.5 cm from centre HTV and 3rd with LN at 14.5 cm from centre HTV. For each HTP, the first measurement was performed at the centre of the HTV, second at 9.5 cm from the centre and the third at 14.5 cm.

Results: PLN improved in 85% of cases, for the S60 28 pLN (73.7%) and Seye 63 pLN (92.7%) (table 1). The TC25 and THQ in the HTP with pLN are significant higher ($p<0.001$) compared to HTP without pLN. For 1 patient (3.6%) it was not possible to optimize the pLN without a loss of <5 % in THQ for HTV. There was no significant difference for the TC25 and THQ for the HTV between both HTP. The maximum distance between centre HTV - centre pLN for the S60 was 14.5 cm and Seye 18.5 cm. Above these values, the pLN did not meet the requirements. Measurements with a lamp phantom showed the focus is steered to the pLN according the HTV + pLNs HTP (Figure 1).

Conclusion: It is feasible to perform a combined HTV + pLNs optimized HTP without loss of the coverage and THQ of the HTV when the distance between a pLN and the HTV is less than 14.5 cm for the S60 and 18.5 cm for the Seye.

Fig. 1

	HTP HTV only	HTP HTV +pLNs	P value
Sigma 60			
HTV TC25 (n=13)	67,15% (18-95)	67,85% (28-94)	0,578
HTV THQ (n=13)	0,457 (0,387-0,562)	0,466 (0,399-0,544)	0,429
pLN TC25 (n=38)	38,95% (0-100)	58,58 (0-100)	<0,001
pLN THQ (n=38)	0,318 (0,098-0,896)	0,409 (0,154-1,03)	<0,001
HTV met requirements	-	12/13 (92.3%)	
pLN met requirement	16/38 (42.1%)	28/38 (73.7%)	
Sigma Eye			
HTV TC25 (n=15)	92.6% (85-99)	92.93% (85-99)	0,625
HTV THQ (n=15)	0.534 (0.451-0.643	0.533 (0.460-0.613)	0,713
pLN TC25 (n=69)	59.91% (0-100)	83.84% (0-100)	<0,001
pLN THQ (n=69)	0.403 (0.033-0.752)	0.522 (0.078-0.82)	<0,001
HTV met requirements	-	15/15 (100%)	
pLN met requirement	41/69 (59.4%)	64/69 (92.7%)	

Fig. 2

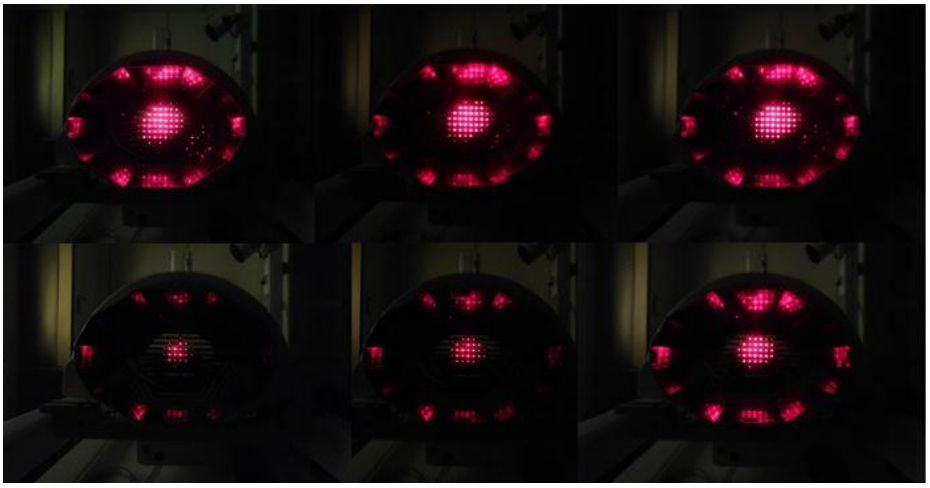

OP-45

Evaluation third year of the H2020 HYPERBOOST consortium: Hyperthermia boosting the effect of radiotherapy

J. Crezee[1], S. Curto[2], H. D. Trefna[3], R. Fietkau[4], B. Frey[5], U. S. Gaipl[5], P. Ghadjar[6], M. R. Horsman[7], H. P. Kok[1], P. M. Krawczyk[8], T. Niendorf[9], O. J. Ott[4], J. Overgaard[7], P. Pavoni[10], G. C. van Rhoon[2], O. Riesterer[11], S. Scheidegger[12], M. Wadepohl[13], B. J. Slotman[1]

[1]Amsterdam University Medical Center, Department of Radiation Oncology, Amsterdam, Netherlands
[2]Erasmus University Medical Center Rotterdam, Department of Radiation Oncology, Rotterdam, Netherlands
[3]Chalmers University of Technology, Department of Electrical Engineering, Gothenburg, Sweden
[4]Universitätsklinikum Erlangen, Department of Radiation Oncology, Erlangen, Germany
[5]Universitätsklinikum Erlangen, Translational Radiobiology, Department of Radiation Oncology, Erlangen, Germany
[6]Charité Universitätsmedizin Berlin, Department of Radiation Oncology, Berlin, Germany
[7]Aarhus University Hospital, Experimental Clinical Oncology - Department of Oncology, Aarhus, Denmark
[8]Amsterdam University Medical Center, Department of Medical Biology, Amsterdam, Netherlands
[9]Max-Delbrück-Center for Molecular Medicine, Berlin Ultrahigh Field Facility, Berlin, Germany
[10]Medlogix srl, Rome, Italy
[11]Centre for Radiation Oncology KSA-KSB, Cantonal Hospital Aarau, Aarau, Switzerland
[12]ZHAW School of Engineering, University of Applied Sciences, Winterthur, Switzerland
[13]Dr. Sennewald Medizintechnik, Munich, Germany

Background: Hyperthermia is a clinically proven radiosensitizer and is used combined with radiotherapy (RT). Optimal therapeutically effective clinical application requires well-designed clinical protocols and experienced staff with a good multidisciplinary understanding of hyperthermia. HYPERBOOST was created to bridge these gaps in a 4-year European Horizon 2020 Innovative Training Network (ITN) project with 11 beneficiaries in 6 European countries, and 7 partner organizations (H2020-MSCA-ITN-2020-955625). The scientific aim of HYPERBOOST is to develop an advanced personalized combined radiotherapy and hyperthermia treatment planning platform based on extensive (pre)clinical data, and training a new generation of hyperthermia experts.

Methods: HYPERBOOST started December 2020 to integrate efforts from multiple disciplines, including physics, pre-clinical and clinical studies to train dedicated staff. Scientific work was divided over 3 work packages aiming at 1) gaining more preclinical insight into hyperthermia effects, 2) translating these insights into development of a personalized planning platform and 3) clinical implementation, evaluation and quality assurance. Fourteen PhD students are trained to become next-generation hyperthermia professionals with multidisciplinary skills and expertise to develop, apply and optimize advanced multi-modality cancer treatments through close interaction with academic and industrial consortium partners. Novel training methods are applied for hyperthermia, radiotherapy and translational skills. Joint training courses and secondments at partner institutes are a key part of HYPERBOOST.

Results: HYPERBOOST is progressing well. Joint training courses included successful online courses and onsite training weeks in the Netherlands, Sweden, Germany and Switzerland. Secondments helped to establish fruitful research collaborations between different partners and across different work packages. This in turn promoted collaboration between European and American hyperthermia centers both within and outside HYPERBOOST. The midterm evaluation by the EU was very positive about the progress and scientific results achieved. Achieved HYPERBOOST results are promoting high quality assurance standards for hyperthermia protocols and high level treatment delivery standards with much attention for safeguarding and documenting therapeutically effective temperature levels. A final report is in preparation summarizing results and providing recommendations for the clinical hyperthermia field. The HYPERBOOST project will end in December 2024.

Conclusion: HYPERBOOST is contributing to high-level hyperthermia research and clinical practice by initiating, stimulating and facilitating multidisciplinary cross-pollination between the disciplines involved in hyperthermic oncology. This leads to consolidation and expansion of the infrastructure and industry for hyperthermia research and effective clinical application.

OP-46

Reintroducing head and neck hyperthermia treatments using the HyperCollar3D at Erasmus MC; the medical device regulation process and hard- and software enhancements

A. Rink[1], M. Kroesen[1], S. Curto[1], M. Zanoli[1], M. Paulides[2], K. Sumser[2], I. Lieben[1], D. de Regt[1], G. C. van Rhoon[1], P. Granton[1]

[1]Erasmus University Medical Center Rotterdam, Hyperthermia, Rotterdam, Netherlands
[2]Eindhoven University of Technology, Eindhoven, Netherlands

Introduction: From 2008 to 2019, 89 patients at Erasmus MC, with recurrent head and neck cancer were treated with re-irradiation combined with hyperthermia treatments (HT). Retrospective analysis of the clinical results by Kroesen et al. (2021) reported promising outcomes. In May 2021, the European Union revised the laws governing medical devices and introduced the medical device regulation (MDR). Recognizing the clinical importance of these treatments and the requirements posed by the MDR, the radiotherapy department initiated a process to reintroduce the HyperCollar3D (HC3D) for primary treatment by a clinical phase I dose-escalation trial. Herein, we report on this multi-faceted process requiring multidisciplinary collaboration.

Methods:The reintroduction process involved several key steps:
- creation of a MDR file in compliance with European regulations;
- enhancements in patient comfort through personalized head support;
- improvements in patient fixation and positioning reproducibility;
- technical upgrades to the HC3D, including redesign of the water bolus, hydraulic system, and electrical safety measures;
- implementation of automatic CT segmentation combined with an AI-assisted segmentation of organs at risk;
- integration of the new clinical workflow for the phase I study protocol.

A multidisciplinary workgroup was established comprising a tailored mix of clinical and research personnel, assisted by the Medtech Innovation Support, the Quality Assurance office, the mold laboratory and the instrumentation laboratory of the radiotherapy department.

Results:
- MDR approval for the use of the HC3D in a clinical trial was obtained.
- A personalized headrest with nose-forehead fixation was developed to reduce patient movement to millimeters while enhancing comfort and alignment between treatment plan and execution.
- A new AI assisted CT segmentation routine was integrated into the planning workflow, decreasing personnel workload and improving repeatability.
- The water bolus and hydraulic system were redesigned to simplify clinical operations, reduce failure rates, and diminish electrical safety risks.
- A comprehensive clinical treatment and QA protocols were established for supporting the Phase I dose escalation study.

Conclusion: The adoption of in-house developed equipment for clinical trials requires oversight by a multidisciplinary team and extends beyond the expertise of a single department. We found that, when not managed effectively, the drafting of an MDR file can result in years of undesired delays. However, when properly addressed, the MDR process streamlines the introduction of novel medical devices into the clinical practice, by identifying and resolving bottlenecks and areas of improvement, as demonstrated by our successful reintroduction of the HC3D. This experience enables optimisation of new hyperthermia approaches and technology, which is crucial to accelerate the acceptance of hyperthermia as oncological treatment modality.

Fig. 1

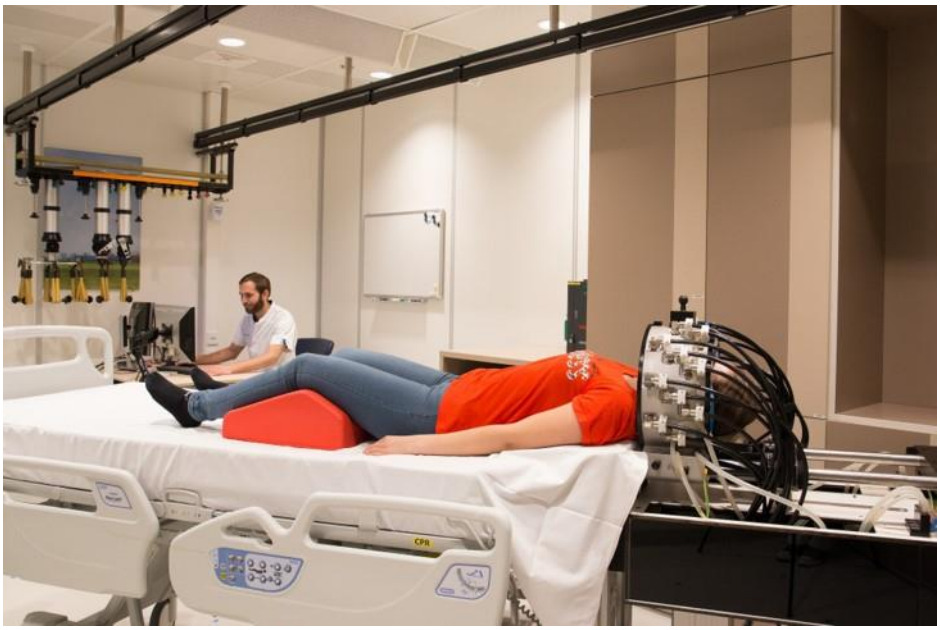

OP-47

Deep hyperthermia and radiotherapy: A promising palliative treatment option for patients with recurrent, bulky tumors

M. Neesen[1], N. Bachmann[1], M. Fürstner[2], M. Reist[1], B. Shrestha[1], E. Riggenbach[1], H. Hemmatazad[1], A. Kollar[3], D. M. Aebersold[1], C. Ionescu[1], E. Stutz[1]

[1]Inselspital Bern, Bern, Switzerland
[2]Division of Medical Radiation Physics and Department of Radiation Oncology, Inselspital, Bern University Hospital, University of Bern, Bern, Switzerland
[3]Department of Medical Oncology, Inselspital Bern, University of Bern, Bern, Switzerland, Bern, Switzerland

Aims: Bulky tumors represent a major challenge in cancer therapy. Due to significant hypoxic areas, systemic therapies and radiation (RT) alone are often of limited effectiveness. However, hyperthermia has shown to effectively target these hypoxic areas in bulky tumors. We combined deep radiative hyperthermia with radiation therapy (dHT+RT) as a treatment option for patients with uncontrolled, recurrent bulky tumors aiming to increase local treatment response and palliation.

Methods: All patients treated in a palliative intent at our institution with dHT+RT with (i) 40Gy/16fx, (ii) a baseline GTV larger than 200cc in the RT planning CT and (iii) at least one diagnostic follow-up CT scan were included. Patient and treatment characteristics, toxicity and follow-up CT data for radiologic tumor volume assessment were analysed.

Results: From 08/2022 until 03/2024, nine patients were included with a median age of 59 years (range 56 - 80) and an ECOG of 0 - 2. The most prevalent tumor type was soft tissue sarcoma (5 out of 9 cases), with all tumors located in the abdomen or pelvis. Mean and median baseline GTV volume and diameter were 1464cc and 560cc (range: 215 – 5169 cc) and 17.7cm and 18.9cm (range: 6.4 – 25.6cm), respectively. Several patients (4/9) had at least two previous systemic treatment lines. Based on volumetric assessment during a median CT follow-up time of 7 months (range 1 - 11 months), seven of 9 patients (77%) achieved a tumor volume reduction of -40% or more from baseline. Mean and median tumor volume reduction were -53% and -43% (range -100% to -5.2%) respectively. The other two patients were (i) patient 2 with a dedifferentiated liposarcoma, G2 and a baseline GTV of 3102cc showing only a volume reduction of -20% and (ii) patient 3 with an undifferentiated pleomorphic sarcoma, G2 and the largest tumor volume (5169cc) of this cohort. Patients 3 was the only patient showing tumor

volume progression after dHT+RT There was no treatment-associated grade 3/4 toxicity. The median number of dHT sessions was 6 (range 3 - 7). Radiative dHT was applied with A4D (Med-Logix, Italy).

Conclusion: With a well tolerated dHT+RT schedule, we observed in most of our cases with recurrent either radio-resistant or highly pretreated bulky tumors a significant tumor volume reduction of at least -40% or more from the baseline CT during the CT follow-up time. Despite limitations such as small sample sizes, short follow-up periods, and heterogeneous tumor entities, this initial analysis indicates that the combination of dHT+RT can not only halt the growth of bulky tumors but also significantly reduce tumor volume, thereby improving palliation and quality of life. We suggest to expand this analysis to a more in-depth retrospective multicenter study to compare its results to a historic control group treated with the same fractionation but with RT alone.

Fig. 1

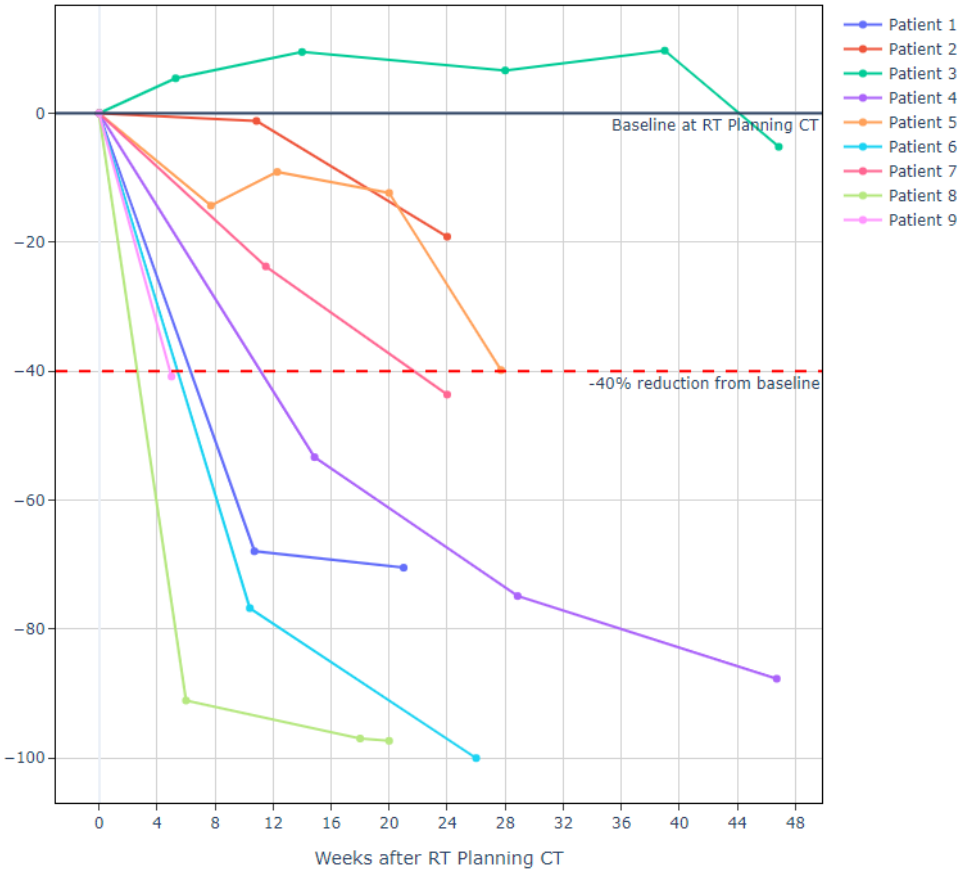

OP-48

Hyperthermia terms and definitions – Initial report from the ASME thermal medicine lexicon subcommittee

H. Dobšíček Trefná[1], S. Curto[2], J. Crezee[3], C. Crouch[4], G. Shafirstein[5], S. Heckel-Reusser[6], D. Marder[7], A. Ademaj[7], H. Ring[8], C. Diederich[9], K. Sumser[10], D. Rodrigues[11]

[1]Chalmers University of Technology, Göteborg, Sweden
[2]Erasmus University Medical Center Rotterdam, Rotterdam, Netherlands
[3]Amsterdam University Medical Center, Amsterdam, Netherlands
[4]University of Tennessee, Knowville, TN, United States
[5]Roswell Park Comprehensive Cancer Center, Buffalo, NY, United States
[6]Heckel-medizintechnik GmbH, Esslingen am Neckar, Germany
[7]Cantonal Hospital Aarau, Aarau, Switzerland
[8]3M Company, Minneapolis, MN, United States
[9]University of California, San Francisco, CA, United States
[10]Eindhoven University of Technology, Eindhoven, Netherlands
[11]University of Maryland, Baltimore, MD, United States

Question: To propose standardized engineering and clinical definitions for hyperthermia therapy (HT) in basic and translational research as well as clinical practice. This initiative is part of the Thermal Medicine (TM) Lexicon Subcommittee of the TM American Society of Mechanical Engineers (ASME) Standards Committee, a collaborative effort between ASME and STM/ESHO.

Method: The HT lexicon subgroup created engineering and clinical definitions for "hyperthermia therapy" as a global term, and for specific HT methods and devices currently employed in clinical settings. Each definition also includes a "sources of confusion" section to address misconceptions and prevent the use of inaccurate or confusing terms. Experts from different disciplines (with technical, clinical, and biological backgrounds) are consulted to validate the definitions from different perspectives.

Results: The team proposes engineering definitions of HT as a thermal therapy during which the tissue temperature is intentionally increased to approximately 39-45°C for a prescribed duration, typically one hour. This therapy is generally used in the treatment of cancer which has both additive (complementary) and synergistic effects when used in combination with radiotherapy, chemotherapy and/or immunotherapy.

HT can be delivered using a variety of heating techniques and technologies, divided into external and internal heating. Further sub-divisions are performed according to the target depth (superficial, deep and whole body) and/or the target volume (local, locoregional or whole body). Perfusion-based heating techniques are covered in a separate section.

HT can be achieved using different heating technologies, for which we present definitions for 1) electromagnetic technologies, including the use of radiofrequency, microwave and infrared sources; 2 ultrasonic heating; and 3) nanoparticle-mediated heating. We also propose heat-activated drug delivery as a clinically relevant HT term.

Conclusions: As a stepping stone towards standardization in thermal medicine, we proposed a series of critical terms and definitions specific to hyperthermia therapy while conveying the differences to other thermal therapies, such as ablation therapy. We followed an established, rigorous and recognized ASME standards development process, which provides the HT Lexicon credibility in the scientific and medical community.

Flash presentation

FP-01

Morphologic and molecular dissection of apoptotic cell death induced by magnetic fluid hyperthermia on cervical cancer cells HeLa.

K. Shah[1], H. Patel[2], K. Parekh[2], N. Jain[2]

[1]Charotar University of Applied Sciences, P. D. Patel Institute of Applied Sciences, Changa, India
[2]Charotar University of Applied Sciences, Dr. K. C. Patel Research and Development Centre, Changa, India

Magnetic fluid hyperthermia (MFH) is emerging as one of the promising cancer treatment strategies. It involves exposing magnetic nanoparticles to an alternating magnetic field to generate controlled localized heat. It is imperative, however, that cell death induced by MFH follows an apoptotic pathway. The present work aimed to look into the effect of Ho-doped iron oxide-based magnetic fluid and comprehend the cellular and molecular response upon exposure to MFH.

Cervical cancer cells HeLa were treated with 0.05mg/mL of Holmium doped temperature sensitive Mn-Zn ferrite and exposed to 11.7 kA/m of magnetic field strength and 332 kHz frequency. The influence of treatment on cellular morphology was analyzed by inverted phase contrast microscopy. Apoptosis-mediated cell death after MFH was confirmed by Hoechst/PI dual staining and examining the state of chromatin under a fluorescence microscope. Quantification of apoptotic cells was carried out using flow cytometry. Molecular dissection of apoptosis was carried out by analyzing expressions of anti-apoptotic proteins Bcl-xL and Mcl-1 and pro-apoptotic protein Bok using immunoblotting.

The findings reveal that one hour of MFH treatment led to apoptosis-mediated cell death in HeLa cells. Hoechst/ PI staining revealed maximum cells in the late stage of apoptosis with fragmented nuclei and a few with condensed nuclei displaying signs of the early stage of apoptosis. Flowcytometric results showed > 92% underwent apoptosis, with ~60% of the cells in late-stage apoptosis. This was further confirmed by immunoblotting, as an increased expression of Bok and decreased expression of Bcl-xL and Mcl-1 were detected in cervical cancer cells after MFH.

MFH using Ho-doped iron oxide-based MF effectively killed cervical cancer cells in vitro by inducing apoptosis, which was evident both at the morphologic and molecular levels. Expression analysis of anti- and pro-apoptotic proteins suggests the expected involvement of the intrinsic pathway of apoptosis. Downstream experiments on cervical cancer spheroids and animal models may further validate the effectiveness of this treatment for clinical applications to treat cervical cancer.

Authors thank the Indian Council of Medical Research, ICMR-NCD/AD-HOC/64/2020-21, and the Department of Science and Technology-Science and Engineering Research Board SERB/CRG/2021/001587 New Delhi, India, for providing financial support.

FP-02

Pulsed alternating fields magnetic hyperthermia in combination with chemotherapy as a cancer treatment for glioblastoma multiform: An *In Vitro* and *In Silico* study

L. Souiade[1], M. R. Rodríguez García[1], T. Samaras[2], D. Rodrigues[3], J. J. Serrano Olmedo[1], M. Ramos Gómez[1]

[1]Universidad Politecnica de Madrid, Centro de tecnología biomedica, Pozuelo de Alarcon, Spain
[2]Aristotle University, Faculty of Sciences, School of Physics, Thessaloniki, Greece
[3]University of Maryland, Radiation Oncology, School of Medicine, Baltimore, MD, United States

Purpose: Our group has shown that trapezoidal pulsed alternating magnetic fields (TP-AMFs) improve the heating efficiency of magnetic hyperthermia (MHT) in killing cancer cells when compared to conventional sinusoidal AMFs [1]. In this study, we will evaluate in vitro the synergistic effect of MHT using TP-AMFs with chemotherapy to kill cancer cells and conduct in silico studies to quantify potential eddy currents effects induced by TP-AMFs in cell culture medium.

Methods: The TP-AMFs were induced using a home-made device describe elsewhere [2, 3] capable of generating a variety of waveforms, with a frequency range of 100 to 500 kHz below, and magnetic field amplitude under 3mT. Magnetic nanoparticles [1] were applied at a biocompatible concentration (1 mg/ml) to a glioblastoma cell line (CT2A), for several cycles of MHT (30 minutes per cycle, 45min of rest between cycles) in combination with 5-fluorouracil at 0.1 µg/ml, a chemotherapeutic drug. The in silico study was performed in Sim4Life (ZMT, Switzerland), after modelling our own home-made coil and cell culture medium designs, to calculate the induced Eddy currents and correspondingly heating. As the simulator is not able to work with TP-AMF currents, we computed the sinusoidal field in Sim4Life, modelled the TP-AMF in MATLAB (Fourier series), and imported the resulting heat source to Sim4Life for the temperature distribution simulation.

Results: An example of the synergetic effect between MHT produced by TP-AMF signals and the 5-fluorouracil is shown in Figure 1. It shows an increase of cell death (58.9±2%) against MHT alone (31.4±3%). We found that cell death was dominated by the necrosis cell death pathway with 47.3 ± 2% and 11.6±2% of apoptosis. In addition, CRT positive cells increased to 17±1% when cells were treated with MHT + 5FU in comparison to MHT alone, which produced 10±1% of positive cells (Figure 1). In silico studies of the experimental setup show a stable magnetic field(1676±183A/m) and temperature (around 37°C) across the cell culture volume in agreement with the measured temperature.

Conclusions: The combination of MHT with chemotherapy enhanced the killing effects against CT2A cancer cells and increased the CRT expression on the cells surface. This indicates that this combination promotes the activation of the immune system to target and destroy remaining cancer cells.

References:

[1] Souiade, L. *et al. International Journal of Molecular Sciences*, 24(21), pp 15933, 2023, doi: 10.3390/ijms242115933

[2] Zeinoun, M. et al. Nanomaterials, 11(12). pp 3240, 2021, doi: 10.3390/nano11123240

[3] Zeinoun, M. et al. IEEE Access, vol. 9, pp. 105805-105816, 2021, doi: 10.1109/ACCESS.2021.3099428

Fig.1

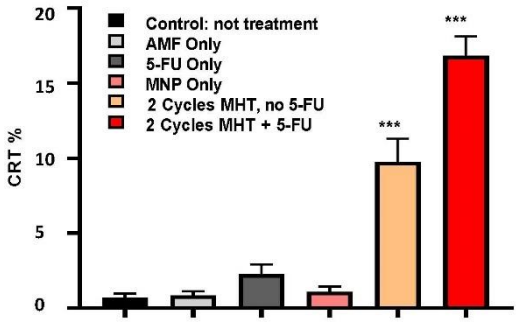

Figure 1. CRT expression on the surface of CT2A cells by immunostaining. CT2A 30000/cm2, 1mg/ml MNP, 0.1ug/ml 5-FU TS 200kHz/2mT. Treatments applied: 30 minutes for each cycle of exposure, 45 minutes rest between cycles, trapezoidal square signal, at 200 kHz, with magnetic field amplitude of 2.14 mT.

FP-03
In vitro modeling of hyperthermic enhancement of immunotherapy in melanoma

K. Kopec[1], N. DeSouza[1], D. Quaranto[1], T. Jarboe[1], M. Carnazza[1], J. Geliebter[1], R. K. Tiwari[1], M. D. Hurwitz[1,2]

[1]New York Medical College, Valhalla, NY, United States
[2]Westchester Medical Center, Radiation Medicine, Valhalla, NY, United States

Purpose/Objective: Despite advancement in understanding and manipulation of immune checkpoint inhibitors (ICIs) in immunotherapeutic design, limitations in treatment efficacy persist. Melanoma lacks T-cell infiltration, therefore ICI response rates are low in these "cold tumors". Strategies to enhance the effectiveness of melanoma treatment include use of multiple immunotherapeutic agents or combination with radiation therapy. Prior studies also demonstrated potential for hyperthermia to augment response to these therapies. We hypothesize that *in vitro* moderate hyperthermia affects the anti-tumor immune response in melanoma thus allowing immune manipulating therapies to be more effective.

Materials/Methods: To understand the consequences of temperature on carcinogenic phenotypes *in vitro*, B16-F10 melanoma cells were grown at 37°C or 41°C and biochemical profiles including protein expression were evaluated. Data obtained was used to define ongoing *in vivo* experiments in which B16-F10 cells are implanted into C57BL/6 mice, grown to palpable tumors then treated with water-filtered infrared radiation (wIRA) in combination with immunotherapy. Future studies based on these initial *in vivo* studies will explore the hyperthermic effects of carcinogenic properties and phenotypes the tumor microenvironment (TME) through immunohistochemistry of obtained organs.

Results: B16-F10 cells grown at 41°C decreased the rate of cell migration over 18hr. Further, at hyperthermic temperatures, live cell population decreased by 62% at 48 hours and then by 94% at 72 hours. With respect to proliferation, expression of pERK and ERK were both significantly decreased, whilst Caspase-3 expression increased. Commonly, sphingomyelinase activation results in CD95 receptor translocation, causing cell death. Cell stress can induce death pathways and the heat shock protein response simultaneously. Thus, we investigated inducible Hsp70 expression which increased by 188% at 41°C vs. 37°C. To evaluate the immune milieu, cytokine array data from conditioned media showed that at 41°C: TNFα expression was increased and IL-4 expression was decreased, suggesting a proinflammatory shift in cytokine profiles at hyperthermic temperatures. In direct relation to clinical practice, we observed that hyperthermic potentiation decreased PD-L1 expression in B16-F10 by 35%.

Conclusion: Our work to date supports the hypothesis that hyperthermia can enhance immunotherapy via several mechanisms. *In vivo* study of hyperthermic induction via wIRA hyperthermia is currently in progress.

FP-04
Use of hyperthermia to treat lymphomas: Results of a systematic literature review

M. Scharr[1], F. Damm[2], P. Krahl[1], A. Dieper[1], P. D. Veltsista[1], A. Hansch[1], M. Beck[1], D. Gerster[1], A. C. Giovannelli[1], L. Bullinger[2], D. Zips[1], P. Ghadjar[1]

[1]Charité Universitätsmedizin Berlin, Radiation Oncology, Berlin, Germany
[2]Charité Universitätsmedizin Berlin, Medical Oncology, Berlin, Germany

Introduction: Hyperthermia (HT) at temperatures between 39°C and 44°C is utilized as an adjunctive cancer therapy, serving as potent radio- and chemosensitizer. Its effectiveness in treating solid malignancies has been well established. This raises the question of whether HT can also benefit patients with non-solid tumors, such as lymphomas.

Objective: To provide an overview of the current literature on research involving the use of HT in the treatment of lymphomas.

Material and Methods: This literature review was conducted following the PRISMA guidelines. For this purpose, a MeSH-term-defined literature search on MEDLINE (Pubmed) and Embase (Ovid) was conducted from June 25 to

June 28, 2024. Included were *in vitro* studies on lymphoma cell lines and pre-clinical studies on animal models with lymphoma that were both treated with HT as monotherapy or HT in combination with another treatment, and studies on patients with lymphoma. Excluded were studies that used thermal ablation, hyperthermic perfusions, ultrasound treatment, and photothermal therapy.

Results: 39 studies were included, predominantly *in vitro* studies (n=32) or studies on animal models (n=5). The *in vitro* studies utilized HT either as monotherapy (n=6), with substances that enhance HT efficacy (n=18) or as a sensitizer for other treatments (n=8). Additionally, two clinical case reports on the treatment of lymphoma patients were included.

Conclusions: *In vitro* results suggest that HT can have anticancer effects on lymphoma cells and may enhance existing treatments. These findings are supported by *in vivo* studies and case reports. However, additional clinical data are needed before translation into the clinic can be implemented.

FP-05
Enhancement of the effectiveness of heat treatments in cells exposed to inhibitors of heat shock transcription factor 1

N. Vilaboa[1,2], M. de Mesa[2], R. Garrido-Punzano[2], M. Mendiola[3,2], R. Voellmy[4]

[1]CIBER de Bioingenieria, Biomateriales y Nanomedicina, CIBER-BBN, Madrid, Spain
[2]Instituto de Investigación Sanitaria del Hospital Universitario La Paz, IdiPAZ, Madrid, Spain
[3]CIBER de Cáncer, CIBERONC, Madrid, Spain
[4]HSF Pharmaceuticals SA, La Tour-de-Peilz, Switzerland

Activation of the heat shock response (HSR) is triggered by protein damage upon exposure of cells to heat or other conditions that induce protein denaturation. The master regulator of the HSR is the heat shock transcription factor 1 (HSF1), which orchestrates the induced expression of heat shock proteins (HSP), molecular chaperones that reduce aggregation of misfolded proteins. HSF1 also regulates the expression of genes related to cell survival, facilitating the oncogenic transformation and maintenance of the malignant phenotype. We have generated inhibitors of HSF1 (IHSF) which are cytotoxic to human cancer cells (1) and cause hundreds of cellular proteins to unfold and aggregate (2). IHSF covalently react with nucleophilic groups of the proteins, resulting in unfolding and aggregation of components of the proteostasis network, including HSF1, chaperones and co-chaperones, components of the ubiquitin/proteasome system, translation initiation factors and autophagy-related proteins. The majority of proteins that aggregate unfold because their conformational stability depends on interactions with proteins that are covalently modified, or on the failing cellular chaperoning system of IHSF-treated cells. These effects magnify the pervasive impact of the IHSF on the proteostasis network.

The efficacy of hyperthermia tumor therapies is often compromised by the abundantly expressed HSP and chaperones in cancer cells as well as by the protective HSR subsequent to hyperthermia, which may render tumor cells less sensitive or even insensitive to subsequent thermal treatments. In this study, we tested the hypothesis that the proteostasis crisis caused by IHSF may enhance the effectiveness of heat treatments. To this aim, triple negative human breast adenocarcinoma MDA-MB-231 cells and human prostatic adenocarcinoma PC-3 were cultured two-dimensionally (2D), incubated for 2 h with IHSF128, a compound of the IHSF series, and then heat-treated at 45 ºC for 10-30 min by partial immersion in a temperature-controlled water bath. After incubation for 72 h, cell viability assays indicated that preincubation with IHSF128 substantially increased the cytotoxicity of heat treatments. The effects were dependent on the doses of IHSF128 and on heat intensity. In another set of experiments, cells were grown three-dimensionally (3D), as spheroids, treated as above-described and further incubated up to 15 days. The morphology of the spheroids that were preincubated with IHSF128 and heat-treated markedly differed from those only treated with the compound or only heat-treated. Thermal treatment of spheroids exposed to IHSF128 dropped cell viability to a much higher extent than thermal treatment alone. These results suggest that the combination of IHSF and hyperthermia shows promise for designing more effective treatments of tumors that acquire heat resistance.

1. Nucleic Acids Res. 2017;45:5797.
2. Pharmaceuticals (Basel) 2023;16:616

FP-06

Modulated electro hyperthermia (mEHT) as single agent or combo-chemotherapy versus palliative chemotherapy in advanced pancreatic cancer: A multicenter retrospective observational comparative study

G. Fiorentini[1], G. Ranieri[2], M. Bonucci[3], S. Bonanno[4], G. Cristina[5], R. Lodico[6], D. Sarti[7], D. Sarti[8]

[1]San Salvatore Hospital, Oncology, Pesaro, Italy
[2]National Cancer Institute, Oncology, Bari, Italy
[3]ARTOI Foundation, Integrative Oncology, Roma, Italy
[4]Regional Hospital, Radiotherapy, Siracusa, Italy
[5]Regional Hospital, Internal Medicine -Complementary Medicine, Merano, Italy
[6]San Camillo Forlanini, Surgical Oncology, Roma, Italy
[7]Oncology Unit, Urbino, Italy
[8]Oncology Unit, Urbino, Italy

Pancreatic cancer (PC) is a severe disease with high lethality and poor chance of cure. The mEHT alone or combined with chemotherapy has been reported present some therapeutic effects.

Objective: to assess survival, tumor response and toxicity of mEHT alone or combined with chemotherapy versus second and third lines of chemotherapy in advanced PC.

Methods: this was a retrospective data collection on patients affected by locally advanced or metastatic PC. From 2003 to 2021, 628 patients with locally advanced or metastatic pancreatic tumor were observed and treated in nine Italian centers, 217 of them were included in this observational study, 89 (41%) of them were treated with mEHT+CHT (mETH group) and 128 (59%) with only CHT (no-mEHT group). CHT regimen was mostly gemcitabine-based in both study groups and was chosen by singular physician. We collected the data when the treatments were already done. The mEHT treatments were performed 1-3 times/week for a total of 4-6 weeks, starting at 60 W/40 minutes and increasing up to 150 W/ 90 minutes in 2 weeks. The efficacy was measured after reaching the final power of 150 W/ 90 minutes. The computer connected to the hyperthermia machine has a program that calculates and converts the Kilojoules dispensed by the machine into degrees of temperature at the treatment site. Results: Median patients age was 67 years (range 31–92 years). Delivered sessions was 16.8 (range 6-25).

Results: The mEHT group had a median overall survival (OS) greater than non-mEHT group (20 months, range 1,6-24, vs 9 months, range 0.4-56.25, p<0,001). mEHT group showed a higher number of partial responses (PR) (45% vs 24%,p=0,0018) and a lower number of progressions (PD) (4% vs 31%, p<0,001) than the no-mEHT group, at the three months follow-up. Adverse events were similar in both groups, skin reactions observed in 2,6% of mEHT sessions. The analysis of OS by age ≥70 years or <70 years showed that there was no difference in OS between mEHT ≥70 years (20 months, 2-43 months range) and <70 years (20 months 3-27 months range) p=0,235, whereas no-mEHT <70 years had a higher OS than no-mEHT ≥70 years group (12 months range 1-56 vs 8 months range 1-47, p= 0.01). Tumor response at three months follow-up was available for 87 (98%) of mEHT and 111 (88%) patients for non-mEHT group. mEHT patients showed a higher number of partial responses (PR) (45% vs 24%, p=0,0018) and a lower number of progressions (PD) (4% vs 31%, p<0,001) than no-mEHT group. Stable disease (SD) had similar value in both groups: 51% for mEHT and 45% for no-mEHT. In 7 pats a nasogastric thermoprobe was placed in the duodenum. In 2 cases, an increase of 0.7 degrees Celsius was observed.

Conclusion: These data suggest that mEHT is effective in term of survival and responses, not increasing toxicity to chemotherapy. We hope that these results will suggest experts to organize a large randomized trial to clarify the usefulness of mEHT in PC.

FP-07
Oncology hyperthermia on pulmonary carcinoma

N. Pantano[1]

[1]Poliambulatorio Orione s.r.l., Palermo, Italy

Local hyperthermia treatment is a procedure adopted in patients affected by cancer disease and used with synergic approach together with other therapies aiming to eradicate or reduce at least the tumoral mass.

This case study presents the outcome of a patient with pulmonary carcinoma of low grade treated with 4 cycle (48 sessions) of local hypertermia and coadjuvant therapies showing to enhance the neoplastic cytoreductive process aid with complementary and integrated therapies.

Fig. 1

FP-08
Oncologic hyperthermia treatment on papillary urothelial carcinoma of low grade

N. Pantano[1]

[1]Poliambulatorio Orione s.r.l., Palermo, Italy

Local hyperthermia treatment is a procedure adopted in patients affected by cancer disease and used with synergic approach together with other therapies aiming to eradicate or reduce at least the tumoral mass. This case study presents the outcome of a patient with papillary urothelial carcinoma of low grade treated with 2 cycles (24 sessions) of local hypertermia and coadjuvatn therapy e.g., infusional theraphy. The hyperthermia treatment has shown to enhance the neoplastic cytoreductive process supported by additional complementary and integrated therapies.

Fig. 1

FP-09

Modulated electro-hyperthermia and radiotherapy, a multimodal treatment approach in a paediatric patient with diffuse intrinsic pontine glioma

C. Minnaar[1,2], K. Bennet[3], T. Naidoo[4]

[1]Wits Donald Gordon Medical Centre, Radiation Oncology, Johannesburg, South Africa
[2]University of the Witwatersrand, Radiobiology, Johannesburg, South Africa
[3]Wits Donald Gordon Medical Centre, Paediatric Oncology, Parktown, South Africa
[4]University of the Witwatersrand, Radiation Oncology, Parktown, South Africa

Introduction: Diffuse Intrinsic Pontine Glioma (DIPG) is a highly aggressive and fatal brainstem tumour, predominantly affecting children. The prognosis remains dire, with a median survival time of 9 to 12 months from diagnosis and fewer than 10% of children surviving beyond two years. Standard treatment primarily involves radiation therapy, which offers temporary symptom relief and slight survival extension. Chemotherapy has shown limited efficacy due to the tumour's location and the blood-brain barrier. Despite these challenges, ongoing research and clinical trials aim to improve outcomes for DIPG patients.

Patient Presentation: A 10-year-old male, presented with a three-month history of severe headaches, occasional vomiting, left-sided ptosis, difficulty swallowing, visual changes, and declining academic performance. Examination revealed brisk reflexes.

Diagnostic Imaging: A diagnostic MRI on February 23, 2023, identified a large, high T2 intensity mass in the pons measuring 6.5x5.1x6.9 cm, extending into the brachium pontis bilaterally (predominantly on the left), left midbrain, and medulla, encasing the basilar artery and attenuating the fourth ventricle. The mass showed no restricted diffusion or post-contrast enhancement, consistent with DIPG.

Treatment: The patient was referred for radiation therapy (54Gy in 1.8Gy fractions) and modulated electro-hyperthermia (mEHT) administered twice weekly. mEHT sessions were conducted before radiation, with a maximum 30-minute interval between treatments. The treatment regime also included six cycles of Perazone (2mg PO BD) and Zofer (4mg SL daily).

Outcomes: Post-treatment MRIs showed progressive reduction in tumour size and signal intensity:

MRI (June 19, 2023): 11% reduction in tumor size.

MRI (August 4, 2023): 30% reduction from baseline.

MRI (October 30, 2023): 37% reduction from baseline.

MRI (January 30, 2024): 44% reduction from baseline.

MRI (May 2, 2024): 48% reduction from baseline.

As of July 31, 2024, 14.5 months post-treatment and 17 months post-diagnosis, the patient remains well, attending school, participating in sports, and maintaining good academic performance. He has received psychotherapy for social struggles.

Conclusion: This case study demonstrates the potential benefits of combining mEHT with standard radiotherapy in treating DIPG. The significant reduction in tumour size and improved quality of life observed in this patient highlights the importance of further research and clinical trials.

Ongoing Research: A Phase I/II clinical trial has been initiated to investigate the addition of electro-hyperthermia to radiotherapy for paediatric brainstem gliomas. The study aims to assess the clinical effects, safety, and overall survival in this patient population.

Fig. 1

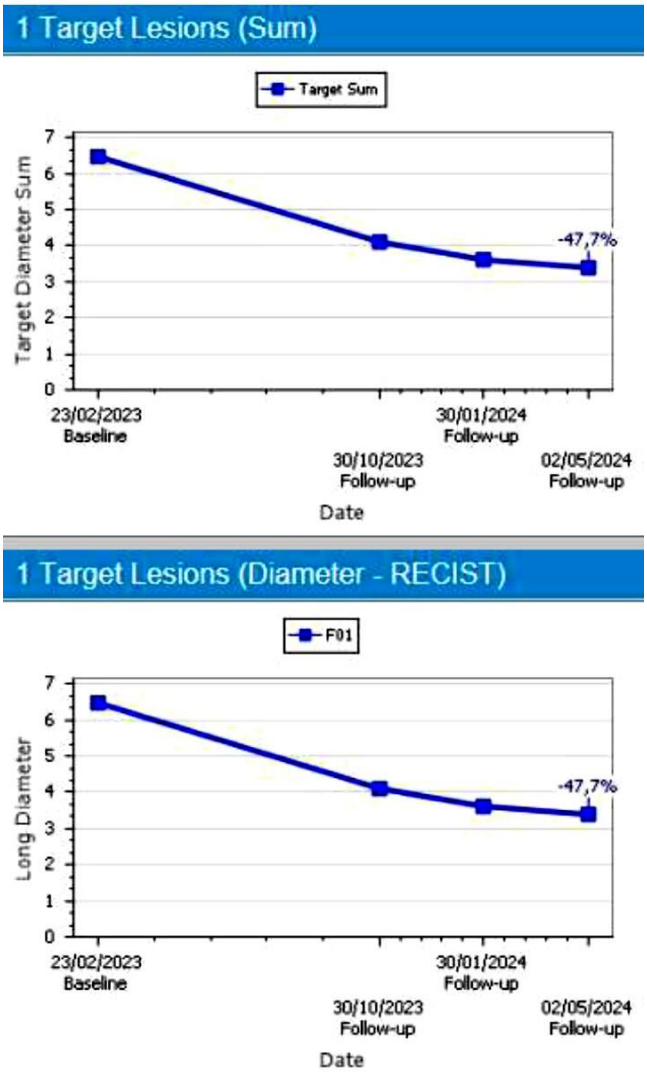

FP-10

Different hydration status of malignant tumors versus corresponding normal tissues and its relevance for hyperthermia using electromagnetic irradiation

H. Piazena[1,2], M. Notter[3], P. Vaupel[4]

[1]Charité Universitätsmedizin Berlin, Berlin, Germany
[2]Charité Universitätsmedizin Berlin, Dept. of Anaesthesiology and Intensive Care Medicine, Berlin, Germany
[3]Lindenhofspital, Dept. of Radiation Oncology, Bern, Switzerland
[4]University Medical Center, University of Freiburg, Dept. of Radiation Oncology, Freiburg, Germany

Introduction: Water content (C_w) of normal human soft tissues is quite variable: ≈ 53 wt.% (female breast) to about 80 wt.% (kidney). C_w-values increase up to a factor of approx. 1.5 in their corresponding malignant tumors (leading to hyperhydration of tumors). The absorption of electromagnetic irradiation significantly depends on C_w of exposed tissue, i.e., on the absorption coefficient μ_a (during wIRA-application), and on the dielectric loss ε'' (using microwaves and radiofrequencies) upon hyperthermia treatments (HT). In addition, differences in C_w can significantly influence key parameters of Pennes´ bioheat transfer equation (i.e., tissue density ρ, specific heat capacity c_p, heat conductivity k), and characteristics of the heat exchange within the tissue (heat diffusivity α and

heat effusivity ε). The aim of this study was to quantify the effect of C_w on these parameters in normal tissues and corresponding malignant tumors in patients.

Method: Values of μ_a, ε'', ρ, c_p, and k are experimental data published by different authors for various human tissues [1-9] which were correlated with the respective values of C_w. Using these data, the values of α and ε were calculated and also correlated with C_w.

Results. All parameters listed increased approx. linearly with rising C_w and were maximal in tumor tissues. The increases in c_p, k, α and ε with rising C_w were similar when comparing various tissue types, different breast tissue layers and skin layers. Highest values of C_w, and of the listed parameters were found in cancers.

Conclusion: Hyperhydration of tumor tissues results in higher absorption of electromagnetic radiation, and in increasing accumulation of thermal energy, but lower heating rates as compared to the corresponding normal tissues. This is counteracted by higher values for thermal conductivity, thermal diffusivity and effusivity of tumors to surrounding tissues, resulting in temporary conductive heat fluxes according to actual temperature gradients until a thermal steady state is reached. Thus, adjusted irradiances and/or electric fields as well as adequate exposure times are required in tissues with significant differences in water content in order to prevent hot spots and to get therapeutically relevant effects.

References:

[1] Jakubowski D. et al. In: Biomedical Optical Imaging (Eds. J. Fujimoto, D. Farkas), 352-377, Oxford University Press (2008).

[2] Bashkatov A.N. et al.: J. Innov. Opt. Health Sci. 4, 9-38 (2011).

[3] Chanmugan A. et al.: Int. Mech. Eng. Congr. Expo. 134-143 (2012).

[4] Jacques S.L.: Phys. Med. Biol. 58, R37-R 61 (2013).

[5] Chen H. et al.: Int. J Heat and Mass Transfer 80, 121804 (2021).

[6] Vaupel P., Piazena H.: Int. J. Hyperthermia 39, 987-997 (2022).

[7] Camillieri J.S. et al.: Sensors 22, 3894 (2022).

[8] Bianchi L. et al.: Int. J Hyperthermia 39, 297-340 (2022). [9] Lüchtenborg A.M. et al.: Adv. Exp. Med, Biol., in press (2024).

FP-11
Use of radiofrequency electromagnetic fields applied by capacitive hyperthermia for glioblastoma therapy

D. Gerster[1], R. Muratoglu[1], P. Krahl[1], A. Hansch[1], A. Dieper[1], D. Kaul[1], P. D. Veltsista[1], J. Onken[2], M. Misch[2], J. Nadobny[1], D. Zips[1], P. Ghadjar[1]

[1]Charité Universitätsmedizin Berlin, Radiation Oncology, Berlin, Germany
[2]Charité Universitätsmedizin Berlin, Neurosurgery, Berlin, Germany

Introduction: Radiofrequency electromagnetic fields applied by capacitive hyperthermia (RF-HT) might be applicable to improve therapy for glioblastoma patients but computer simulation data is scarce. We aimed to perform a numerical analysis of RF-HT treatment in glioblastoma patients.

Methods: The EHY-2030 RF-HT system (Oncotherm, Budapest, Hungary) was studied using a round 20 cm diameter electrode. Realistic head models were created, and quasi-electrostatic finite element simulations were performed (Sim4Life v7.2, ZurichMedTech, Zürich, Switzerland). First, 109 spherical supratentorial glioblastoma localizations

were created within a healthy head model and three different electrode setups were used for simulations of the specific absorption rate (SAR). These simulations enabled us to determine the best setup for each localization. Then, in a total of 20 real glioblastoma patients, the E-field and SAR in the gross tumor volume (GTV) and its boundary zone were simulated using two electrode setups, and transient temperature simulations were performed.

Results: The outcome of the simulation for the 109 artificial tumor localizations indicated enhanced effectiveness when the electrode is setup as close to the GTV as possible. The simulations conducted on 20 patients revealed that the SAR achieved in the GTV and its surrounding boundary zone is highly dependent on the localization of the tumor, with a mean SAR of 24.3 W/kg (ranging from 11.5 to 46.7 W/kg). The mean temperature within the GTV was higher in patients with a resection cavity (mean: 40.2°C) instead of a macroscopic tumor (mean: 37.8°C).

Conclusion: RF-HT induces a substantial SAR within the GTV and its boundary zone in glioblastoma patients. The temperature increase in the GTV is significantly greater in patients with a resection cavity compared to those with a macroscopic tumor. To further clarify the role of RF-HT in glioblastoma therapy, clinical trials would be necessary.

FP-12
Ultra-wideband, high-power hyperthermia system with precision control of steering parameters

R. Nilsson[1], M. Zanoli[1,2], H. Fischer[3], M. A. Pagneux[4], H. D. Trefna[1]

[1]Chalmers University of Technology, Electrical Engineering, Göteborg, Sweden
[2]Erasmus University Medical Center Rotterdam, Rotterdam, Netherlands
[3]Eindhoven University of Technology, Eindhoven, Netherlands
[4]Aix-Marseille university, Marseille, France

Question: Deep-seated intracranial tumors for microwave hyperthermia treatment poses increasingly higher requirements on accuracy as undesired heating in healthy tissues may lead to life threatening consequences. While software-based treatment planning provides optimal steering parameters, it must be cross-linked with a high precision microwave hardware that can accurately deliver the parameters during the treatment session. Especially, the system must accommodate for potential inaccuracies in hardware components or mismatches between system and antennas. This contribution proposes an improvement of an Ultra-Wideband (UWB) microwave system using a novel feedback system to precisely deliver desired parameters. Additionally, the feeding structure of the self-grounded bowtie antennas as well as their operational frequency band were revised.

Method: A multi-channel feedback system composed of a single-board microcontroller (Arduino Mega), microwave magnitude and phase detectors (AD8302), and phase shifters (DTS-11-480/1S) was designed and evaluated. The transformed signal is extracted and compared to the original signal (reference signal) via AD8302 to determine deviations from desired steering parameters. The phase shifters were systematically used to set the phase of the reference signal, enabling the full 360° span. All electrical components are EMC shielded. To ensure an efficient energy transfer between the system and antennas, two attempts to improve the antenna feeding structure were designed and evaluated. The first approach involved a re-design of the current feeding structure, the balun, while the second replaced the balun with a microwave slot structure.

Results: The system was constructed with an input signal feed to the 16 antennas allowing for a frequency range of 10-1000 MHz, phase range of 0-360°, and amplitude power range of 0-53 dBm (200 W). Preliminary tests show a signal control between 2-4° for phase, and 1< dB for amplitude settings. Using the new balun allowed for lower frequencies of 245 MHz to be reached. The slotted structure optimally operated at higher frequencies but showed ideal directivity thus remains a promising candidate.

Conclusion: A 16 channel UWB amplifier system using a control feedback system for precision control of steering parameters was designed and constructed. Self-grounded bowtie antennas were re-optimized to allow for lower frequencies down to 245 MHz. Theoretically, the system allows for simultaneous use of different antenna operating at frequency range between 245 - 1000 MHz.

FP-13
Pareto optimization for prostate cancer focal laser ablation

A. Andreozzi[1], M. Iasiello[1], G. Napoli[2], G. P. Vanoli[2]

[1]Università degli studi di Napoli, Dipartimento di Ingegneria Industriale, Napoli, Italy
[2]Università degli studi del Molise, Dipartimento di Medicina e Scienze della Salute "V. Tiberio", Campobasso, Italy

Laser thermal ablation is a new therapy arising for prostate cancer treatment. Being a low-invasive technique, in many cases it can be preferred to high-invasive ones such as chemotherapy, radiotherapy or surgical operations; besides, it can be an alternative to other thermal therapies like microwave or radiofrequency ablation. Laser induced hyperthermia, allowing to concentrate the thermal energy only on the tumor, without affecting the healthy tissue, permits to kill the tumoral cell without affecting the surrounding healthy one. However, so far, the procedure is based on surgeon experience, since recognized guidelines are still missing, due to lack of ex vivo and in vivo data. Consequently, it is fundamental to develop accurate models to aid the surgeon before, to better plan, and during the procedure, to properly set the protocol, to maximize the tumoral tissue death, while, at the same time, avoiding healthy tissue damaging. For these reasons, this work aims to find the best setting, to perform a laser induced hyperthermia treatment to ablate a prostate cancer, by means a Pareto optimization carried out employing a multi-objective genetic algorithm (MOGA).

The procedure optimization object of this work aims to find the best trade-off among the procedure design parameters to improve the outcomes. To pursue this goal, a multi-objective genetic algorithm, based on the natural evolution theory, is implemented in MATLAB environment, employed to set and update the decision variables[MI1] , which are provided to the finite commercial code COMSOL, that allows to solve the governing equations describing laser hyperthermia, namely the Pennes"s equation for the heat transfer in biological tissues and the laser beam propagation inside it, simulated with the Beer-Lambert"s law. As a constraint[MI2] , it is assumed that the tumor is a sphere that always presents the same volume, and also the surrounding tissue has always the same geometrical sizes. With the same code, the objective functions, namely the thermal damage in the tumor and in the healthy tissue, are evaluated and provided to the MATLAB MOGA, which iteratively continues until a stop criterion is reached and the Pareto front is obtained.

The results point out that a multi-objective optimization allows to properly set the protocol parameters, choosing for the best trade off among complete tumor ablation and healthy tissue conservation, achieved with the optimal set of points along the Pareto front. This allows to choose the best protocol (time, laser number, power, position, and dimension) to guarantee the maximum necrosis in the tumor and to avoid damaging the healthy tissue. This method could establish a framework to aid the surgeon to plan the hyperthermia protocol reducing the outcome uncertainty.

FP-15
First measurements with a phantom for infrared hyperthermia devices according to ESHO guidelines

D. Marder[1], P. Janssen[1], O. Timm[1], R. A. Hälg[1], A. R. Thomsen[2], P. Zucchetti[3], W. Arnold[3], H. Schneider[1], A. Ademaj[1], E. Puric[1], O. Riesterer[1]

[1]Kantonsspital Aarau, Radio-Onkologie-Zentrum Mittelland, Aarau, Switzerland
[2]University of Freiburg, University Medical Center, Freiburg/Brsg, Germany
[3]Luzerner Kantonsspital, Radio-Onkologie, Luzern, Switzerland

Question: Hyperthermia (i.e., heating at 40-43°C for an hour) is a potent sensitizer in combination with radiation therapy, enhancing the treatment outcome for malignant tumours. For large superficial tumours, water filtered infrared-A (wIRA) is a common technique of hyperthermia. The minimum requirements for such devices are defined in the published guidelines of the European Society for Hyperthermic Oncology (ESHO) [1]. To test the abilities of a device applying wIRA, a skin tissue equivalent phantom was produced and the characteristics of a commercial hyperthermia treatment device in terms of heating ability, thermal effective penetration depth (TEPD) and thermal effective field size (TEFS) were evaluated.

Methods: To test the abilities of the commercial wIRA device hydrosun-TWH1500 (heckel medizintechnik GmbH, Esslingen, Germany), a silicone-based phantom according to Lualdi et. al. [2] was produced. The phantom consists of multiple square sheets with an individual thickness of 5-9 mm and a side length of 25 cm. In total of 22 experiments were performed with four irradiators for heating at the Kantonsspital Aarau and the Luzerner Kantonsspital. According to ESHO guidelines the stack of phantom sheets was exposed to irradiation by the wIRA device for 6 minutes. Instantly after the irradiation, high resolution infrared images (VarioCAM® HD, Dresden, Germany) were taken of the surface at various depths. From the pixelwise substraction of the temperature images before and after irradiation, the maximum temperature rise at 5 mm, TEPD and TEFS were determined using the software of the IR camera.

Results: For the maximum temperature rise achieved in 5 mm phantom depth, which is the indicator for the heating abilities of the wIRA heating device, the value of 11.4 ± 0.71 K was found, when keeping the surface temperature below 43°C. The TEPD was equal to 10.6 ± 0.62 mm (see *Figure 1*). At 5mm depth an area of 357 ± 17 cm2 was found for TEFS (see *Figure 2)* which is equivalent to a circular coverage area with a radius of 10.6 ± 0.25 cm.

Conclusion: With the suggested phantom a reproducible measurement of TEPD, TEFS and maximum temperature rise at 5 mm depth is possible. Further investigations into the thermal properties of the produced phantom are necessary to evaluate its tissue equivalence.

Acknowledgements: This work was financially supported by the Dr. med. h.c. Erwin Braun Stiftung.

References:

[1] Dobsicek Trefna, H., Crezee, J., Schmidt, M. et al (2017). Quality assurance guidelines for superficial hyperthermia clinical trials: II. Technical requirements for heating devices. Strahlentherapie und Onkologie, 193(5): 351-366. http://dx.doi.org/10.1007/s00066-017-1106-0

[2] Lualdi, M., Colombo, A., Farina, B., Tomatis, S. and Marchesini, R. (2001), A phantom with tissue-like optical properties in the visible and near infrared for use in photomedicine. Lasers Surg. Med., 28: 237-243. https://doi.org/10.1002/lsm.1044

Fig. 1

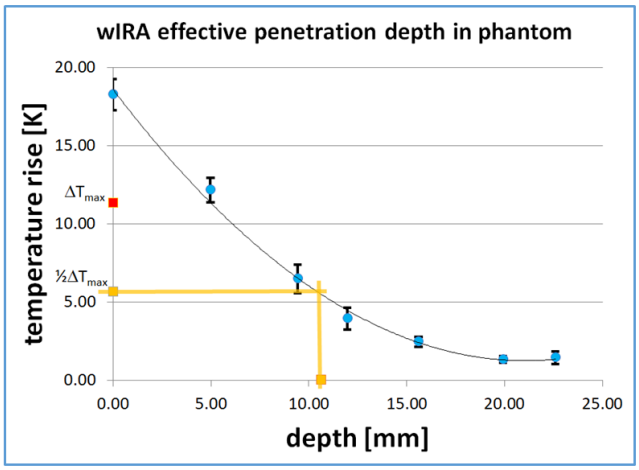

Figure 1: TEPD determined from penetration depth

Fig. 2

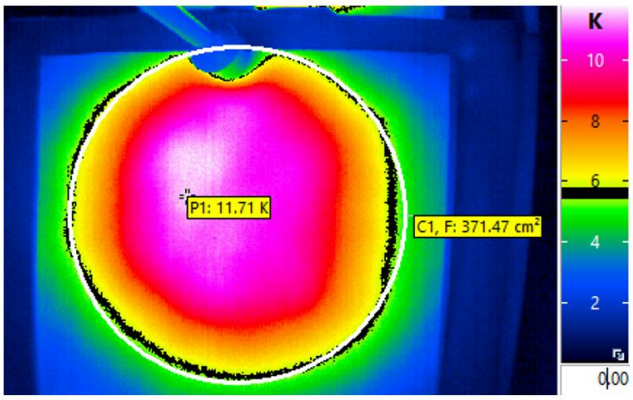

Figure 2: example for TEFS at 5mm penetration depth; black outline defines the 50% T_{max} temperature rise and is approximated by the white circle as the TEFS

FP-16

Reirradiation and hyperthermia in patients with recurrent previously irradiated angiosarcoma in head and neck

T. Lushchaeva[1], V. Vasilevska[1], D. Milanovic[1], D. Medenwald[1]

[1]University Hospital Magdeburg, Department of Radiation Oncology, Magdeburg, Germany

Objective: The treatment of locally recurrent previously irradiated angiosarcomas of the head and neck remains a multidisciplinary challenge. Radical surgical treatment can be difficult and the use of a second course of radiotherapy (RT), known as reirradiation (re-RT), may be limited due to the development of radioresistance and previous radiation exposure to normal tissue.

Hyperthermia treatment (HT) is the controlled application of heat to the body, which is known for its radiosenticising properties. It reduces hypoxia-induced radioresistance, causes inhibition of DNA damage repair and probably activates immune cell expression. All the mechanisms described can lead to increased sensitivity to radiation and consequently to better local control.

The combination of re-RT and HT has been demonstrated to be a safe and efficacious approach in the management of recurrent breast cancer. The use of HT and RT has also been shown to be a potential approach in the treatment of soft tissue sarcomas, with an improvement in 5- and 10-year overall survival (OS).

In the treatment of locally recurrent, previously irradiated angiosarcomas in the head and neck area, the combinatin of HT and re-RT has not yet been investigated.

Methods: The proposed study will be conducted as a multicenter trial. Patients with a local recurrence of an angiosarcoma in the head and neck area who have previously undergone irradiation will be included in the study. We plan to recruit 53 [MD1] patients (with a 10% drop-out rate) based on a power of 90% with 95% confidence intervals with a null-hypothesis of a local control rate after one year of 40% vs. 65% in the study group. Patients will be treated with total dose of 20 Gy in five weekly fractions. HT will be applied prior to irradiation with tissue temperature of 42°C to 20 mm and exposure time 45-60 minutes.

Primary objective of this trial is to determine local control and our secondary objectives are toxicity, quality of life and cancer-specific survival. Primary endpoint of this trial is progression-free survival while secondary endpoints

are quality of life according to the EORTC QLQ-HN43 questionnaire, toxicity according to CTCAE (version 5.0), overall and cancer-specific survival, adverse events and metastasis-free survival.

Cases will be matched with historic controls in order to estimate the clinical effect. Based on a non-inferiority approach (PFS of 10% vs. 30%, non-inferiority limit 2%) the power is 85%.

Results: We intend to discuss this topic with our colleagues in order to organise a clinical trial. Our hypothesis is that the combination of re-RT and HT may lead to better local control than treatment with re-RT alone.

Conclusion: In the treatment of recurrent angiosarcoma of the head and neck, re-irradiation in combination with hyperthermia may be a valuable treatment strategy, and to confirm our hypothesis, we plan to conduct an multicentre study.

FP-17
Characterization of 434 MHz CFMA applicators for superficial hyperthermia for various realistic curvature and bolus thickness scenarios

T. D. Herrera[1], R. Zweije[1], J. Crezee[1], H. P. Kok[1]

[1]Amsterdam University Medical Center, Radiation Oncology, Amsterdam, Netherlands

Objectives: Contact flexible microstrip applicators (CFMA) operating at 434 MHz, are used for superficial hyperthermia treatments. These applicators come in different sizes and are flexible or precurved to permit clinical use following the patient curvature. A water bolus is used to couple the emitted power to the patient tissue, with a thickness that depends on patient anatomy. This work investigates the influence of curvature and bolus thickness on the performance of CFMAs.

Methods: We characterized the E-field distribution of the 3H (28.7x20.7 cm2) and 5H (19.7x28.5 cm2) CFMAs. We placed the applicators on an acrylic tank filled with 100x40.5x20 cm3 of saline water (6 g/L NaCl, electrical conductivity σ = 1.1 Sm-1, relative permittivity εr = 78), connected to an ALBA signal generator applying 50 W at 434 MHz. The applicators were put in contact with the saline water using a bolus filled with demineralized water over a 1 mm thick acrylic surface, either flat or with curvature radii of 175 and 280 mm. The bolus thickness was kept constant, with values of 7, 13, 19, 25 and 31 mm. We measured E-field using a robotic scanner moving a diode dipole antenna, oriented parallel to the main E-field direction. The surface at 1 cm depth parallel to the contact surface was measured, as well as orthogonal planes perpendicular to the CFMA. We evaluated the SAR distribution, effective field size (EFS) and effective heating depth (EHD) for varying bolus thicknesses and curvatures. We also performed finite difference time domain (FDTD) simulations using Plan2Heat and compared the SAR distributions, EFS and EHD to the measurement results.

Results: EFS values were between 300 and 400 cm2 for both applicators for the flat contact surface. Excessive bolus thickness showed a split SAR focus, probably due to the interference of oscillations in the bolus with the incident field. This results in a decreased EFS, especially for very large bolus thickness, which a larger impact for the 3H. EFS was reduced with curved contact surfaces, showing also a split focus for large bolus thickness, especially for the smaller curvature radius. Earlier measurements and analysis showed an absence of the split focus effect due to bolus interference for CFMAs smaller than the 3H and 5H, likely because these antennas are smaller with respect to the wavelength at 434 MHz. Simulations confirm the overall shape of SAR distributions and depth penetration of the 3H and 5H CFMAs. Simulation results provide valuable insights into the impact of curvature and bolus thickness on SAR distributions, which makes them useful to optimize treatment delivery.

Conclusions: FDTD simulations are a valuable tool to assess SAR distributions considering variations in curvature and bolus thickness for CFMAs. The impact of the set-up geometry on SAR distributions is reflected, which makes treatment planning using the patient model a useful tool to optimize treatment conditions in individual patients.

Fig. 1

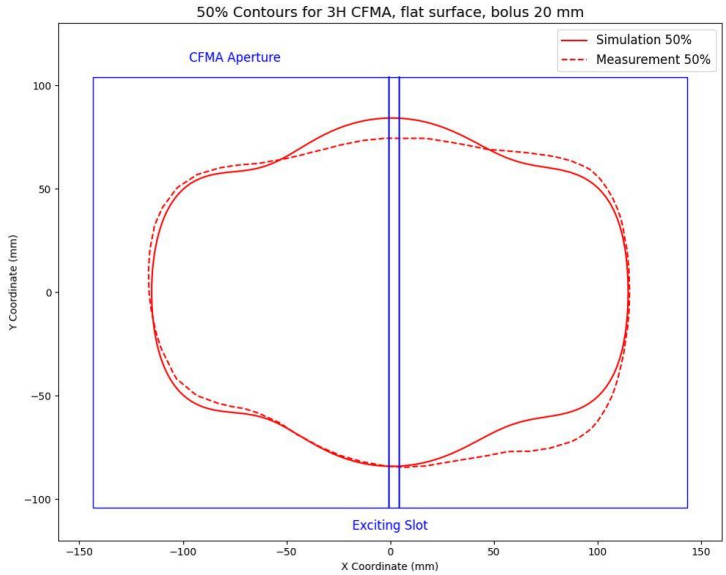

Figure 1. Comparison of the 50% contours at 1 cm depth in saline water for measurement and simulation of SAR distribution for the 3H CFMA, with a flat surface contact and bolus thickness of 20 mm. The geometry for the applicator and exciting slot is shown in blue. Simulation was performed with Plan2Heat, with voxels of 2x2x1 mm^3. Measurement was made with an E-field sensor in saline water 6 g/L.

Fig. 2

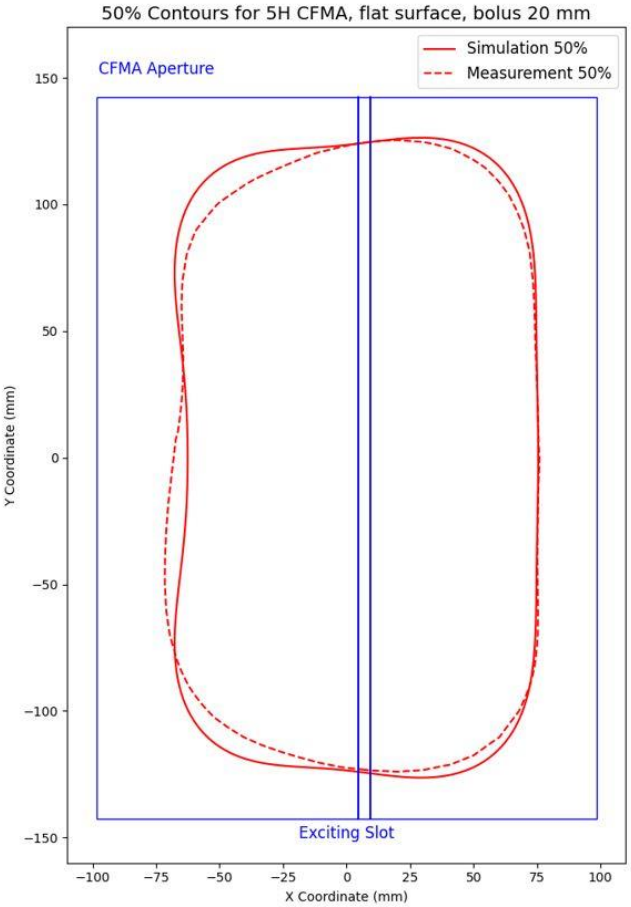

Figure 2. Comparison of the 50% contours at 1 cm depth in saline water for measurement and simulation of SAR distribution for the 5H CFMA, with a flat surface contact and bolus thickness of 20 mm. The geometry for the applicator and exciting slot is shown in blue. Simulation was performed with Plan2Heat, with voxels of 2x2x1 mm^3. Measurement was made with an E-field sensor in saline water 6 g/L.

FP-18

Fast tumor volume reduction in fungating bulky breast cancer following combined palliative radiotherapy and hyperthermia: Case reports of two patients

M. Blatti[1], E. Riggenbach[1], M. Fürstner[2], M. Reist[1], N. Bachmann[1], B. Shrestha[1], M. Rabaglio[3], C. Rauh[4], D. M. Aebersold[1], K. Lössl[1], E. Stutz[1]

[1]Inselspital Bern, Bern, Switzerland
[2]Division of Medical Radiation Physics and Department of Radiation Oncology, Inselspital, Bern University Hospital, University of Bern, Bern, Switzerland
[3]Department of Medical Oncology, Inselspital Bern, University of Bern, Bern, Switzerland, Bern, Switzerland
[4]Department of Gynecology, University Hospital Inselspital Bern, Bern, Switzerland, Bern, Switzerland

Aims: The treatment of fungating bulky breast tumors is challenging. A phase III randomized study with locally advanced breast cancer patients treated with definitive radiotherapy (RT) (Overgaard, 2024) demonstrated that local control can be significantly improved by adding hyperthermia (HT). Based on this data, we offered RT+HT to patients with bulky, fungating breast tumors.

Methods: All patients treated in our institution from 04/2022 until 06/2024 with fungating bulky inoperable breast tumors with (i) definitive HT+RT, (ii) a baseline gross target volume (GTV) larger than 200cc and (iii) at least one diagnostic follow-up CT scan 3 months after treatment were included. The GTV was contoured on the RT planning CT scan and used as baseline for assessing tumor volume reduction during RT+HT (based on CBCT scans) and after treatment (follow-up CT scans).

Results: Two patients fulfilled the inclusion criteria. A 36 year old woman with a bulky (GTV=2946 cc) fungating triple negative breast cancer with lung metastases (cT4 cN3 cM1) was treated with chemotherapy with paclitaxel and pembrolizumab with transient response but consecutive tumor regrowth. Systemic treatment was stopped and palliative RT+HT with 39Gy/13fx was initiated. After observing a fast tumor shrinking, additional 20Gy/10fx were applied to a total dose of 66Gy EQD2 (a/b3) concurrently with 10 HT sessions in total (A4000, Med-Logix, Italy) and followed by epirubicin. We observed a remarkable GTV reduction during RT+HT of - 55% at 3 weeks after baseline CT, -88% at 12 weeks and -92% at 19 weeks. Three months after completing RT+HT, the remaining tumor hole was excised showing histologically no malignant cells. The second patient was a 78 year old woman with a hormonal receptor positive fungating inoperable breast tumor (GTV=216cc) with brain metastasis (cT4 cN0 cM1). She was treated with palliative RT+HT with 42Gy/14fx (EQD2 50.4Gy) combined with 5 radiative HT sessions (A4000, Med-Logix, Italy) and aromatase inhibitors. Ribociclib was not tolerated. Similarly, we observed a fast GTV reduction during RT+HT of -58% at 3 weeks after baseline CT, -91% at 11 weeks and -95% at 25 weeks. The toxicity was within the expected range, especially as a bolus was used. The first patient developed a grade 3, the second only a grade 1 radiodermatitis (CTCAE v5.0). This tumor volume reduction was accompanied with a subjectively reported improvement of pain, reduced odor and improved quality of life.

Conclusion: In both patients with bulky fungating breast cancers we observed a fast tumor volume regression of nearly -60% from baseline within the first two weeks under treatment, independent of their initial size and nearly -90% after 3 months. This combination seems to be a fast-active and effective method and should be taken earlier into account for such challenging tumor situations with limited treatment options.

Fig. 1

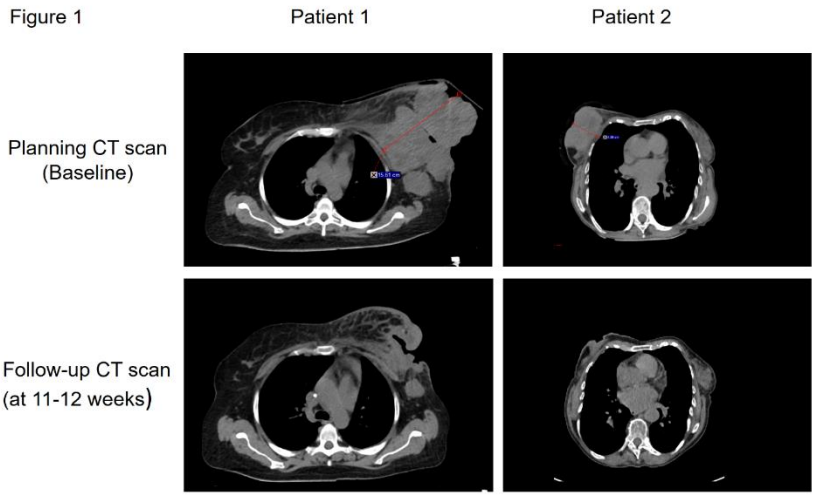

Fig. 2

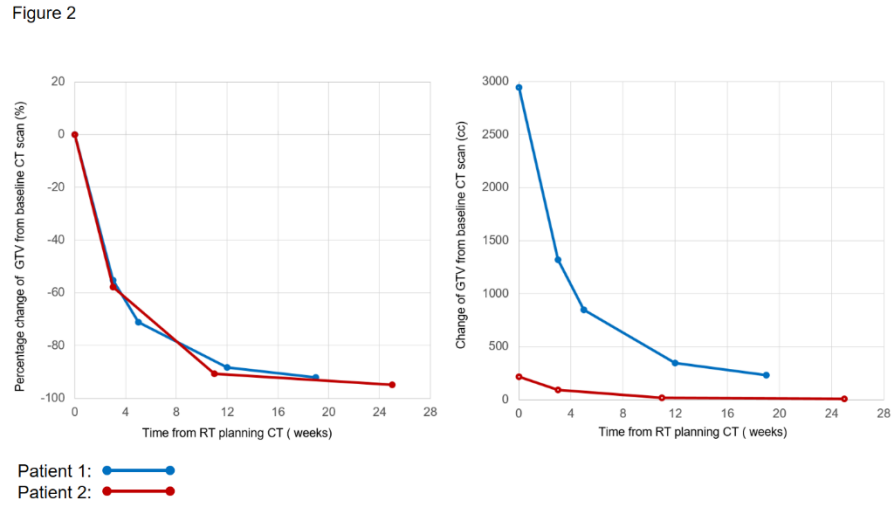

FP-19

Impact of Schottky diodes feeding traces on E-field characterization of 434MHz hyperthermia applicators

D. Phal[1], K. Sumser[1], I. Androulakis[2], S. Curto[2], M. Paulides[1]

[1]Eindhoven University of Technology, Eindhoven, Netherlands
[2]Erasmus University Medical Center Rotterdam, Cancer Institute, Rotterdam, Netherlands

Question: Quality assurance (QA) of hyperthermia applicators ensures their accurate functionality, thereby guaranteeing that the delivered dose aligns with the planned dose. According to ESHO guidelines, QA should be fast, reliable and accurate. However current SAR based QA methods are either time-consuming (e.g., IR camera, thermal probes) or both expensive and limited to compatible applicators (e.g., MRT). E-field sensing sheets, with their 2D array of sensors, enable fast QA. In this study, we aim to assess the effect of Schottky diode sheets on the E-field distribution through both simulations and measurements.

Materials and methods: Previously, E-field measurement using Schottky diodes arranged in a 2D array have been shown feasible (Van Rhoon, IJH, 2009). Building on this knowledge, we designed printed circuit boards (PCB) of various shapes and sizes with multiple diodes to study if they generate E-field distortions. First, we used Sim4Life to investigate the effect of the Schottky diode sheets on the heating pattern of a clinically used lucite cone

applicator (LCA). We analysed the impact of the PCB on the E-field patterns inside a phantom, as shown in Fig 1A. Additionally, we examined the voltage across the diode pins in two scenarios: first, when the traces are perfect electrical conductors, and second, when the traces are high impedance carbon. Carbon traces represent the ideal case due to their high impedance properties, which minimizes E-field distortions by reducing current flow and interaction with the E-field. We designed a PCB with 9 diodes arranged in a 3x3 grid fed by copper leads facing the applicator's propagation region to validate our simulations.

Results: Fig. 1 shows the E-field distribution 5cm inside the phantom (deep region), in front of the applicator aperture without PCB (Fig 1B), and with PCB with copper traces (Fig 1C) or carbon traces (Fig 1C). These simulations show that conventional PCBs with copper traces (Fig 1C) modify E-field patterns. Simulations show that increasing the impedance of these traces by alternative materials effectively reduces the E-field distortion (Fig 1D). Namely, the E-field values in the evaluated region are reduced by up to 123% on average. Fig. 2 shows the normalized voltage across the dipole pins of the simulated PCB with copper traces and high impedance traces.

Conclusion: Conducting feeding traces of E-field sensors in 2D sheets disturb the E-field pattern. Our simulation study show that high impedance traces are necessary for accurate E-field sensing and improved SAR-based QA.

Fig. 1

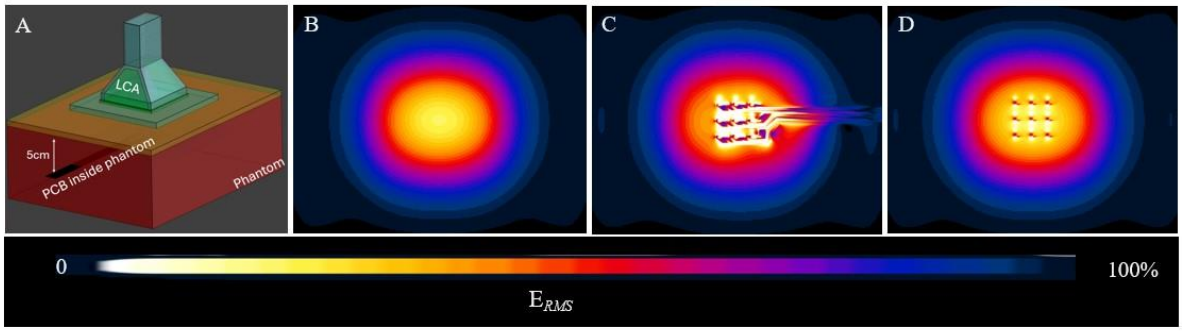

Fig. 1 (A) The simulation setup with the PCB inside the applicators propagation region (B) E-field pattern from LCA without the PCB in the phantom (C) E-field pattern with PCB with copper traces (D) E-field pattern with PCB with ideal high impedance traces.

Fig. 2

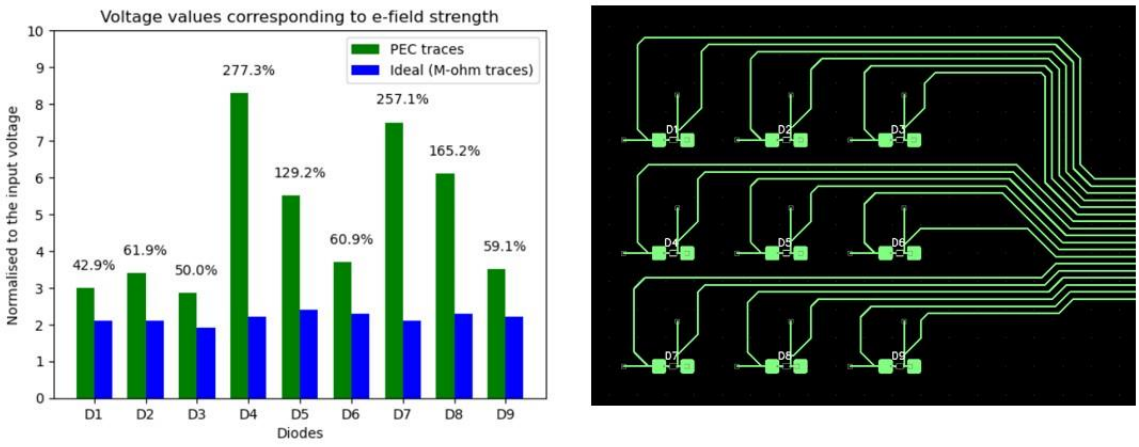

Fig.2 (left) The normalised voltage across diode pins from the simulation (right) the designed 3x3 PCB

FP-20
Effect of positioning on SAR and temperature in head and neck microwave hyperthermia

E. van Wesel[1,2], S. Curto[1], G. C. van Rhoon[1], M. Paulides[1,2]

[1]Erasmus University Medical Center Rotterdam, Radiation Therapy, Rotterdam, Netherlands
[2]Eindhoven University of Technology, Electrical Engineering, Eindhoven, Netherlands

Introduction: In microwave (434MHz) hyperthermia, electromagnetic (EM) waves are simulated and optimized for delivering maximum heat in the tumor while suppressing possible hotspots by using the target-to-hotspot quotation (THQ) [1]. However, the scan for pre-treatment planning is not performed in the actual treatment position. The position inside the applicator deviates from the planned position, causing the tumor to shift out of focus and new hotspots to occur. These expected THQ differences will also lead to changes in temperature profile [2]. Positioning measures in microwave hyperthermia restrict errors to 5mm in all directions, considering current developments in treatment and applicator design [3]. Hence, our question is: What is the effect on THQ and temperature profile following position changes of 5mm?

Methods: Twelve patients were simulated using finite difference time domain simulations inside the MR Collar to determine the treatment planning for each patient. Phases and amplitudes of the simulated EM waves were optimized to obtain the highest THQ. To simulate positioning errors, each patient was simulated with negative and positive position shifts of 5mm in either x, y and z direction. The phases and amplitudes optimized for the nominal position were applied to the shifted scenarios, and the THQ difference with the nominal position was calculated. Based on these EM simulation results, the impact of incorrect position on temperature was quantified as well. For this step, thermal simulations were done with the input power set for each simulation to reach 44°C in healthy and tumor tissue, according to the ESHO benchmarks for hyperthermia treatment modeling.

Results: Figure 1A shows the effect of positioning on THQ, with an average decrease in THQ of 6.9%(x), 3.2%(y), and 1.3%(z). The temperature in the tumor quantified by T50 (median) shows a different directional dependent result with an average decrease in T50 of 0.3°C(x), 0.4°C(y), and 0.5°C(z) (Figure 1B). Associating T50 to THQ (Figure 2) shows a moderate relation between T50 and THQ (R^2=0.63) of +0.4°C for +0.1 in THQ. No pronounced linear relationship between the tumor temperature change and THQ change was found.

Conclusion: A 5mm change in positioning between the treatment and planning positions affects the accuracy of the optimized parameters in focused microwave hyperthermia. Our simulations predict that these changes also directly impact the temperatures reached during treatment.

[1] Drizdal T, Int. J. of Hyperth. 2018; 34(6)
[2] Canters R, Phys Med Biol. 2009; 54(12)
[3] Rijnen Z, Int. J. of Hyperth. 2015; 31(8)

Figure 1: The relative difference in THQ (calculated using: $\Delta THQ=(THQ_r-THQ_{r+\Delta r})/THQ_{r+\Delta r}x100\%$ (THQ_r: treatment position, $THQ_{r+\Delta r}$: planned position) for positioning errors in x, y and z direction, whereas B shows the respective positioning errors and ΔT50 ($\Delta T50=T50_r-T50_{r+\Delta r}$).

Figure 2: The optimized THQ is shown with its relation to the tumor temperature (T50).

Fig. 1

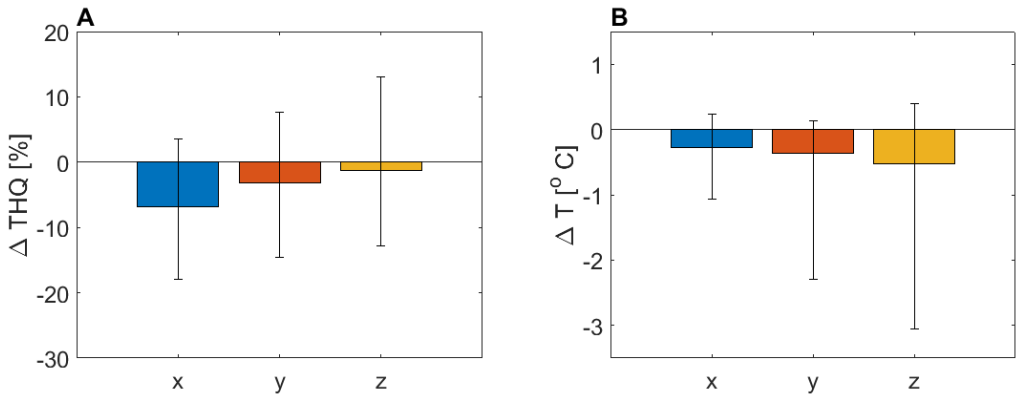
A
B
Δ THQ [%]
Δ T [° C]
20
10
0
-10
-20
-30
1
0
-1
-2
-3
x
y
z

Fig. 2

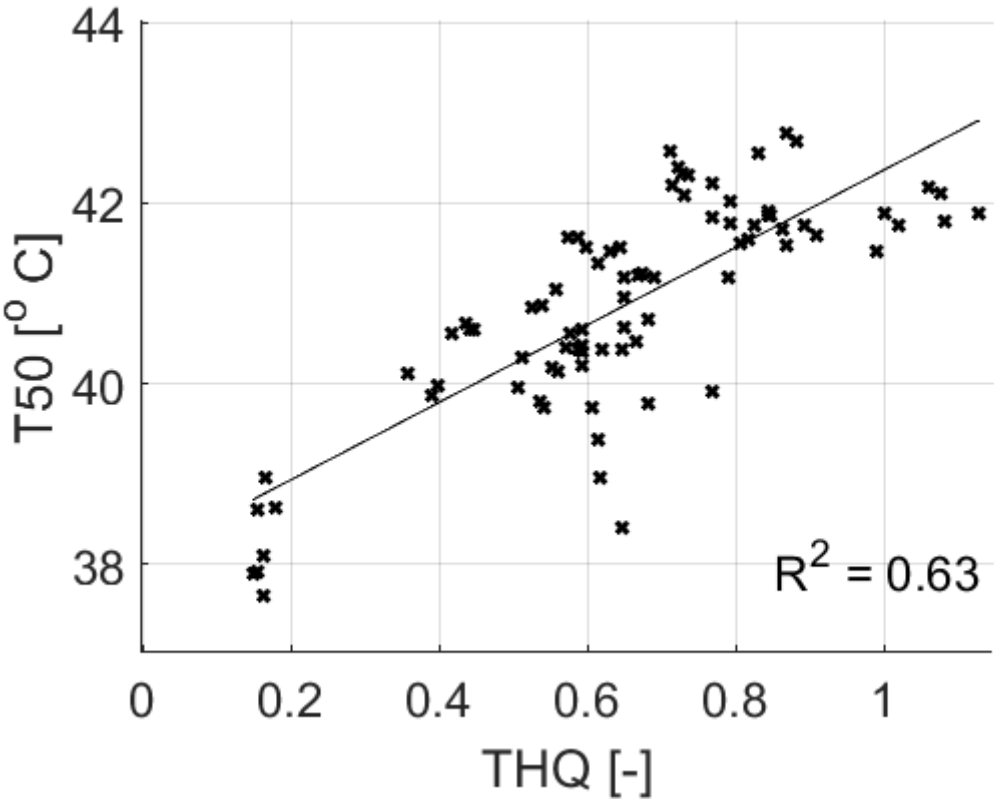
T50 [° C]
44
42
40
38
0
0.2
0.4
0.6
0.8
1
THQ [-]
R2 = 0.63

FP-21
Implementation of surrogate optimization algorithm for hyperthermia treatment

M. Mrázková[1], T. Drizdal[1]

[1]Czech Technical University in Prague, Department of Biomedical Technology, Faculty of Biomedical Engineering, Kladno, Czech Republic

In deep regional hyperthermia, temperature target increase is standardly applied using constructive interference of several electromagnetic fields radiated from phased array setups. However, creating target conformal heat distribution while minimizing exposure to nearby healthy tissues is challenging. A possible solution is to use optimization algorithms to adjust the amplitude and phase of the antenna input signals in the hyperthermia treatment planning process (HTP).

This paper aims to maximize the Specific Absorption Rate (SAR) in the target area while minimizing the SAR in the healthy tissue. Surrogate Optimization (SGO) uses a static model that can accurately approximate the output function concerning the inputs. The advantage of surrogate modeling is its speed, since one evaluation of the surrogate model is much faster than the evaluation of the original simulation. The algorithm starts by selecting a set of points in the search space, where the objective function is evaluated. These selected points are used to train a surrogate model, which is then used to predict the values of the objective function at unexplored points in the defined space. Based on these predictions, SGO iteratively selects new points and evaluates the merit function at these points. If the candidate solution is of higher quality, the surrogate model is updated, and this process is iteratively repeated until the candidate solution is accepted as a global minimum or maximum [1].

For evaluation purposes, the results of the SGO algorithm were compared with those of the clinically utilized Particle Swarm Optimization (PSO) algorithm. Both algorithms used the Target Hotspot Quotient (THQ) function as a fitting function. The comparison focused on the SAR-based target coverage parameters TC25, TC50, and TC75. The HTP process was done for ten patients, specifically for five patients with tumors in the head and neck area and five patients with glioblastomas. For electromagnetic simulation, *Sim4Life* was used. Then, the E-field was exported to *Matlab*, where the optimization was performed. The results show that SGO is more efficient for glioblastomas. There was no statistically significant difference between SGO and PSO for head and neck tumors.

[1] Wang, Y., & Shoemaker, C. A. (2014). *A General Stochastic Algorithmic Framework for Minimizing Expensive Black Box Objective Functions Based on Surrogate Models and Sensitivity Analysis*. http://arxiv.org/abs/1410.6271

FP-22
Hazard of biliary stent heating in radiative deep regional hyperthermia (RHT)

S. Abdel-Rahman[1], M. Göger-Neff[2], B. Zilles[2], R. D. Issels[2], D. Di Gioia[2], L. Lindner[2]

[1]University of Munich, Medical Clinic III, Munich, Germany
[2]University of Munich, Medical clinic III, Munich, Germany

Introduction: RHT with radiative heating technics to temperatures of 41-43°C as a supplement to chemotherapy and/or radiotherapy has proven to be beneficial in the treatment of gastrointestinal tumours. Tumours in this area usually cause a blockage of the bile duct. A biliary metallic stent implantation keeps the bile duct open so that bile can flow into the small intestine and aid digestion. Therefore, RF-induced extensive heating of the stent must be excluded prior to HT to avoid damage to the adjacent tissue.

In this study, the influence of biliary stents on the specific absorption rate (SAR) and temperature was investigated.

Material/Methods: SAR and temperature in the identical metal stent of a patient with pancreatic carcinoma awaiting treatment were examined in the phantom.

It is a commercially available Wallflex Biliary metallic Stent partially covered with a permalume™ coating provided by Boston Scientific, Ireland. For the Temperature measurements the stent was placed inside an elliptic phantom,

which was inserted in the Sigma30-MR applicator of the BSD2000-3D/MR deep hyperthermia system (Pyrexar, USA) integrated in a 1.5T Ingenia MRI (Philips, Netherlands). Inside the phantom Bowman probes were moved along the stent axis and their temperature was recorded. We applied 80 W at 100 MHz in 1 kg of Tx151 phantom, which corresponds to four times the power applied to the patient during treatment (20W/kg). In a second test the stent was embedded in a 25 kg phantom and a max. Power of 800 W (32W/kg) was applied with the Universal applicator of the BSD2000-3D/MR deep hyperthermia system.

Results: MR Thermometry estimated approx. 9-10°C heating in the Tx151 phantom in agreement with the Bowman probes (Tstart=24°C Tend=34°C). In the MRT maps there was no temperature excess at the stent location observed. The temperature along the stent showed only a moderate temperature increase (2.5 °C). In the 25kg-phantom, MR temperature measurement T50 was 5.4 °C (T90 was 4.3 °C) during a heating period of 14 minutes. The Bowman probes measured a max. temp. of 35 °C after 37 minutes. The max. ΔT between center and end of the stent was 4 °C. In a patient in perfused tissue the temperature increase is expected to be lower.

Conclusion: Such stents are not an exclusion criterion for RHT treatment. Between April and July 2024 the patient underwent 4 courses of Gemcitabine+ Cisplatin in combination with 8 RHT´s (max. power: 700 W) applied without any hyperthermia related complications or patient discomfort. The current CT shows significant regress in liver metastases with only discrete hypodense residues and size-regressed lymph nodes emphasized periportally.

FP-23
Muscle equivalent tissue material for superficial hyperthermia quality assurance

A. Kanagaratnam[1], C. Carrapiço-Seabra[1], S. Curto[1]

[1]Erasmus University Medical Center Rotterdam, Hyperthermia Unit, Radiotherapy department, Rotterdam, Netherlands

Introduction: Current quality assurance (QA) guidelines for superficial hyperthermia describe possible phantom recipes aiming to mimic dielectric and thermal properties of muscle tissues. However, these recipes have a limited time span, due to deterioration and moulding. Additionally, their fabrication process can be challenging.

Purpose: This study presents and characterises a new muscle-mimicking phantom material that is (1) viable for a relatively long period of time and (2) easy to produce through a simple mixing process.

Materials and methods: The newly developed muscle-mimicking phantom material is created by mixing deionised water (at 3 °C), TX-151, and polyethylene powder (PEP) in a mass ratio of 1000:200:120. The dielectric properties (measured between 50-450 MHz and 500-950 MHz) and thermal properties of this phantom material were evaluated both immediately after production and monitored over a period of six weeks. Measured values were compared to muscle tissue literature values from the IT"IS database [1]. Moreover, heating experiments were performed on a full-size split phantom to verify its compliance with superficial hyperthermia QA guidelines. The results were then compared to previous experiments that used the muscle phantom recipe prescribed in the QA guidelines [2].

Results: Figures 1a and 1b show the measured baseline values of relative permittivity and conductivity of the phantom material (50-450 MHz and 500-950 MHz), as well the literature values (50-950 MHz). In Table 1, the dielectric and thermal property values after production as well as during the weekly assessments are presented. We found differences up to 6% between the literature and measured values for all parameters and frequencies of interest at the baseline measurements. Over the six-week period all properties were stable within 14% from week 0. The thermal effective penetration depth (TEPD) for the newly proposed muscle phantom was compared to the TEPD of the standard QA muscle phantom [3]. We obtained 3.54 cm while previous work reported 3.17 cm. The TEPD measurements were performed within a week of when the phantom was created.

Conclusion: The proposed muscle phantom recipe was shown to have good dielectric and thermal properties at baseline and over time (at 434 and 915 MHz), being a sustainable new option as it does not grow mould as previous used versions. However, longer testing is required to further confirm these findings.

References:

[1] Baumgartner, C. et al. IT"IS Database for Thermal and Electromagnetic Parameters of Biological Tissues, Version 4.2.[(accessed on 15 July 2024)]; 2024.

[2] Dobšíček Trefná, H. et al. Quality assurance guidelines for interstitial hyperthermia. International Journal of Hyperthermia, 36(1), 276–293.

[3] Carrapiço-Seabra, C. et al. (2023). Application of the ESHO-QA guidelines for determining the performance of the LCA superficial hyperthermia heating system. International Journal of Hyperthermia, 40(1).

Fig. 1

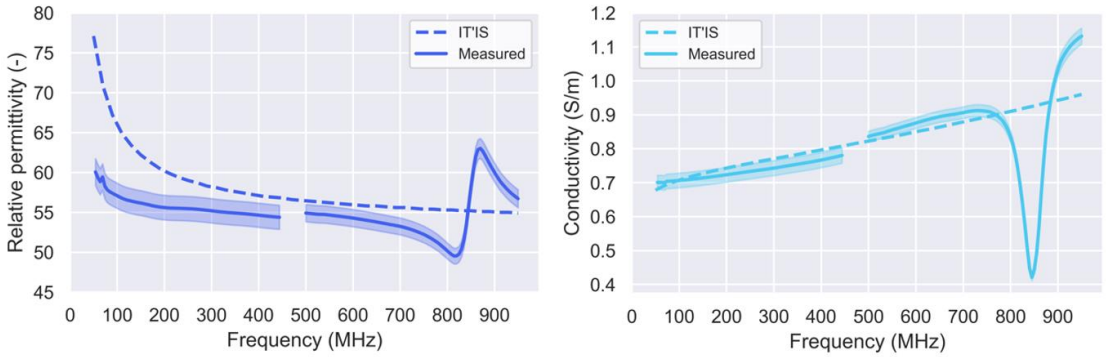

(a) (b)

Figure 1: Measured (average ± standard deviation) and literature values of (a) relative permittivity and (b) conductivity for a range of frequencies of 50 – 950 MHz.

Fig. 2

Table 1: Measured dielectric and thermal properties for muscle-mimicking phantom for two different frequencies of interest (434 and 915 MHz). Literature values from IT'IS database [1] are also given for comparison. Week 0 corresponds to the baseline measurements when the phantom was created.

		Dielectric properties				**Thermal properties**	
Parameter		Relative permittivity		Conductivity (S/m)		Specific heat capacity (J/kg K)	Thermal conductivity (W/m K)
Frequency (MHz)		434	915	434	915		
Literature		56.9	55.0	0.805	0.948	3421 ± 460	0.49 ± 0.04
Week	0	55.3 ± 2.1	52.3 ± 1.6	0.79 ±0.03	0.98 ± 0.03	3269 ± 136	0.52 ± 0.02
	1	55.8 ± 0.8	53.3 ± 0.7	0.77 ± 0.02	0.95 ± 0.01	3279 ± 224	0.50 ± 0.04
	2	53.2 ± 2.1	51.8 ± 1.3	0.76 ± 0.04	0.92 ± 0.03	3421 ± 91	0.53 ± 0.03
	3	54.4 ± 1.7	58.7 ± 1.3	0.78 ± 0.03	1.08 ± 0.02	3417 ± 134	0.52 ± 0.01
	4	53.8 ± 1.4	52.6 ± 1.5	0.77 ± 0.02	1.00 ± 0.02	3452 ± 55	0.54 ± 0.01
	5	55.9 ± 1.0	53.4 ± 2.9	0.81 ± 0.02	1.02 ± 0.06	3422 ± 125	0.56 ± 0.01
	6	55.1 ± 1.8	51.8 ± 1.4	0.83 ± 0.03	1.00 ± 0.04	3424 ± 99	0.56 ± 0.02

FP-24

Experimental measurement of the specific absorption rate of magnetic nanoparticles in magnetic hyperthermia when using non-harmonic asymmetric magnetic field waveforms

M. R. Rodríguez García[1], D. Pinto Llorente[1], L. Marrodán Bretón[1], I. Martínez Ramírez[1], C. Alcaide León[1], M. Ramos Gómez[1], J. J. Serrano Olmedo[1]

[1]Universidad Politecnica de Madrid, Centro de tecnología biomedica, Pozuelo de Alarcon, Spain

Purpose: A homemade apparatus, capable of functioning between 100 kHz and 1 MHz with various trapezoidal waveforms, including triangular and sinusoidal, has been previously employed to demonstrate that the utilization of non-sinusoidal symmetrical waveforms enhances the heating efficiency of magnetic nanoparticles [1] and the mortality of tumor cells in *in vitro* experiments [2]. Theoretical calculations have also demonstrated that the use of (a)symmetrical trapezoidal-shaped waveforms improve the Specific Absorption Rate (SAR) of magnetic nanoparticles [3]. The objective of the present study is to experimentally investigate the capabilities of a new, homemade apparatus developed to generate a wide variety of waveforms, including symmetrical and asymmetrical waveforms, to further enhance the SAR of a variety of magnetic nanoparticles.

Methodology: The new design is based on the previous one [4], which underwent a significant redesign. This involved the use of an H-bridge based on power MOSFETs, a couple of power sources, and a meticulous timing of switching. Both voltage sources are coupled in order to maintain a balanced ratio between their respective voltages, taking into account the rising and setting times. While the main source (master) is commercially available, the other (slave) is based on a DC-DC buck converter, offering a more cost-effective alternative.

Results: Figure 1 provides a detailed illustration of an exemplar waveform. Figure 2 depicts a number of real waveforms, accompanied by their corresponding MOSFET commutation schemes. Given that the initial prototype was developed just a few weeks ago, it is hoped that a comparison of the SAR obtained for different magnetic nanoparticles in a number of conditions will be presented at the conference.

Conclusions: It is feasible to develop magnetic hyperthermia equipment based on switching systems that facilitate the implementation of magnetic induction techniques on nanoparticles with enhanced heat production capacity. This paves the way for novel applications of magnetic hyperthermia in oncological therapy, exploiting intense, brief, and highly localized thermal shocks.

References:

[1] Zeinoun, M. *et al. Nanomaterials*, 11(12). pp 3240, 2021, doi: 10.3390/nano11123240

[2] Souiade, L. *et al. International Journal of Molecular Sciences*, 24(21), pp 15933, 2023, doi: 10.3390/ijms242115933

[3] Allia, *et al.* , *Physical Review Applied*, 12(3), pp 034041, 2019.

[4] M. Zeinoun, *et al.* IEEE Access, vol. 9, pp. 105805-105816, 2021, doi: 10.1109/ACCESS.2021.3099428

Fig 1. This signal has a ratio of 1:3, since the leading slope is three times larger than the ending one. The active cycle is also asymmetrical since the high flat period is 1.5 larger than the lower one.

Fig 2. A) 50% flat – asymmetrical ratio 2:1. B) 25% flat – asymmetrical ratio 4:1. C) 75% flat divided in 80% upper part and 20 % bottom part – asymmetrical ratio 3:1. D) Triangular – asymmetrical ratio 6:1.[JS1]

Fig. 1

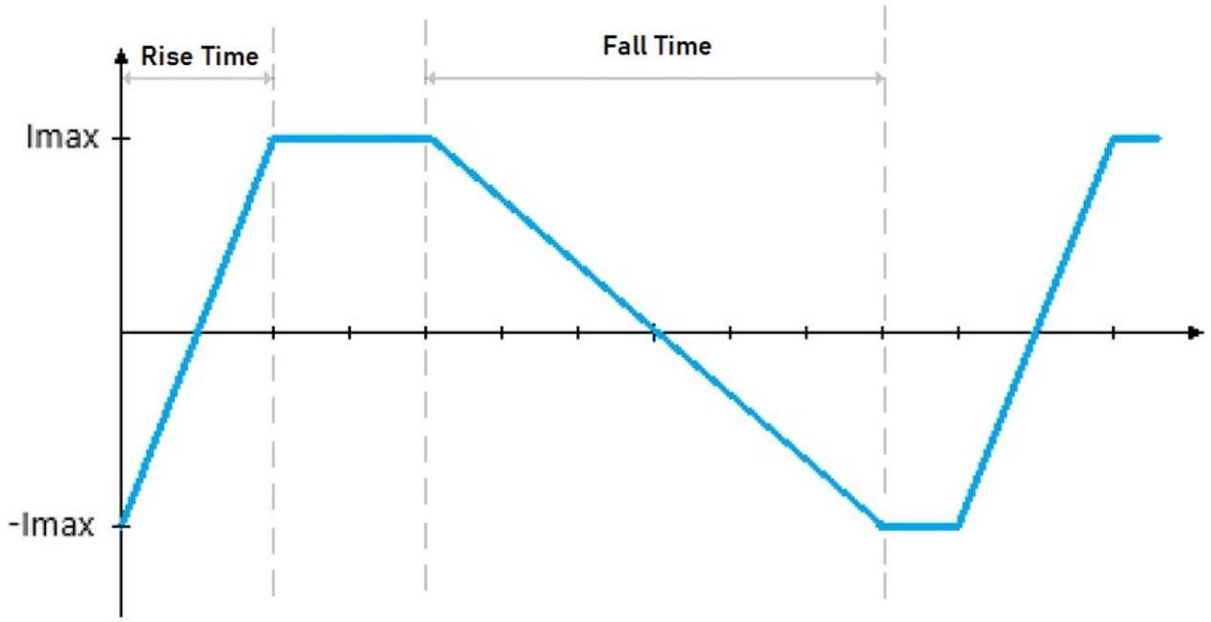
Rise Time
Fall Time
Imax
-Imax

Fig. 2

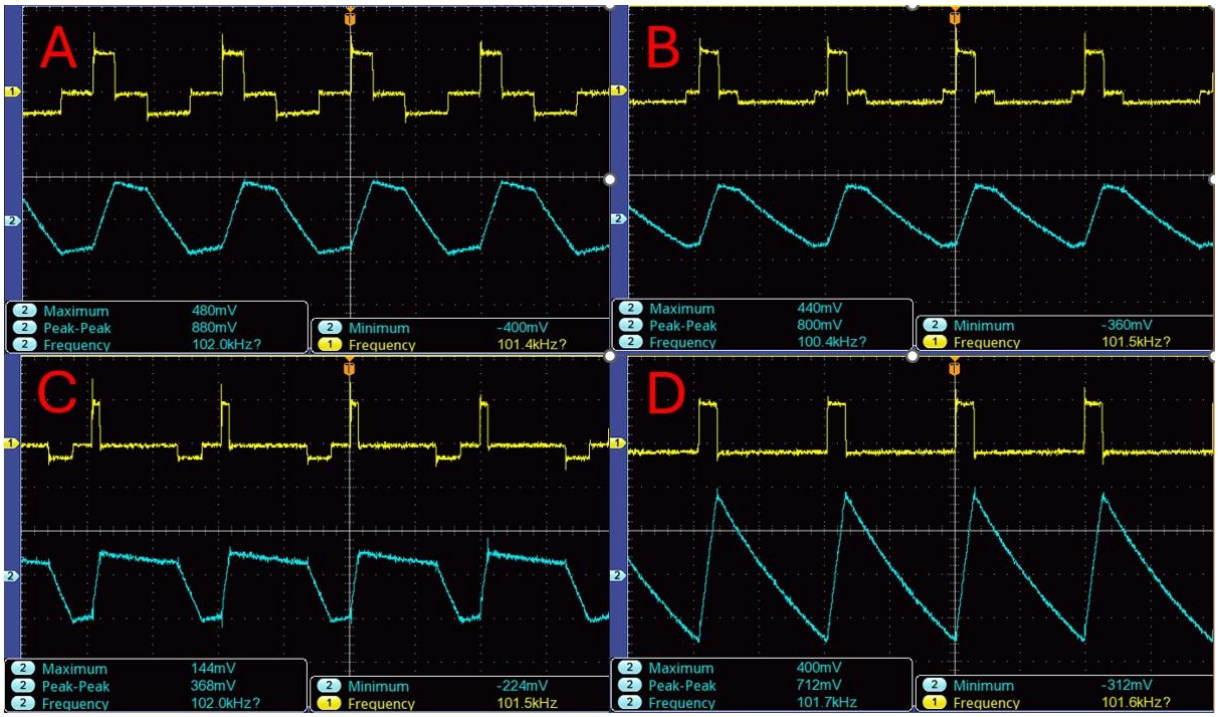
A
Maximum 480mV
Peak-Peak 880mV
Frequency 102.0kHz?
Minimum -400mV
Frequency 101.4kHz?
B
Maximum 440mV
Peak-Peak 800mV
Frequency 100.4kHz?
Minimum -360mV
Frequency 101.5kHz?
C
Maximum 144mV
Peak-Peak 368mV
Frequency 102.0kHz?
Minimum -224mV
Frequency 101.5kHz
D
Maximum 400mV
Peak-Peak 712mV
Frequency 101.7kHz
Minimum -312mV
Frequency 101.6kHz?

FP-25
Enhancing quality of life in bladder cancer patients: leveraging hyperthermia and chemotherapy

S. Badzgaradze[1], M. Kutchava[1]

[1]Immuno and Oncothermia center INTEGRA, Oncology, Kutaisi, Georgia

When pathogens become aggressive, the immune system triggers fever, mobilizing natural defenses, supplying tissues with increased oxygen and nutrients, aiding in detoxification, and enhancing infection resolution. Inspired by this natural response, a hyperthermia device using water-filtered infrared-A (wIRA) was developed to control skin burns and body temperature.

Fever-range infrared hyperthermia (FRIH) leverages natural self-healing mechanisms to treat chronic conditions and malignant diseases. This study investigates the molecular and cellular mechanisms of FRIH as immunotherapy for cancer, combined with standard chemotherapy and immunotherapy protocols. The protocol included gemcitabine 1000 mg/m² over 30-60 minutes on days 1, 8, and 15, and cisplatin mg/m² on day 2, repeated every 4 weeks for up to 6 cycles. For gemcitabine with carboplatin, dosing was adjusted based on creatinine clearance, with carboplatin dosed at 4.5× [glomerular filtration rate +25] on day 1 over 1 hour IV every 3 weeks. Pembrolizumab 200 mg was administered every 3 weeks for treating distant metastases. For bladder tumors, gemcitabine, cisplatin, and pembrolizumab were combined. On the second day of the course, 1 hour after cisplatin infusion, local hyperthermic therapy was administered for 3 hours at 43-44°C.

FRIH enhances the immune system's anti-tumor activity through several molecular pathways. Increased body temperature induces the expression of heat shock proteins (Hsps), which serve as molecular chaperones and play crucial roles in protein folding, repair, and degradation. Hsps also enhance the presentation of tumor antigens by antigen-presenting cells (APCs) such as dendritic cells. These APCs migrate to lymphoid tissues, where they activate cytotoxic T lymphocytes (CTLs), which then target and destroy cancer cells.

Additionally, hyperthermia promotes the infiltration of immune cells, including natural killer (NK) cells and macrophages, into the tumor microenvironment. This increased immune cell presence enhances tumor visibility to the immune system, facilitating targeted immune responses. Hyperthermia also upregulates the expression of adhesion molecules and chemokines, supporting the recruitment and retention of immune cells at the tumor site.

Preclinical and clinical data demonstrate improved anti-tumor responses with mild hyperthermia. The molecular mechanisms underlying these improvements include the activation of the immune system via Hsps, enhanced antigen presentation, and increased immune cell trafficking to the tumor. Hyperthermia may sensitize tumor cells to treatments like chemotherapy and radiation by disrupting their protein homeostasis and inducing apoptosis.

Hyperthermia shows significant potential as an adjunct to cancer immunotherapy.

Fig. 1

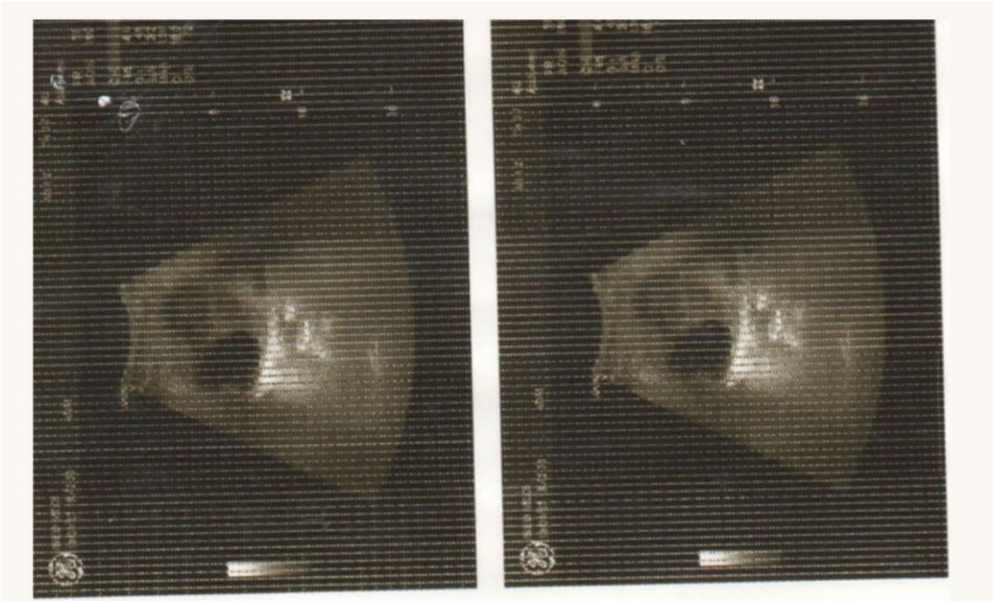

Fig. 2

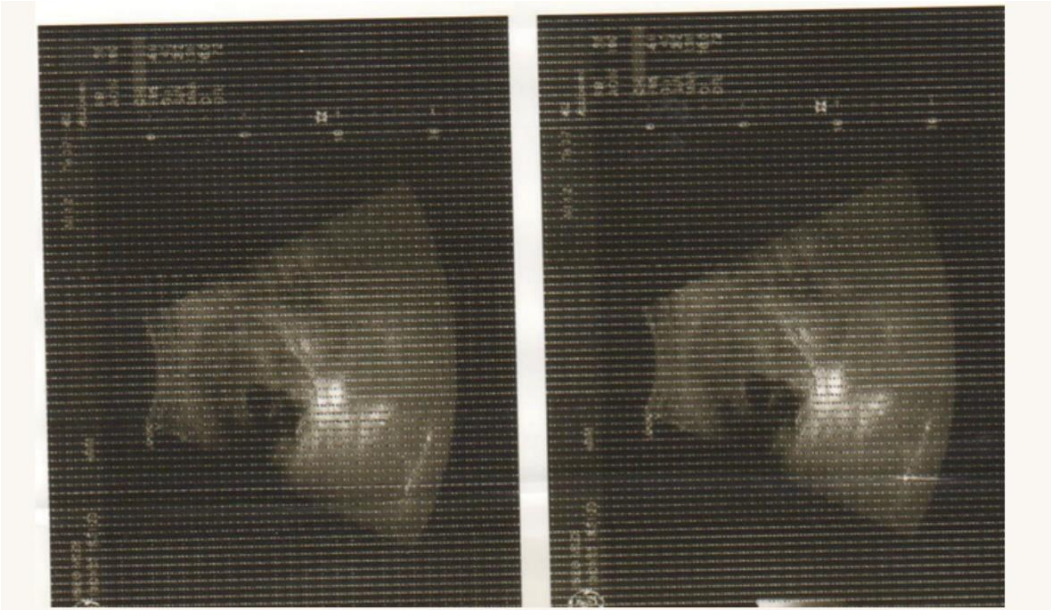

FP-26

Numerical study of hyperthermia application for head and neck tumour with varying complexity of the human model

M. Di Cristofano[1], M. Cavagnaro[1]

[1]Sapienza University, Rome, Italy

Question: Radiative oncological hyperthermia is a therapy based on the application of electromagnetic (EM) fields to heat the tumour. A superficial applicator allows to treat targets up to a depth of 3-4 cm. In this work the application of two superficial hyperthermia antennas (α antennas – Medlogix srl), to produce a deeper focus (~ 6 cm) in head and neck applications, is presented. The study is focused on the evaluation of the complexity, in term of number of reported tissues, of the human model that must be simulated.

Methods: The scenario was modelled in CST Microwave Studio (Dassault Systèmes, France) using a male voxel human model. The two α antennas were positioned at the two sides of the head of the model, with the water bolus between the skin and the antenna, as shown in Fig. 1.

Fig. 1: Antenna positioning.

The specific absorption rate (SAR) was evaluated with EM simulation, considering an input power of 50 W and a 0° phase for both the antennas, and given as input for the thermal simulation. The results were evaluated in five cases with different complexity. The considered tissues were:

- Case 1: all tissues (complex model);
- Case 2: muscle, fat, bone, air;
- Case 3: muscle, fat, bone, air, brain;
- Case 4: muscle, fat, bone, air, brain, nerve;
- Case 5: muscle, fat, bone, air, brain, nerve, skin.

In the simplified cases, the neglected tissues were present in the model, but in the simulation their dielectric and thermal properties were set equal to the muscle ones. Only the properties of teeth were set equal to those of bone. The temperature of the water bolus was set at 15 °C and the convection heat transfer coefficient at 100 W/m^2K.

Results*:* The simulative results show the possibility to obtain a SAR and temperature focus at 5.8 cm of depth. With reference to the SAR distribution, there are no significant variations among the different studied cases (e.g. between case 1 and case 2 $\Delta SAR_{\%} \cong 8.58 \pm 8\%$). Different results are obtained for the temperature: the worst approximation of the complex model is obtained in the case 2, because in that case the brain thermal properties are neglected. In the cases 3 and 4 the temperature distribution better resembles that of the complex case, but there is an error in the detection of the temperature peak of about 2 °C, while the case 5 provides an optimum approximation of the complex model.

Conclusion*:* In this work the application of two superficial hyperthermia antennas on the head of a human model was studied. SAR distribution is in a good agreement between the simplest and the most complicated cases considered, but the temperature distribution shows significant variations. The presence of the brain and the skin tissues allows to obtain an optimum approximation of the most complex model for the evaluation of the temperature distribution.

Fig. 1

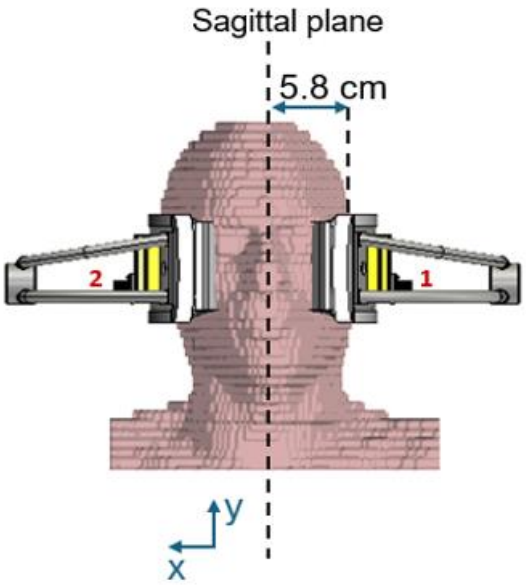

FP-27

Synergistic nanoparticle-mediated therapies: Enhancing antitumor efficacy through immune modulation and targeted hyperthermia

D. Sharma[1]

[1]Institute of Nano Science and Technology, Chemical Biology Unit, Mohali, India

Magnetic hyperthermia stands at the forefront of targeted cancer therapy, harnessing the extraordinary properties of magnetic nanoparticles (MNPs) to achieve a remarkable potential for eradicating tumors. This cutting-edge, non-invasive method capitalizes on MNPs' ability to generate cytotoxic reactive oxygen species (ROS) under an alternating magnetic field (AMF), resulting in precise and potent suppression of tumor cells. The quest for successful magnetic hyperthermia cancer therapy (MHCT) has been driven by the critical investigation of factors like MNP size, coating, and morphology, leading to optimal parameters that overcome clinical limitations and unlock the therapy's full prowess in both in vitro and in vivo applications.

The advancements in MNP synthesis have played a crucial role in enhancing the efficacy of MHCT. We have focused on tailoring the size, shape, and surface coating of MNPs to improve their biocompatibility, stability, and heating efficiency. For instance, the use of carboxymethyl-stevioside-coated magnetic dots has shown significant improvements in magnetic hyperthermia performance and glioblastoma treatment. Similarly, manganese-doped magnetic nanoclusters have been developed to enhance hyperthermia and photothermal therapy for glioblastoma.

One of the significant challenges in magnetic hyperthermia is ensuring the MNPs can reach and accumulate in the tumor site effectively. The blood-brain barrier (BBB) poses a substantial obstacle for treating brain tumors. However, we have studied that the transmigration of magnetite nanoparticles across the BBB can be influenced by external and alternating magnetic fields, providing a viable strategy for treating glioblastomas.

The role of immune modulation in magnetic hyperthermia is another exciting area of research. Combining magnetic hyperthermia with immune checkpoint inhibitors or other immunotherapeutic agents can enhance the antitumor immune response, leading to more effective and sustained tumor regression. For instance, targeted inhibition of Heat Shock Protein 90 (HSP90) has been shown to unveil immune-mediated therapeutic synergy in glioma treatment, significantly enhancing the efficacy of magnetic hyperthermia.

Additionally, the development of synergistic therapies, such as Vitamin K3-loaded magnetic nanoparticles, has demonstrated remarkable results. This approach evokes massive ROS production and immune modulation, leading to augmented antitumor potential. The combination of hyperthermia and ROS generation creates a highly hostile environment for cancer cells, promoting their destruction through multiple pathways.

Magnetic hyperthermia, empowered by MNPs, promises to reshape the landscape of cancer therapy, setting the stage for a new era of hope and healing. The integration of advanced materials science, targeted delivery systems, and immunotherapy paves the way for more effective and personalized cancer treatments.

Fig. 1

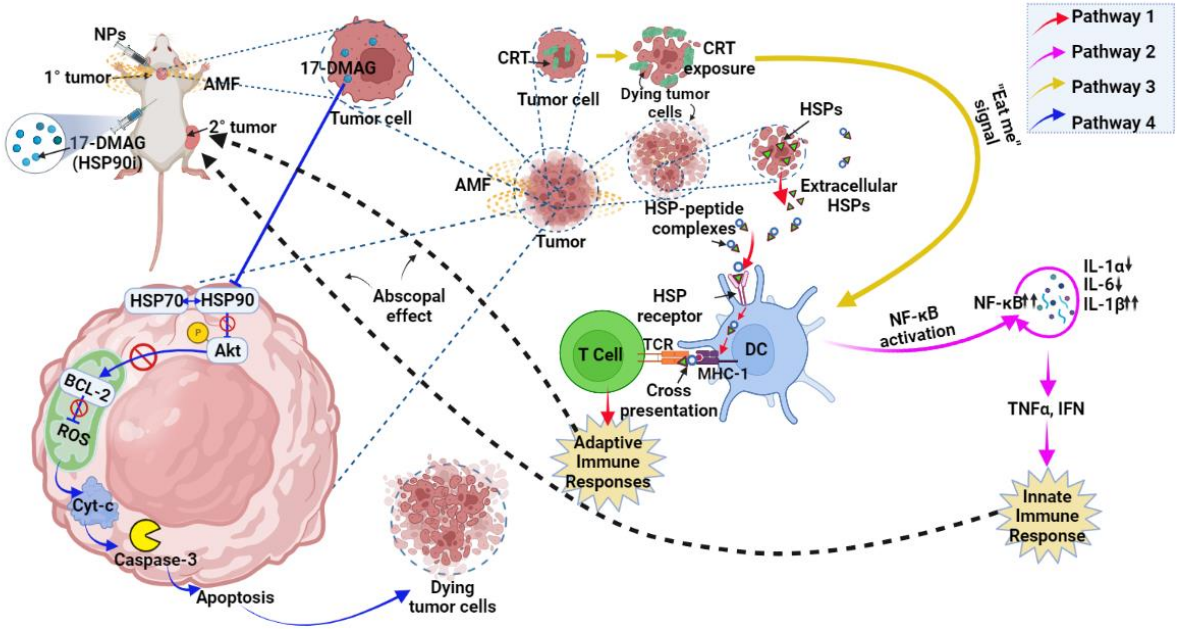

FP-28

Effect of biocompatible polyacrylic acid-coated iron oxide-based magnetic fluid in inducing programmed cell death in breast cancer cells MCF-7 subsequent to magnetic fluid hyperthermia

N. Jain[1], T. Patel[2], K. Parekh[1]

[1]Dr. K C Patel Research and Development Centre, Charotar University of Science and Technology, Anand, India
[2]P D Patel Institute of Applied Sciences, Charotar University of Science and Technology, Anand, India

Question: Over the past few decades, magnetic fluid hyperthermia (MFH) has drawn attention in oncology research due to its higher efficacy and minimal side effects compared to chemo- and radiation therapy. However, the clinical practice of MFH is challenged by factors such as precise temperature control, biocompatibility of the magnetic nanoparticles, and the induction of apoptotic cell death during MFH sessions. Therefore, identifying suitable magnetic fluid and standardization at the in vitro level is crucial in establishing MFH as a reliable anti-cancer treatment for proceeding in vivo.

Methods: The present study focused on the hyperthermic potential of a self-regulating temperature-controlled polyacrylic acid (PAA) coated Mn0.9Zn0.1Fe2O4 ferrite nanoparticle-based magnetic fluid on breast adenocarcinoma cell line MCF-7, while maintaining magnetic field amplitude (10 kA/m) and frequency (300 kHz) within safety limits. The biocompatibility of the magnetic fluid (MF) was examined by MTT-cell viability assay. Percentage internalization and Fe content per cell was quantified using a colorimetric-based method. The cytotoxic effect of MFH was determined using an MTT assay, whereas the mode of cell death subsequent to MFH session was visualized using Hoechst-Propidium Iodide staining.

Results: Our findings indicate that the MF was biocompatible, with 100% cell viability at concentrations up to 2 mg/ml and 70% cell viability even at higher concentrations of 2.4 mg/ml. Internalization studies revealed that 60% of the MF was internalized, with each MCF-7 cell containing approximately 1.068 ± 0.03 ng of Fe after 12 hours of MF incubation. MFH resulted in 75% cell inhibition after 1 hour of induction heating, and Hoechst-Propidium Iodide staining confirmed late-stage apoptosis in most cells post-MFH session.

Conclusions: PAA-coated Mn0.9Zn0.1Fe2O4 ferrite nanoparticle-based magnetic fluid demonstrated a promising hyperthermic response in inducing apoptosis in breast cancer cells at in vitro level. The findings suggest that this fluid holds significant potential, and further analysis on 3D-spheroid and animal models is warranted to develop it for clinical applications. Authors thank the Indian Council of Medical Research, ICMR-NCD/AD-HOC/64/2020-21, and the Department of Science and Technology-Science and Engineering Research Board SERB/CRG/2021/001587, New Delhi, India, for providing financial support.

FP-29

Biological modeling shows thermal enhancement of radiation dose in a pediatric sarcoma patient treated with proton beam therapy and regional deep hyperthermia

M. De Lazzari[1], R. Wessalowski[2], S. Karkavitsas[3], O. Mils[2], U. Kontny[4], B. Timmermann[5], R. Richter[5], D. Rodrigues[6], H. Dobšíček Trefná[1]

[1]Chalmers University of Technology, Electrical Engineering, Göteborg, Sweden
[2]Heinrich-Heine University, Medical Faculty, Pediatric Hematology and Oncology, Duesseldorf, Germany
[3]Dr. Sennewald Medizintechnik, Munich, Germany
[4]RWTH Aachen University, Pediatric Hematology Oncology and Stem Cell Transplantation, Aachen, Germany
[5]University Hospital Essen, West German Proton Therapy Centre Essen, Essen, Germany
[6]University of Maryland School of Medicine, Radiation Oncology, Baltimore, MD, United States

Introduction: The radiosensitization effect of hyperthermia (HT) is well-documented and can be quantified through biological modeling. This evaluation requires accurate temperature data induced by HT in tissues, which can be estimated via computational simulations or measured using MR thermometry (MRT). However, these two technologies are still in development and only some clinical centers use them. In this study, we aim to evaluate the radiation dose enhancement provided by HT using MRT and simulation data from a pediatric patient case study treated with HT and radiation.

Methods: The patient was a 2-year-old female with recurrent rhabdomyosarcoma of the pelvis, treated with proton beam therapy (PBT) combined with deep HT (DHT). DHT was delivered using the BSD Sigma-30 applicator, which consists of an annular phased-array with 8 antennas operating at 100 MHz. The Equivalent Dose (EQD) of the HT enhancement was computed using an extension of the linear-quadratic (LQ)-model, which incorporates oxygenation effects. A 3D model of the patient segmented into 12 different tissues was created using CT scans with a 1×1×1 mm resolution. Electromagnetic and thermal simulations were performed in COMSOL Multiphysics, using an accurate model of the Sigma-30 applicator. The temperature distribution at steady-state was computed using the same power and phase settings used in the treatment. The radiation dose distribution was registered to the 3D patient model using a MATLAB routine. The segmented tissue matrix, along with the temperature and dose distributions were then used to compute the dose enhancement given by HT using an in-house MATLAB algorithm.

Results: An initial attempt to use MRT data to calculate EQD for the HT+PBT treatment was unsuccessful, mainly due to difficulties in image registration from differences in patient anatomy and positioning between the planning CT and MR imaging. In addition, MRT data presented a low signal-to-noise (SNR) ratio, with temperature readings significantly higher than temperature probes. Thus, we limited our EQD study to simulated temperature only, which showed an EQD enhancement of 40% when adding HT to PBT: 21.7 Gy (PBT only) vs. 37.0 Gy (PBT+HT). This result closely aligns with previous theoretical calculations, which estimated an enhancement of 36%. Of note, the simulated temperature distribution was comparable to the treatment data collected by MRT and internal temperature probes. However, there were a few hotspots predicted by simulations that were not visible in the MRT, likely due to low SNR.

Conclusion: The present study revealed several challenges associated with current image acquisition protocols that lack standardization, making image registration not possible. The use of MRT data was also limited due to its

poor imaging quality. However, the simulation tools developed by our group proved to be effective to evaluate the radiobiological effects of combining HT with PBT in pediatric sarcoma patients.

FP-30
Neoadjuvant concurrent gemcitabine and radiotherapy for soft tissuesarcoma: Assessment of toxicity and efficacy

P. trecca[1], C. Greco[1], M. Fiore[1], E. Ippolito[1], C. Demofonti[1], S. Minuti[1], S. Valeri[2], B. Vincenzi[3], S. Ramella[1]

[1]Fondazione Policlinico Campus Bio-Medico di Roma, Radiation oncology, Rome, Italy
[2]Fondazione Policlinico Campus Bio-Medico di Roma, General Surgery, Rome, Italy
[3]Fondazione Policlinico Campus Bio-Medico di Roma, Medical Oncology, Rome, Italy

Aims: Surgery is the mainstay of treatment for Soft tissue sarcomas (STS) and is the only curative treatmentoption. The integration of surgery with neoadjuvant radiotherapy (RT) or chemotherapy for resectable tumoris an option that needs multidisciplinary discussion. Gemcitabine (gem) is a radiosensitizer with activity inSTS. The purpose of this study was to evaluate the efficacy and toxicity of concomitant RT and gemcitabinein the neoadjuvant setting for STS.

Methods: A retrospective analysis of 19 patients treated with concurrentRT and gem from 2018 to 2022 in a neoadjuvant setting was performed. Radiative hyperthermia treatmentwas also performed in 9 patients since available in our Center. The RT prescription dose was for all patients50 Gy in 25 fractions over 5 weeks. Gem was administered at 300 mg/m2 once weekly for the duration of RT.

Results: The mean age was 61 years (range, 36-83) with ECOG Performance Status 0-1. The mean sizeof the treated tumor was 6.9 cm (range 2-20). Pathological response was evaluated in 17 patients. In 12patients (70.5%) the tumor was localized in the extremities. 7 (41.2%) patients had been pre-treated with anthracycline-based chemotherapy (mean number of cycles performed 3.5, range 2-4) and 10 (58.8%) were naïve. The radiotherapy technique used was 3D-CRT, 2 IMRT, 11 VMAT in 4 patients. All patients followed 25 RT sessions in 5 weeks and the mean number of chemotherapy cycles performed was 4.4 (range 3-5). No patients reported acute and late toxicity >/= CTCAE (vers.5.0) grade 3. Six (35.2%) patients reported grade1-2 hematologic toxicity. Of these, three had previously undergone chemotherapy and 5 also underwenthyperthermia during the integrated treatment. All patients (17/17) underwent radical surgery. An R0 resection was obtained in all but one patient (94%). 7 (41.2%) patients achieved a complete pathological response. 2/17 (11.8%) patients had post-surgical complications (anastomotic leaks). Five (29.5%) patients had disease progression, (3 local progression and 2 distant metastases). At the time of the analysis, 15/17 (88.2%) patients were alive, 3 with disease and 12 without.

Conclusions: The combination of RT and Gemcitabine in patientswith STS is feasible and well tolerated, even after previous chemotherapy or in combination withhyperthermia. It might be more potent than radiation alone in achieving tumor regression and local control for high grade STS.

FP-31
In silico analysis of step-up heating protocols to improve the effectiveness of oxaliplatin-based HIPEC

P. Namakshenas[1,2,3], J. Crezee[1,2,3], A. L. Oei[1,2,3,4], H. P. Kok[1,2,3]

[1]Department of Radiation Oncology, Amsterdam UMC Location University of Amsterdam, Amsterdam, Netherlands
[2]Cancer Center Amsterdam, Cancer Biology and Immunology, Amsterdam, Netherlands
[3]Cancer Center Amsterdam, Treatment and Quality of Life, Amsterdam, Netherlands
[4]Laboratory for Experimental Oncology and Radiobiology (LEXOR), Amsterdam, Netherlands

Question: The administration of oxaliplatin-based Hyperthermic Intraperitoneal Chemotherapy (OXA-HIPEC) followed by cytoreductive surgery is considered a curative treatment option for colorectal peritoneal metastasis. However, the high recurrence rate reported in recent trials indicates that the standard HIPEC protocol, involving a 460 mg/m2 dose of oxaliplatin for a 30-minute perfusion at 42°C, is suboptimal. Longer duration would increase the efficacy, but also yields an increased risk of complications. This study applied computer simulations to investigate whether the duration of OXA-HIPEC treatments can safely be extended using a heating protocol based on step-up heating that involves 30 min of HIPEC at high temperatures preceded by 60 min at lower temperature.

Methods: Using our in-house developed HIPEC simulation software, we implemented various step-up heating protocols in open-belly OXA-HIPEC using a 3D anatomical model of a rat abdomen (Figure 1A). The duration was scaled down to 20 min low + 10 min high, or one third to meet faster equilibration due to smaller dimensions of rat. Hence, the control case consists of a short-duration, high-temperature treatment for 10 minutes, while the step-up approach involves a temperature escalation from low to high over an extended duration of 30 minutes. We conducted analyses to assess thermal and chemotherapeutic toxicity and determine the feasibility of this prolongation of the OXA-HIPEC duration. Additionally, we compared the pharmacokinetic advantages of the step-up heating approach with those of the control case.

Results: According to the CEM43 thermal dose results, extending HIPEC duration via a step-up heating approach appears to be safe, except when it is conducted at temperatures > 42°C (Figure 1B). Prolonging the duration by step-up heating improved the homogeneity of oxaliplatin distribution in various quadrants of the peritoneum (Figure 1C). However, it also increased local and systemic concentrations of oxaliplatin, suggesting that dosage should be regulated based on the maximum tolerated toxicity (Figure 2A and 2B). As a pharmacokinetic advantage, the accumulation of OXA in the tumor interstitium, especially in regions with higher risks of heterogeneity and poor OXA coverage rates, was predicted to increase with longer duration through step-up heating (Figure 2C).

Conclusion: This *in silico* study indicates that step-up protocols have the potential to safely extend the duration of OXI-HIPEC treatments, thereby improving treatment efficacy. Simulation results offer valuable insights for future translational research aiming to implement step-up heating in a clinical HIPEC protocol.

Fig. 1

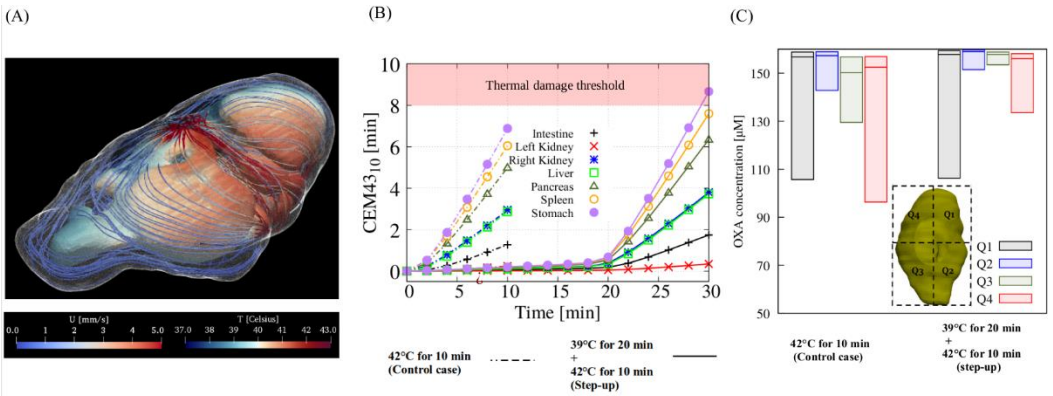

Figure 1. (A) Conjugate heat transfer at t = 30 min in the rat abdomen model. The streamlines represent the flow velocity, while the thermal map shows the temperature distribution of the visceral peritoneal surface. (B) The thermal dose (CEM43$_{10}$) of the abdominal organs during HIPEC using the step-up heating protocol (39°C for 20 min + 42°C for 10 min) compared to the control case (42°C for 10 min). (C) Compares the interquartile range of oxaliplatin concentration in various quadrants of the rat abdomen between the step-up heating and control case.

Fig. 2

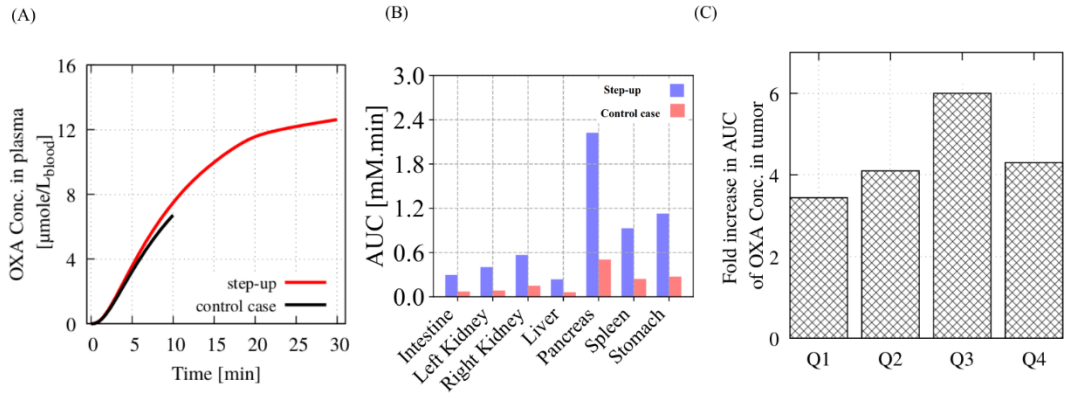

Figure 2. (A) The temporal average oxaliplatin concentration in the plasma (systemic compartment), (B) the AUC of oxaliplatin in normal tissues, and (C) the fold increase in oxaliplatin AUC in a 2 mm tumor, calculated as the AUC of the step-up heating protocol divided by the AUC of the control case.

FP-32

Advancement in the development of a modular, human body-mimicking phantom with active thermoregulation capabilities

L. Van den Bossche[1], W. Vertessen[1], J. Van den Bossche[1], O. Rudenko[1], J. P. Bogers[1], L. Brancato[1]

[1]ElmediX, Leuven, Belgium

Objective: A human body mimicking phantom is used for quality assurance and validation in hyperthermia applications. Interpatient variability in thermal regulation mechanisms, including varying sweating rate, metabolic heat production, and blood redistribution, currently limits the accuracy of existing models. This work aims to surpass these limitations by designing and fabricating a phantom with the aforementioned thermal regulation capabilities.

Methods: Connecting identical units enables mimicking different patient types with distinct physical and thermal regulation properties. Our prev phantom (1) consisted of an agar-based block with an embedded water circulation, a passive sweating system and an external heating source. The current version includes an agar-based block, an ethyl cellulose-based top layer, an internal heat source, a deep and a superficial water circulation and a sweating system. Agar gel and ethyl cellulose gel are produced to mimic the thermal properties of the average human tissues and fat tissue respectively. Each block is wrapped with PVC foil to limit water evaporation. A heating wire, coiled around an embedded aluminium tubing water circulation, simulates metabolic heat generation. A superficial water circuit is placed on top of the fat-mimicking layer. A water pump mimicking the cardiovascular system ensures a 1000ml/h flow rate. Sweat production is simulated using a water pump and perforated tubing. Two units are combined to obtain a phantom of 40kg. A heat production of 40W and 50W is designed for a normal and a shivering mode respectively (2), with the latter being activated whenever the core temperature drops below 36.3°C. Our phantom is operated by a controller, designed to regulate the core temperature.

Results: Our phantom was able to regulate its core temperature to a setpoint of 37.0°C with an accuracy of ±0.7°C. The maximum temperature gradient within the phantom decreased from 6°C to 2°C after activating the water circulation. The internal heating and increased water flow reduced local temperature gradients significantly.

Conclusion: Our phantom models heat exchange by convection, conduction, radiation and evaporation, with the latter being the most significant in the loss of heat in the human body. Thermal conductivity properties, dimensions, heat production and extraction rates can be easily tuned to mimic different patient models. The phantom shows promising results as an effective tool for hyperthermia device validation and verification, offering accurate representation of physiological responses. We continue to validate our phantom, focusing on its thermal regulation capabilities under different environmental conditions as one of the ongoing tests.

1. *Van den Bossche L. et al., A modular phantom with sweating, circulation and metabolic heat production capabilities for personalized thermal treatment planning, ESHO 2022.*
2. *UofG, Basal metabolic rate in man, https://www.fao.org/4/m2845e/m2845e00.htm 2018*

Fig. 1

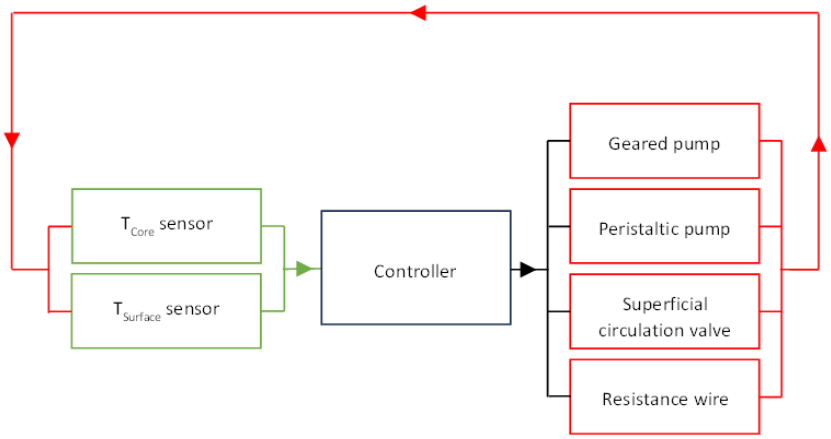
T Core sensor
T Surface sensor
Controller
Geared pump
Peristaltic pump
Superficial circulation valve
Resistance wire

FP-33

Increasing the quality of life in bladder cancer patients by Heckel-HT3000

S. Badzgaradze[1], M. Kutchava[1]

[1]Immuno and Oncothermia center INTEGRA, Oncology, Kutaisi, Georgia

With the Heckel-HT3000, we have managed to enhance the quality of life for patients and achieve clinical remissions in advanced cases within a short timeframe. Combined chemotherapy with hyperthermia allowe us to a significant improvement in the overall condition of patients in the shortest possible time.

Aim: The aim of the study was geriatric oncology patients aged 70 years and above, who had bladder cancer with far-fetched metastases.

Methods and Materials: The protocol recommended gemcitabine and cisplatin courses which were selected in the methods. Gemcitabine 1000 mg/m² over 30-60 minutes on days 1, 8, and 15. Cisplatin mg/m² on day 2. Repeated every 4 weeks for a maximum of 6 cycles. For gemcitabine with carboplatin, the dose of cisplatin and carboplatin was selected according to the determination of creatinine clearance. Carboplatin 4.5× [glomerular filtration rate +25] on day 1 over 1 hour IV. Every 3 weeks, for the treatment of distant metastases, we additionally added the drug Pembrolizumab 200mg every 3 weeks, which was selected by immunomorphological research. In the third phase in bladder tumors we used gemcitabine in combination with cisplatin and pembrolizumab. In order to enhance the effect and since the patients were geriatric patients, we recommended hyperthermic therapy with a hyperthermic machine. On the second day of the course when cisplatin is used 1 hour after cisplatin infusion, we conducted Heckel's hyperthermic therapy for 3 hours at 43-44 degrees Celsius.

Results: We will represent to you two interesting cases, one with distant metastases that are also fixed in the lung, and second that are fixed in the nodules or lymph nodes. In this case, in a short time, the patient I.K. received gemcitabine, pembrolizumab, and 2 courses of cisplatin. Already, the lymph nodes have completely cleared up. The patient then switched to a mono-regimen, only receiving a weekly regimen of gemcitabine for 1 week, and the patient is already in clinical remission. As for the second patient, B.T. the invasion was in the muscle, and there was metastatic damage to the liver lymph node. In this case, 3 courses of hyperthermia, gemcitabine, and carboplatin were used with the patient, and he achieved clinical remission too.

Conclusion: Instead of the 6-8 courses recommended by the guidelines, the result of the development of clinical remission was obtained after 3 courses using the Heckel-HT3000 hyperthermia machine. The use of the hyperthermia machine was recommended due to the patient's geriatric age, taking into account the toxic effects of platinum on the body. Patients are currently under observation.

Fig. 1

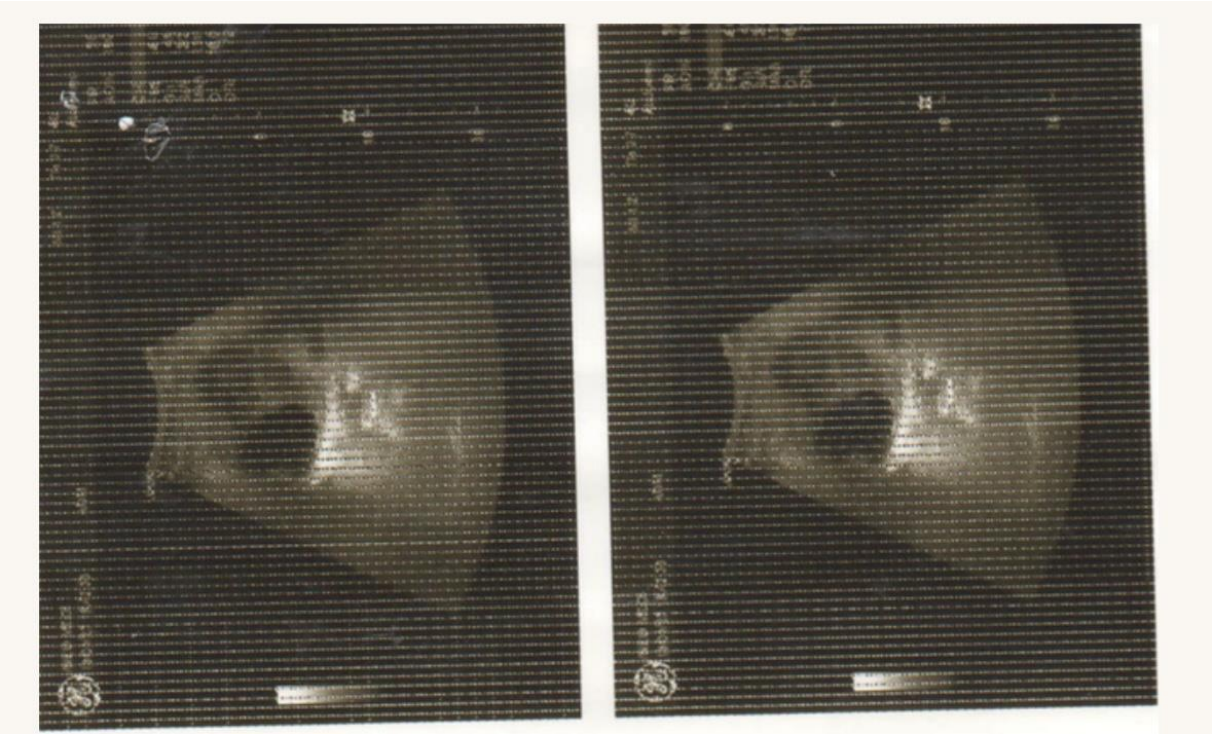

Fig. 2

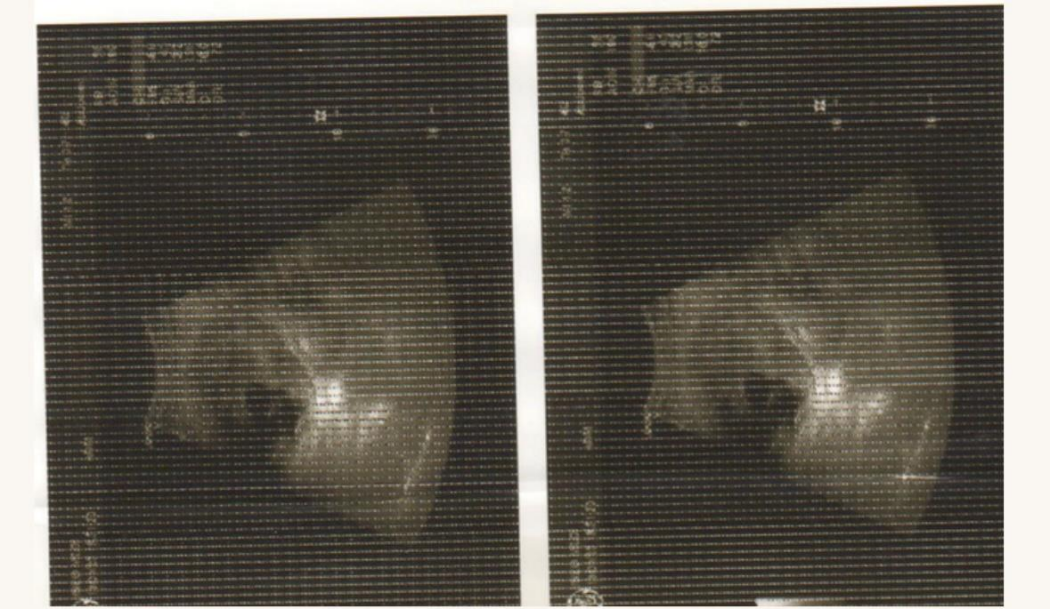

FP-34
The pleiotropic effects of whole-body hyperthermia in synergizing chemotherapy and enhancing immune response in pancreatic ductal adenocarcinoma

T. Logghe[1], R. Colenbier[2], G. Boulet[1], J. P. Bogers[1,2]

[1]ElmediX, Mechelen, Belgium
[2]University of Antwerp, Laboratory of Cell Biology and Histology, Antwerp, Belgium

Introduction: Pancreatic ductal adenocarcinoma (PDAC) is a highly lethal cancer characterized by a dense stroma and outspoken genomic instability, leading to therapeutic resistance, immune evasion and rapid progression. Whole-body hyperthermia (WBHT) may offer synergistic effects with conventional chemotherapies and could enhance anti-tumor immune responses.

Methods: We present a comprehensive preclinical vision of WBHT effects on PDAC based on data available from literature and own research. We illustrate the tumor microenvironment and the cellular processes driving its aggressiveness. The multifaceted potential of WBHT, alone or in combination with chemotherapeutics, comprises vascular modulation, cellular stress, cell cycle disruption, and immune system activation.

Results: PDAC tumors are characterized by a robust extracellular matrix (ECM) produced by cancer-associated fibroblasts (CAFs), creating a barrier to immune cell infiltration and therapy. Key oncogenic and tumor suppressor proteins are dysregulated (e.g., KRAS, p53, SMAD) and can act as growth-regulating receptors (e.g., HGFR, EGFR, FGFR), promoting uncontrolled cell proliferation and resistance to conventional treatment. Hypoxia-inducible factor 1-alpha (HIF1α) mediates angiogenesis and metabolic reprogramming, further facilitating tumor survival and growth.

WBHT improves vascular perfusion and oxygenation, reduces hypoxia and enhances immune cell access to the tumor. WBHT and chemotherapeutic agents (e.g., oxaliplatin, paclitaxel, gemcitabine) exhibit synergistic effects by disrupting the cell cycle, impairing DNA repair mechanisms and enhancing drug accumulation, thereby leading to cellular stress on several levels. WBHT interferes with the normal progression of the S-phase, which must be taken into account when it is considered for combination therapy with base analogs such as gemcitabine. Additionally, WBHT disrupts mitotic spindle function, offering potential synergy with compounds such as (Nab)-paclitaxel.

The immune response would be significantly augmented by WBHT, enhancing dendritic cell maturation, T-cell activation and homing of cytotoxic T-cells. Furthermore, WBHT likely induces immunogenic cell death, releasing danger-associated molecular patterns (DAMPs) such as HSPs, HMGB1, CRT and ATP into the tumor microenvironment, which further aid in mounting an effective anti-tumor response.

Conclusion: WBHT exhibits pleiotropic effects that may synergize with conventional chemotherapeutics and boost the immune response in PDAC. As such, WBHT holds promise as a multifaceted therapeutic strategy in pancreatic cancer treatment. Future research should focus on optimizing WBHT and chemotherapy scheduling to maximize therapeutic outcomes.

FP-35
Development of an anticancer tissue adhesive for intraperitoneal chemotherapy as an adjuvant to HIPEC

M. T. Perelló-Trias[1], A. Rodríguez-Fernández[1], A. J. Serrano-Muñoz[1], J. J. Segura-Sampedro[1], P. Tauler[1], J. M. Ramis[1], M. Monjo[1]

[1]Hospital Universitario La Paz, Cirugía Oncológica, Madrid, Spain

Question: Hemostatic patches (HP) are used during surgeries to prevent complications such as uncontrolled bleeding. Typically made from biomaterials like oxidized cellulose or collagen with a binding agent, HPs have the potential to serve as drug delivery systems (DDS) for localized intraperitoneal chemotherapy. This study aimed to characterize and compare three commercial HPs: TachoSil®, Hemopatch®, and Veriset™.

Methods: The properties of TachoSil®, Hemopatch®, and Veriset™ were analyzed, focusing on degradation rate, hydrophilicity, biological fluid absorption capacity, and adhesive capacity. Hemopatch® was selected as the most suitable candidate. Subsequently, Hemopatch® was used as a scaffold to develop a hybrid device incorporating a hyaluronic acid hydrogel loaded with cisplatin or olaparib.

Results: Hemopatch® demonstrated an optimal combination of slow degradation, high hydrophilicity, excellent absorption capacity of biological fluids, and moderate adhesive capacity while maintaining hemostatic properties. The hybrid device utilizing Hemopatch® facilitated sustained drug release over six days, maintaining the anticancer efficacy of cisplatin and olaparib on OVCAR-3 cells.

Conclusions: Integrating DDS into HPs shows significant potential for delivering chemotherapeutic agents precisely to residual microscopic disease in peritoneal carcinomatosis following cytoreductive surgery (CRS). This innovative approach not only enhances localized drug delivery but also offers additional advantages, including adhesion and hemostatic properties, preventing further growth and metastasis of cancer cells. Therefore, the combination of DDS and HPs opens new avenues for achieving localized chemotherapy in peritoneally affected tissues.

Fig. 1

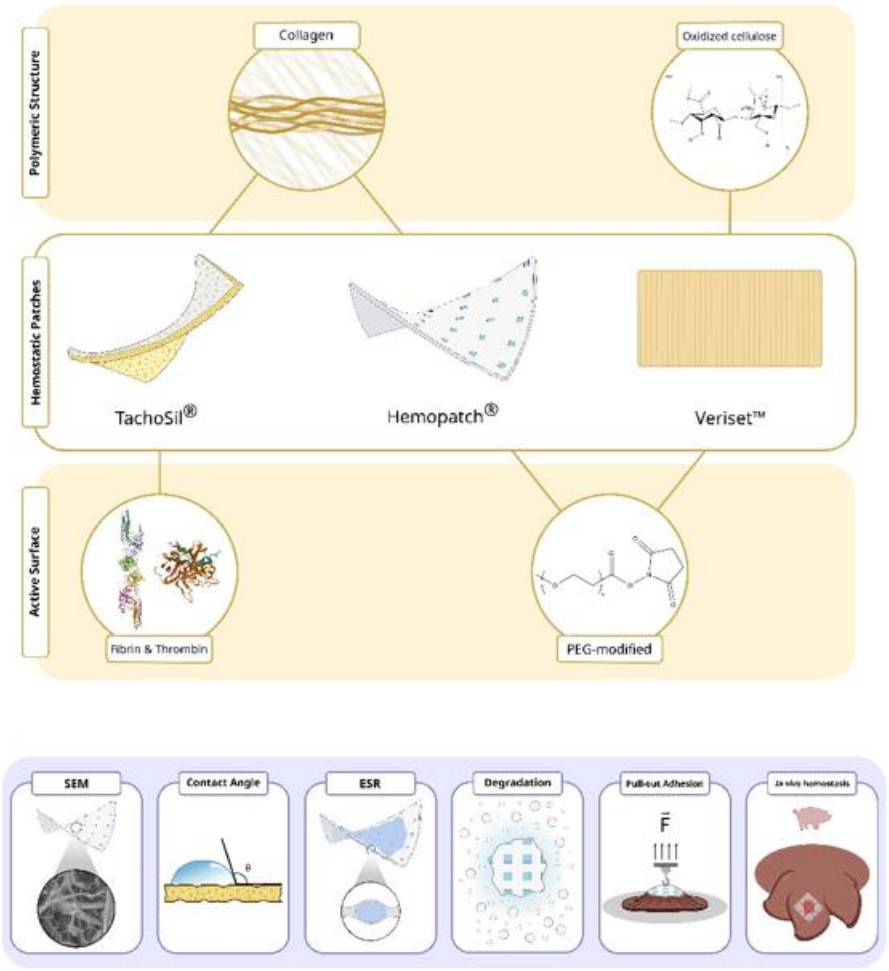

FP-36

Establishment of a murine model of localised advanced ovarian cancer to test this novel intraperitoneal drug delivery system

M. T. Perelló-Trias[1,2,3], A. J. Serrano-Muñoz[1,2,3], J. J. Segura-Sampedro[2], A. Quintero-Duarte[2], J. M. Ramis[1,2,3], M. Monjo[1,2,3]

[1]Hospital Universitario La Paz, Sección de Cirugía Oncológica Peritoneal, Retroperitoneal y de Partes Blandas, Servicio de Cirugía General y del Aparato Digestivo, Madrid, Spain
[2]Universidad de las Islas Baleares, Profesor asociado de Cirugía, Facultad de Medicina, Palma de Mallorca, Spain
[3]Instituto de Investigación Sanitaria de las Islas Baleares (IdISBa), IP en Grupo de Investigación en Cirugía Oncológica Avanzada, m-Health e Innovación en Tecnología Quirúrgica, Palma de Mallorca, Spain

Question: Is it possible to implant genetically engineered OVCAR-3 cells expressing firefly luciferase (OVCAR-3Luc) into the preperitoneal space of athymic nude mice, with or without basement membrane extract (BME), influence tumor formation and progression?

Methods: OVCAR-3 cells were genetically engineered to stably express the firefly luciferase gene (OVCAR-3Luc), and luciferase activity was confirmed post-transfection. The absence of mycoplasma contamination was verified using PCR. OVCAR-3Luc cell suspensions, either with or without BME, were implanted into the preperitoneal space behind the posterior sheath of the anterior rectus abdomen in athymic nude mice. Tumor progression was monitored weekly using bioluminescence in vivo imaging. Mice were sacrificed at various time points, and samples of tumor tissue, plasma, and ascitic fluid were collected for histological, immunohistochemical, and biochemical analyses.

Results: Bioluminescent imaging confirmed localized tumor formation. Tumor volume was not significantly impacted by cell concentration (1x10^6 vs. 4x10^6 cells). However, the inclusion of BME with 1x10^6 cells significantly increased tumor volume. Histopathological analysis revealed peritoneal infiltration and a papillary pattern in the tumors.

Conclusions: The study demonstrated that the use of BME in combination with OVCAR-3Luc cells significantly promotes tumor growth in the preperitoneal space of athymic nude mice. This model can be effectively used for studying tumor progression and the effects of potential therapeutic interventions in a controlled environment.

Fig. 1

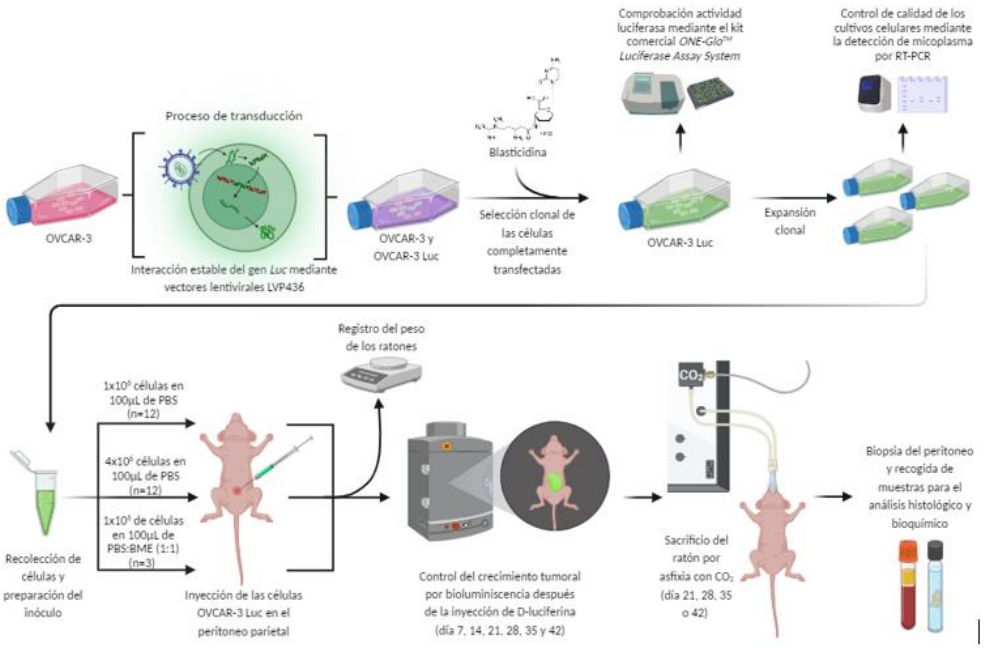

FP-37
Does repeated fever-range whole body hyperthermia treatments reduce patient's capacity to rise body temperature?

J. Moreira Pinto[1]

[1]Hospital da Luz, Medical Oncology, Lisboa, Portugal

Question: Does repeated fever-range whole body hyperthermia treatments reduce patients" capacity to rise body temperature?

Methods: Case report of a 63yo female patient with metastatic gastric adenocarcinoma treated with infrared whole-body hyperthermia (WBHT) system heckel-HT3000 during first line CAPOX + nivolumab and second line FOLFIRI. WBHT treatments were performed every 2-3 weeks after 5-FU infusion (48-72 hours after oxaliplatin/irinotecan infusion). Fever-range WBHT treatment consists in an induction phase until a body temperature of 38.5°C is reached, followed by a retention phase for 1h and 15 minutes.

Results: 63 yo female patient, diagnosed with localized gastric adenocarcinoma treated initially with partial gastrectomy (pT1N1, MSS, HER2 negative, PDL1 CPS 0%) and adjuvant CAPOX for 8 cycles. There was lymph node (peri-aortic and common iliac) recurrence after 14 months. The patient started first line treatment with CAPOX plus Nivolumab in association with WBHT every 3 weeks with complete radiological response. After 8 months, disease progression occurred with increased size and number of peri-aortic and common iliac lymph nodes, and de-novo external iliac lymph nodes. Second line treatment with FOLFIRI was initiated in association with WBHT. After 4 cycles (total 14 cycles WBHT) the induction phase was progressively prolonged, from average 45 min in previous treatments to 1h 30 min and more than 2 hours in the last 2 cycles, without reaching the intended body temperature of 38.5°C. FOLFIRI chemotherapy was maintained and WBHT therapy was suspended. After a total of 15 cycles of FOLFIRI, CT scan showed partial response and lymph node resection was performed. Histological results showed complete pathological response.

Conclusion: Fever-range WBHT in association with chemotherapy may develop thermal tolerance, with increase difficulty to reach intended 38.5°C. Further prospective studies evaluating WBHT optimal number of cycles, treatment duration and best timing related to standard of care anti-neoplastic treatments are needed.

FP-38
Does shape and size of magnetic nanoparticles Influence magnetic fluid hyperthermia? A representative study of Mn0.5Zn0.5Fe2O4 ferrite nanoparticles based magnetic fluid

H. Patel[1]*, K. Parekh*[1]

[1]Charotar University of Science and Technology, DR. K. C. Patel Research and Development Centre, Changa, India

Magnetic fluid hyperthermia is gaining more interest as a therapy option as it is less painful and more targeted than conventional treatments. The magnetic fluid based on Mn0.5Zn0.5Fe2O4 ferrite nanoparticles is notable for its temperature-sensitive magnetic response, with a slightly higher Curie temperature than the ambient temperature. This unique property makes them highly promising for various applications ranging from engineering (coolants in heat transfer devices) to biomedicine, like cancer therapy via controlled hyperthermia. This study examines the impact of different shapes of Mn0.5Zn0.5Fe2O4 ferrite nanoparticles on magnetic fluid hyperthermia within a safety limit of magnetic field amplitude and frequency at the lowest concentration of magnetic nanoparticles. The hydrothermal method is used to synthesize different shapes of particles, including needles, flowers, rings, cubes, octahedrons, rods, etc. The analysis of structure and morphology is conducted by X-ray diffraction (XRD) and transmission electron microscopy (TEM). FTIR and TGA are used to investigate the nature of the coating and its percentage binding to the particle surface. A vibrating sample magnetometer (VSM) is used to determine the magnetic susceptibility and fluid magnetization. The sample's hydrodynamic diameter and stability were verified by the DLS and zeta-potential analyzer. The magnetic fluid induction heating efficiency was studied using the Embrell Easy Heat model LA6310, operating at a frequency of 332 kHz. The findings of the study are shown in Figure 1 and have great practical significance for investigating the potential applications of Mn0.5Zn0.5Fe2O4 ferrite nanoparticles in biomedicine.

Figure 1: Hyperthermia response of different shapes of particle-based fluid at 2 mg/mL concentration.

Acknowledgement: HP thanks Government of Gujarat for financial support under SHODH scheme (student Reference no. 202001300004). KP thanks GOI, New Delhi for providing grant no. SERB/CRG/2021/001587.

Fig. 1

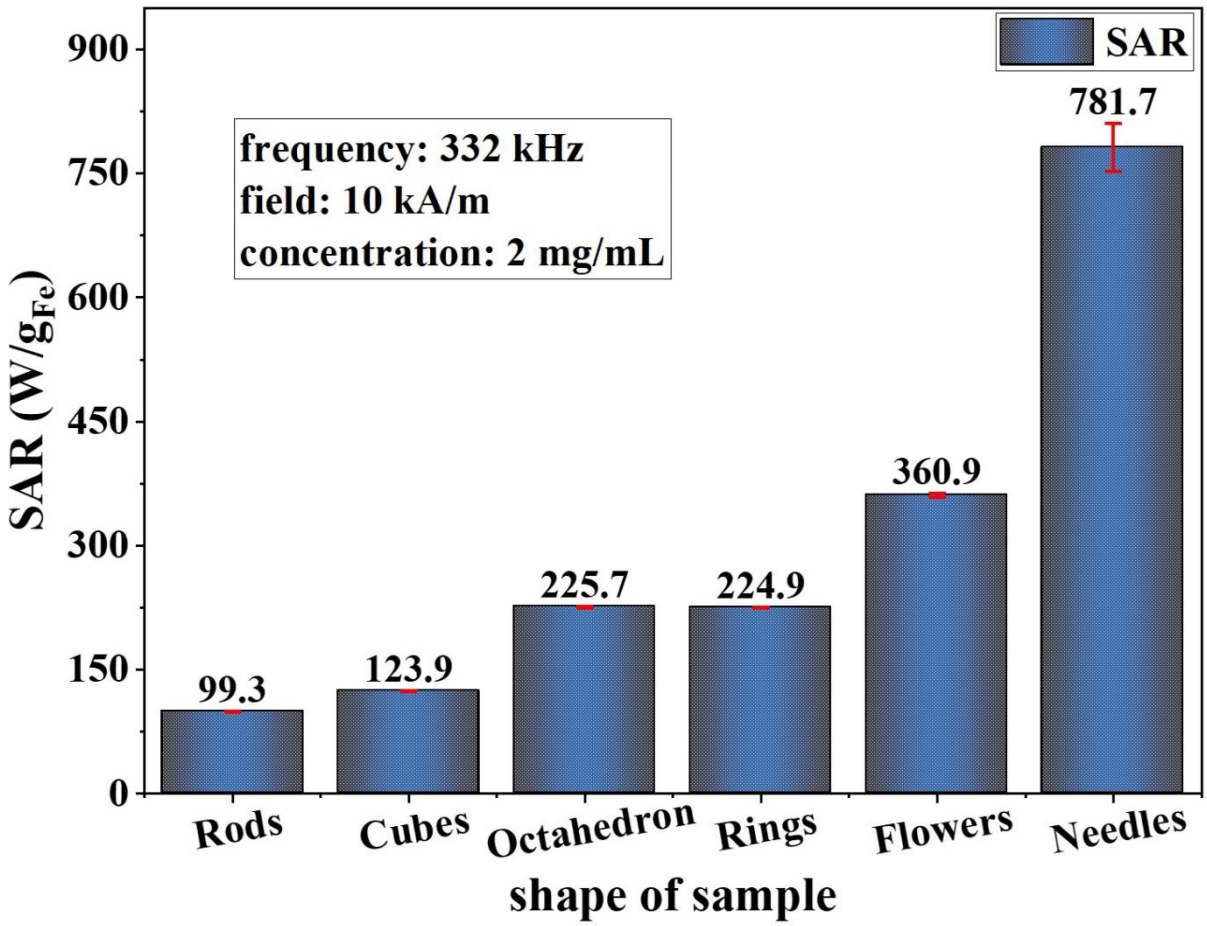

FP-39

Multifunctional plasmonic nanoparticles for combined photothermal therapy and chemotherapy

O. A. Rosas de la Rosa[1], A. Granja[2], C. Nunes[2], S. Reis[2], C. Tavares de Sousa[1]

[1]UAM - Autonomous University of Madrid, Applied Physisics, Madrid, Spain
[2]Faculdade de Farmácia, Universidade do Porto, LAQV, REQUIMTE, Departamento de Ciências Químicas, Porto, Germany

Breast cancer is one of the leading causes of mortality in women worldwide. Multifunctional nanosystems loaded with drug and photothermal agents represent a promising alternative to improve anticancer efficiency and control drug release [1]. In the present work, solid lipid nanoparticles (SLNs) functionalized with folic acid and loaded with Mitoxantrone (Mito) and gold nanorods (AuNRs) as chemotherapy and photothermal therapy (PTT) agents, respectively, for breast cancer treatment were synthesized from temperature-controlled ultrasonication [2]. The obtained nanosystems demonstrated high encapsulation efficiency and optimal physicochemical characteristics for application on tumor cells. The release of Mito was faster at acidic pH (5.2, simulating endosomal pH) and sensitive to changes in near-infrared (NIR) irradiation power. Finally, NIR-promoted PTT and chemotherapy (808 nm, 5 min) increased MCF-7 cell mortality [3]. Overall, the results verify the effectiveness of systems with Mito and AuNRs encapsulated in SLN as an alternative for the treatment of breast cancer by synergy of photothermal therapy and chemotherapy.

[1] Granja, M.Pinheiro, C.T. Sousa and S.Reis, *Biochemical Pharmacology* 190 (2021) 114639.

[2] Granja, C.Nunes, C.T. Sousa and S.Reis, *Biomedicine & Pharmacotherapy,* 154 (2022)

[3] Granja,…, S.Reis, Biomaterials Advances, 151 (2023) 213443.

FP-40
Sorbitan ester-based lipid nanospheres containing Fe3O4 nanoparticles for magnetic hyperthermia

J. Eguia-Sanchez[1], D. Iglesias-Rojas[2], K. Nader[2], J. Azkarate-Irigoras[1], G. García-García[1], U. Telleria[1], A. Martin-San Sebastian[1], I. Castellanos-Rubio[2], J. Marquez[1], I. Badiola[1], M. Insausti[2]

[1]University of the Basque Country, Cell Biology and Histology, Leioa, Spain
[2]University of the Basque Country, Organic and Inorganic Department, Leioa, Spain

Fe3O4 nanoparticle-based systems (NPs) are very versatile platforms due to the properties related to the magnetic core and a proper functionalization. New possibilities can be achieved as specific drug delivery systems, as contrast agents for magnetic resonance imaging or in selective tumor therapies such as magnetic hyperthermia.1 Another delivering systems that have acquired great interest are those based on sorbitan esters (Span®80) combined with oleylamine which has turned out to be very effective for delivering genetic species, such as microRNAs.2 This nanosystem is able to carry different species of both biological and inorganic nature. The low toxicity together with a high versatility allows the delivery of noticeable amounts of magnetic NPs, playing important roles in its development as a therapeutic agent.

Thus, we have prepared Fe3O4 NPs from thermal decomposition of previously synthesized FeOl in a mixture of octadecene and benzyl ether (volume ratio 2:1) and oleic acid. Also, Mn-Zn doped magnetite NPs (Fe2.95Mn0.02Zn0.03O4) have been produced from the mixture of two bimetallic oleates MnFeOl and ZnFeOl. The magnetic NPs have been characterized by XRD, electron microscopy (TEM), DC (M vs H, FC-ZFC) and AC (magnetic hyperthermia) magnetometry. The dimensions of the particles are 24 nm and 26 nm for Fe3O4 and Mn-Zn doped NPs, respectively. These nanosystems present saturation magnetization values of 89 and 86 Am2/kg at RT and the Mn-Zn doped sample reaches SAR values of 495 W/g under clinically safe magnetic excitation (27mT and 234kHz).

After checking their versatility as nano-heaters, an amount of nanoparticles have been combined with sorbitan monoleate (Span®80) and oleylamine to form a combined lipomagnetic nanospheres (LM) whose morphology is malleable, in that case LMs were decorated with hyaluronic acid. The morphology and size of the nanoparticles can be varied depending on various factors during preparation.

In order to evaluate the therapeutic capacity of the nanospheres, they have been incubated with different cell lines. The heterogeneous typology of the lines used covers cancers of different natures, including two colon cancer lines, two pancreatic cancer lines, and one sarcoma line. In all of them, the non-toxicity of the lipomagnetic nanoparticle and its effectiveness have been corroborated when exposing the cells with the LM nanospheres under an AC field. Mortality rates close to 100% were observed except for one pancreatic cancer line (HPAFII) known for its resistance to various treatments [3].

References:

[1] Castellanos-Rubio, I. et al. Chem. Mater. 2021, 33 (22), 8693.

[2] Marquez, J. et al. I. *Inter. J. of Cancer*, 2018, *143*(3), 709.

[3] Felt, S. A. et al, V. Z. *J. of Virology*, 2017, *91*(16), 10-1128.

FP-41

A cost-effective air cooled benchtop device to study magnetic hyperthermia in magnetic nanoparticle systems

Y. Hadadian[1], L. Dieke[1], N. Löwa[1], F. Wiekhorst[1]

[1]Physikalisch-Technische Bundesanstalt, Biosignals, Berlin, Germany

Question: Magnetic hyperthermia (MH) as a stand-alone or complementary method for cancer treatment has received extensive attention, ranging from basic research in physics and chemistry to biomedicine for preclinical and clinical applications. These applications either induce apoptosis/necrosis in cancerous cells through elevated temperature or use heat as a stimulus for temperature responsive nanocarrier drug delivery. Beyond the challenges associated with magnetic nanoparticles as heat mediator for MH, the apparatus for delivering an appropriate radiofrequency magnetic field is challenging. Although a few established commercial devices exist, they are often expensive, bulky, and require water cooling systems, leading to higher maintenance complexity, increased energy consumption, and the need for dedicated space. In addition, integration of such systems with another modality, for instance magnetic particle spectroscopy (MPS) or optical methods for drug release monitoring, can be very challenging. In this regard, we have designed an air-cooled coil system which not only provides a homogenous radiofrequency field within 32 mm on its axis, but also allows the integration with an MPS drive/receive coils system.

Methods: The system comprises a parallel LC circuit with a double-layered coil having an inner diameter of 50 mm. The coil length is 110 mm with 2*25 turns made of 4.4 mm Litz wire to reduce the power requirement and minimize the skin effect. The system is powered by a function generator connected to an amplifier. We developed a comprehensive solver in Python, where all circuit characteristics such as its impedance to match the amplifier"s impedance, coil characteristics, resultant magnetic field, the power consumption, etc. can be adjusted and estimated. The entire circuit is housed in a 3D printed tower (Fig. 1a) that allows airflow of 160 m3/h using a fan at 6300 rpm. The frame is designed such that the airflow passes only through the outer layers of the coil and other components. The sample location will not experience any airflow and sample will be isolated to minimize any possible heat exchange.

Results: In the present study we optimized the system for a maximum12 kA/m field amplitude at 300 kHz, however, the solver allows for easy optimization at a wide range of frequencies. With the current cooling system design, operation of the system at frequencies not higher than 300 kHz is possible. The coil is expected to provide a homogenous magnetic field within 32 mm space at its center (Fig.1b). The power consumption of the system will be approximately 25 W (20 A in the coil).

Conclusion: A cost-effective MH system was designed for field amplitudes up to 12 kA/m and 300 kHz. The system is intended to be used as a benchtop MH device. Its large inner diameter easily allows integration with a drive/receive coil of an MPS system, potentially upgrading the system to an independent tool for drug release and monitoring in temperature-responsive nanocarriers

Fig. 1

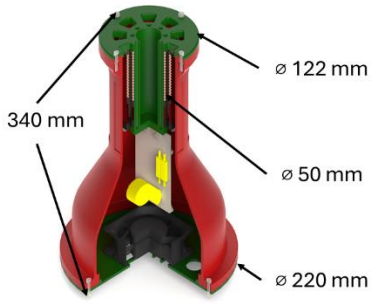

Fig. 1a: Coil system

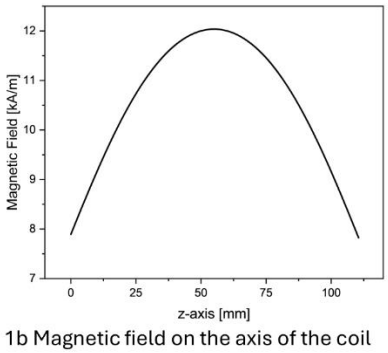

1b Magnetic field on the axis of the coil

FP-42
Cutting-edge dual-responsive magnetite nanorods in magneto-photothermal treatment

Zhila Shaterabadi[1], Ángel Delgado, Guillermo Iglesias

[1]Department of Applied Physics, University of Granada, Avda. de Fuente Nueva sn, 18071, Granada, Spain

Magnetite nanorods, as an important group of one dimensional (1-D) magnetic nanostructures, are among the best candidates for biomedical applications, thanks to their excellent heat-generating ability under an alternating magnetic field (magnetic hyperthermia) and/or infrared laser irradiation (photothermia) [1, 2].

In this work, multi-core magnetite nanorods (MMNRs) were first synthesized through a multi-step procedure using single magnetite nanorods and then characterized in term of the physicochemical properties. The MMNRs were finally subjected to magnetic hyperthermia and photothermia experiments under different conditions of nanorods concentration and stimuli intensity. Our results reveal that the self assembly of magnetite nanorods to a multi-core state causes them to show so prominent heating efficiencies under both stimuli (heating efficiency of 878 W/g in the magnetic yperthermia and 471 W/g in the photothermia) that can introduce them as the novel privileged dual-responsive candidates in thermal therapy.

Fig.1 TEM image of the MMNRs as well as magnetic hyperthermia and photothermia measurements at different concentrations and stimuli intensities.

Acknowledgment

This project has received funding from the European Union's Horizon 2020 research and innovation programme under the Marie Sklodowska-Curie grant agreement No 101064263. Z. Shaterabadi acknowledge the European Union.

References

[1] Z. Shaterabadi, Á. Delgado, and G.R. Iglesias, Journal of Magnetism and Magnetic Materials, 596 (2024), p.171990.
[2] S. El Mousli, Y. Dorant, E. Bertuit, E. Secret, E. and J.M Siaugue, Journal of Magnetism and Magnetic Materials, 589 (2024), p.171571.

Fig. 1

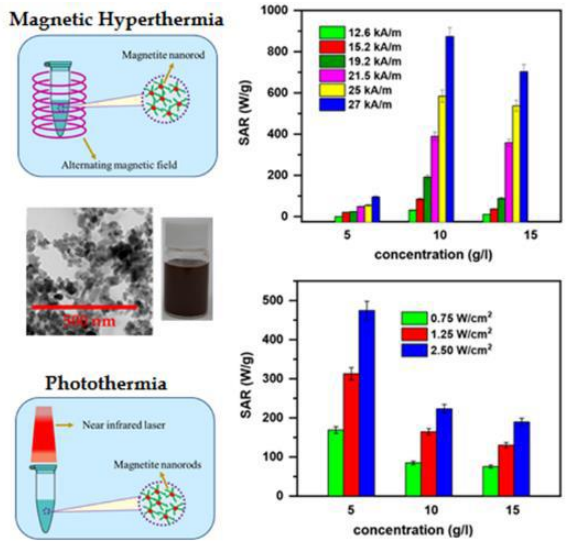

FP-43
Investigation of non-invasive temperature estimation during hyperthermia treatment under ultrasound image guidance

M. R. S. Ramu[1], K. Arunachalam[1], A. K. Thittai[2]

[1]Indian Institute of Technology Madras, Department of engeneering design, Tamilnadu, India
[2]Indian Institute of Technology Madras, Applied Mechanics and Biomedical Engineering, Chennai, India

Non-invasive tissue temperature monitoring is desirable for hyperthermia treatment monitoring as it avoids the use of invasive temperature probes. Furthermore, invasive probes do not provide the complete spatial temperature information inside the tumor target and the surrounding healthy tissues. In this work, we present our progress on the use of two-dimensional (2D) clinical ultrasound back-scattered data for extracting tissue temperature distribution during hyperthermia treatment. It is well known that spatial variation in the speed of sound in tissue exposed to thermal therapy induces thermal strain in the received back-scattered ultrasound echoes. Time shift estimates of thermal strain obtained using gradient technique are known to be prone to measurement inaccuracies and signal decorrelation due to echo straining at elevated temperatures. To enhance temperature estimation, we propose a one-step technique that directly estimates thermal strain from the ultrasound back-scattered data. The technique involves range gating the back-scattered data and temporally stretching thermally strained back-scattered data relative to a pre-heating reference. We explore various stretch factors and select the one yielding the maximum value from the normalized cross-correlation function. Estimated stretch factors are low-pass filtered along lateral direction to generate thermal strain maps. The proposed methodology was assessed using a 128-element ultrasound linear array transducer operated at 6.6 MHz. 2D temperature change maps generated from 2D thermal strain estimates were confirmed with infrared images pre and post heating of muscle equivalent tissue phantom at 434 MHz.

FP-44
Italian Society of Oncological Hyperthermia (Società Italiana di Ipertermia Oncologica - SIIO): foundation, activities and future projects to develop thermotherapy and hyperthermia in Italy

G. Fiorentini[1], G. Ranieri[2], M. Bonucci[3], S. Bonanno[4], G. Cristina[5], R. Lodico[6], D. Sarti[7]

[1]San Salvatore Hospital, Oncology, Pesaro, Italy
[2]National Cancer Institute, Oncology, Bari, Italy
[3]ARTOI Foundation, Integrative Oncology, Roma, Italy
[4]Regional Hospital, Radiotherapy, Siracusa, Italy
[5]Regional Hospital, Internal Medicine -Complementary Medicine, Merano, Italy
[6]San Camillo Forlanini, Surgical Oncology, Roma, Italy
[7]Oncology Unit, Urbino, Italy

The Italian Society of Oncological Hyperthermia (SIIO) was founded in September 2023 to promote oncological hyperthermia in Italy and develop it on the national territory to better serve cancer patients (CP).

Methods: SIIO is recruiting up to now 20 centres including public hospitals and private clinics. All hyperthermia centres have adhered to the proposed statute and code of ethics of SIIO. The following themes were approved and proposed: 1) To promote dissemination of knowledge in Thermotherapy and related fields through publications, meetings and educational symposia. 2) To encourage the advancement of Hyperthermia in all areas of medical sciences. 3) To facilitate cooperative research among the disciplines of physics, engineering, biology, chemistry, and medicine in the study of the properties and effects of Hyperthermia in Medicine including limb and visceral hyperthermic perfusions, Laser treatments and Radiofrequency ablations. 4) To organize a national database regarding tumours treated with hyperthermia: which type, stage, line of therapy, therapeutic results, calculation of the duration of response, toxicities and survival. 5) To define new integrated protocols phase II and III of chemo-hyperthermia, radio-hyperthermia, immuno-hyperthermia, palliative medicine-hyperthermia.

Results: The collections of the preliminary data obtained are being processed. Approximately three thousand patients were treated with hyperthermia every year in Italy, 86% in private clinics and 14% in public Hospitals, all in the metastatic phase relapsing after chemotherapy and radiotherapy with a life expectancy ranging from 3 months to 24 months. No patients are currently enrolled in research studies.

Each patient received eleven hyperthermia sessions (range 3-28) with different type of machines: Andromedic, Oncotherm, BSD, Celsius, Syncrotherm. The duration of treatment was 55 minutes (range 50-110), 2-3 weekly sessions were administered on alternate days, 50% of CP also received single chemotherapy at personalized doses and 90% received integrative and supportive therapies. Particular attention was given to evaluating the improvement in patients' quality of life and compliance using the ESAS scale.

Conclusions: SIIO wants to expand the therapeutic paradigm of CP through the numerical increase of hyperthermia centres and the training of new doctors, technicians and nurses who are experts in hyperthermia. SIIO is a scientific society open to the participation of groups of patients and their families. SIIO wants to collaborate with the Italian Ministry of Health, with the Regional Health Departments, with all medical associations to provide truthful and real information on the use of hyperthermia to allow and obtain the best results by optimizing costs and facilitating CPs' access to hyperthermic treatments on the National Territory and European Nations.

FP-45
Occurrence and management of discomfort during deep hyperthermia treatments

M. L. Fernando[1], R. de Kroon- Oldenhof[1], C. P. Tello Valverde[1], H. P. Kok[1], C. B. M. van den Broek[1], K. Brück[1], E. D. Geijsen[1], D. de Vries-Huizing[1], J. Crezee[1]

[1]Amsterdam University Medical Center, Amsterdam, Netherlands

Question: Long-term adverse events after deep hyperthermia treatment (DHT) are rare, but discomfort regularly occur during treatment. There are several options to reduce discomfort, which may vary in effectiveness. We retrospectively investigated the effectiveness of the applied interventions, aiming to optimize DHT quality.

Methods: 71 DHT sessions of a consecutive series of 15 patients treated between September 2023 and July 2024 were retrospectively reviewed. All patients were treated using the Alba4D, a phased array system with four radiofrequency antennas. The location and type of complaint, power, antenna ratio, phase-amplitudes, type of intervention, achieved temperature and effect of the intervention were documented. Interventions were considered successful when no additional actions were applied within 10 minutes.

Results: DHT was indicated to treat pelvic malignancies in 14 patients, and a median temperature in the treatment area (T50) of 39.8°C (range 38.5-41.5°C) was achieved. One patient was treated for para-aortal lymph node metastases without local temperature measurements. The median number of DHT sessions per patient was 5 (range 2-8). All patients experienced complaints or discomfort at some stage during treatment, with a total of 139 reported complaints. Complaints in the abdomen were most common: 56/139 (40.3%) reported in 14/15 (93.3%) of patients. All locations of discomfort are shown in Figure 1. Pain (55.4%) or pressure (17.9%) in the abdomen was mainly addressed by change in power ratio (37.5%), reduction of total power (26.8%), and the addition of air layers (21.4%). Discomfort in the bladder region occurred in 6/15 (40.0%) patients, mainly due to urinary urgency (77.8%) and was solved by (partially) emptying the bladder (55.6%). Complaints of leg discomfort, such as pain and tingles, were often due to a long lying period in one posture and could be resolved by changing posture, mild sedatives, addition of textiles or pillows. The most frequent solutions for heating associated complaints were changes in power ratio (28.8%), creation of local air layers (23.0%), and change in total power (17.3%). Interventions were immediately successful in 64.0%, while additional interventions were required in 23.0%. Successful actions from previous treatment sessions were often applied upfront in subsequent sessions. Four sessions were prematurely ended in two patients (after 21 and 49 min, and 28 and 40 min, respectively) due to severe discomfort.

Conclusion: Complaints were mostly resolved by one or two adjustments, typically by changing power ratios and addition of local air layers. Adequate communication with patients and timely interventions proved essential to ensure a good, uninterrupted and well-tolerable DHT. Analysis of the effects of interventions on target temperatures is ongoing. The results of this study will be useful to develop more detailed guidelines to effectively reduce complaints, thereby improving DHT delivery.

Fig. 1

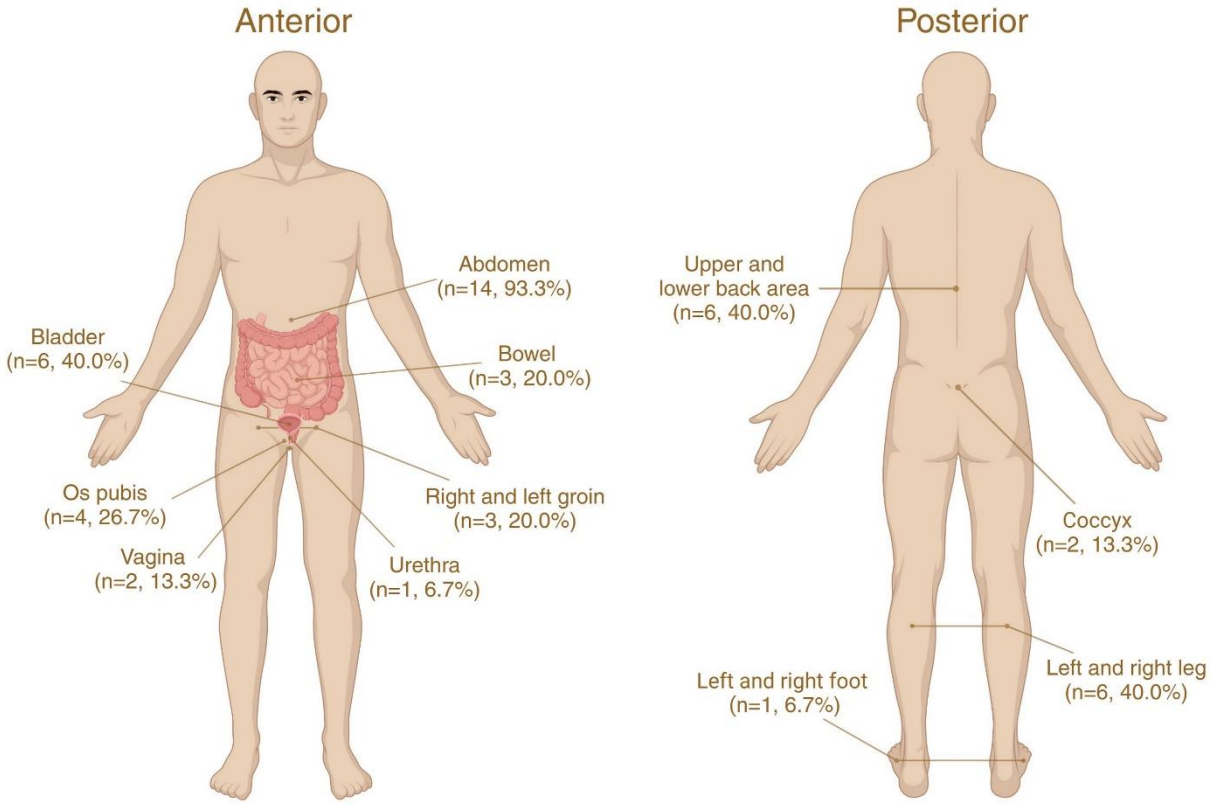

Figure 1. Location of complaints during hyperthermia sessions.
Patients experienced multiple complaint locations. Complaints such as general mild pain, general discomfort, hot/burning/pressing/stinging pain, urinary urgency, nausea, tingling or itching, were reported.

FP-46

Impact of air in the rectum on target dose coverage and specific absorption rate during hyperthermia treatments

I. popescu[1], A. Rink[1], H. Westerveld[1], M. Franckena[1], P. Granton[1], S. Curto[1]

[1]Erasmus University Medical Center Rotterdam, Hyperthermia, Rotterdam, Netherlands

Introduction: At Erasmus MC, approximately 90% of deep hyperthermia treatments (DHT) are administered to patients with cancer in the pelvic area. From radiotherapy (RT) research, it is known that air in the rectum can significantly affect both the planning and delivery of treatments. In CT-scans for hyperthermia treatment planning (HTP), we observed discrepancies between the hyperthermia target volume (HTV) due to air pockets and anatomical displacements when compared to CT-scans for RT planning. Additionally, given that HT treatments last for 90 minutes, the presence and potential movement of air pockets within the pelvic region can potentially impact the quality of the HT treatment due to the long treatment duration. This work aims to investigate the influence of air in the rectum on HTP, evaluating 25% target dose coverage (TC25) and specific absorption rate (SAR).

Methods: We retrospectively analyzed RT and HT planning CT scans from our database, covering the period from 2021 to 2024. We specifically concentrated on cases where air in rectum was present in HT scans but not in RT scans. From this analysis, 10 patients were selected. The two scans were matched on bony anatomy with the segmentation software MIM. The position of the HTV on the RT scan was rigidly transferred to the HT scan. Based on the HT-scan and HTV delineated in that scan, a first HTP was performed (HTP1) in our in-house optimization software VEDO. Afterwards, the delineated HTV on the RT-scan was rigidly transferred to the HT-scan. With this new HTV position, air in the rectum segmented as muscle or fat, antenna settings from HTP1, a second HTP was

performed (HTP2). The TC25, SAR and THQ values were compared between HTP1 and HTP2. To evaluate the movement and variability of rectal air and the HTV during HT, we reviewed the MRI images of 8 treatments, taken every 10 minutes throughout treatment.

Results: When comparing both HTP a significant change in TC25, THQ and SAR is found (Fig. 1). The presence of rectal air substantially affect those values. For instance, with a 2 cm ventral-to-dorsal target shift, the TC25 decreased from 99% to 58%. Similarly, SAR within the target area diminishes significantly with SAR values dropped by 64%, from 3.4W/Kg to 2.2W/Kg. THQ dropped 34% from 0.53 to 0.35. Larger air volumes and greater target shifts result in more pronounced decreases in both parameters. From MRI scans during the treatment, we can see displacement of the HTV of up to 2.5 cm in all directions (figure 2).

Conclusion: This analysis underlines the critical impact of rectal air on HT treatment quality. Both the volume of air and the displacement of the HTV compromise the coverage and SAR, highlighting the need for strategies to manage rectal air during HT planning and delivery to ensure optimal treatment outcomes. This abstract report the preliminary results on one patient, ongoing work will extend this study to the entire patient cohort and these will be presented at the conference.

Fig. 1

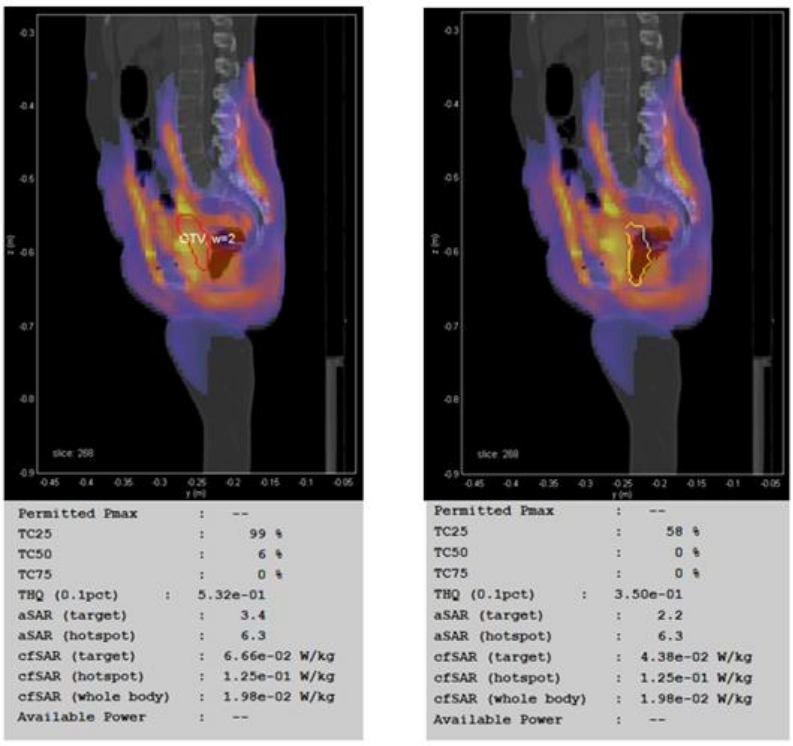

Fig. 2